

# APPENDIX A

## PBPK Modeling of TCE and Metabolites— Detailed Methods and Results

*This document is a draft for review purposes only and does not constitute Agency policy.*

10/20/09

A-i

DRAFT—DO NOT CITE OR QUOTE

**CONTENTS—Appendix: PBPK Modeling of TCE and Metabolites—Detailed Methods and Results**

LIST OF TABLES.....	A-iv
LIST OF FIGURES .....	A-v
APPENDIX A. PBPK MODELING OF TCE AND METABOLITES—DETAILED METHODS AND RESULTS.....	A-1
A.1. THE HIERARCHICAL BAYESIAN APPROACH TO CHARACTERIZING PHYSIOLOGICALLY BASED PHARMACOKINETIC (PBPK) MODEL UNCERTAINTY AND VARIABILITY .....	A-1
A.2. EVALUATION OF THE HACK ET AL. (2006) PHYSIOLOGICALLY BASED PHARMACOKINETIC (PBPK) MODEL .....	A-4
A.2.1. Convergence.....	A-4
A.2.2. Evaluation of Posterior Distributions for Population Parameters .....	A-6
A.2.3. Comparison of Model Predictions With Data .....	A-7
A.2.3.1. Mouse Model .....	A-8
A.2.3.2. Rat Model.....	A-15
A.2.3.3. Human model.....	A-23
A.3. PRELIMINARY ANALYSIS OF MOUSE GAS UPTAKE DATA: MOTIVATION FOR MODIFICATION OF RESPIRATORY METABOLISM .....	A-33
A.4. DETAILS OF THE UPDATED PHYSIOLOGICALLY BASED PHARMACOKINETIC (PBPK) MODEL FOR TRICHLOROETHYLENE (TCE) AND ITS METABOLITES .....	A-38
A.4.1. Model Parameters and Baseline Values .....	A-38
A.4.2. Statistical Distributions for Parameter Uncertainty and Variability .....	A-46
A.4.2.1. Initial Prior Uncertainty in Population Mean Parameters.....	A-46
A.4.2.2. Interspecies Scaling to Update Selected Prior Distributions in the Rat and Human .....	A-46
A.4.2.3. Population Variance: Prior Central Estimates and Uncertainty.....	A-56
A.4.2.4. Prior distributions for Residual Error Estimates.....	A-60
A.5. RESULTS OF UPDATED PHYSIOLOGICALLY BASED PHARMACOKINETIC (PBPK) MODEL .....	A-63
A.5.1. Convergence and Posterior Distributions of Sampled Parameters.....	A-63
A.5.2. Comparison of Model Predictions With Data .....	A-63
A.5.2.1. Mouse Model .....	A-63
A.5.2.2. Rat Model.....	A-63
A.5.2.3. Human Model .....	A-74
A.6. EVALUATION OF RECENTLY PUBLISHED TOXICOKINETIC DATA.....	A-74
A.6.1. TCE Metabolite Toxicokinetics in Mice: Kim et al. (2009) .....	A-74
A.6.2. TCE Toxicokinetics in Rats: Liu et al. (2009) .....	A-78
A.6.3. TCA Toxicokinetics in Mice and Rats: Mahle et al. (2001) and Green (2003a, b).....	A-79

*This document is a draft for review purposes only and does not constitute Agency policy.*

**CONTENTS (continued)**

A.7. UPDATED PHYSIOLOGICALLY BASED PHARMACOKINETIC (PBPK) MODEL  
CODE ..... A-81

A.8. REFERENCES ..... A-106

*This document is a draft for review purposes only and does not constitute Agency policy.*

**LIST OF TABLES**

A-1. Evaluation of Hack et al. (2006) PBPK model predictions for *in vivo* data in mice .... A-10

A-2. Evaluation of Hack et al. (2006) PBPK model predictions for *in vivo* data in rats ..... A-16

A-3. Evaluation of Hack et al. (2006) PBPK model predictions for *in vivo* data in humans ..... A-24

A-4. PBPK model parameters, baseline values, and scaling relationships ..... A-39

A-5. Uncertainty distributions for the population mean of the PBPK model parameters..... A-47

A-6. Updated prior distributions for selected parameters in the rat and human ..... A-52

A-7. Uncertainty distributions for the population variance of the PBPK model parameters ..... A-57

A-8. Measurements used for calibration ..... A-61

A-9. Posterior distributions for mouse PBPK model population parameters ..... A-64

A-10. Posterior distributions for mouse residual errors ..... A-66

A-11. Posterior distributions for rat PBPK model population parameters..... A-67

A-12. Posterior distributions for rat residual errors ..... A-69

A-13. Posterior distributions for human PBPK model population parameters..... A-71

A-14. Posterior distributions for human residual errors..... A-73

*This document is a draft for review purposes only and does not constitute Agency policy.*

**LIST OF FIGURES**

A-1. Hierarchical population statistical model for PBPK model parameter uncertainty and variability (see Gelman et al., 1996) ..... A-2

A-2. Schematic of how posterior predictions were generated for comparison with experimental data ..... A-8

A-3. Limited optimization results for male closed chamber data from Fisher et al. (1991) without (top) and with (bottom) respiratory metabolism ..... A-36

A-4. Limited optimization results for female closed chamber data from Fisher et al. (1991) without (top) and with (bottom) respiratory metabolism ..... A-37

A-5. Respiratory metabolism model for updated PBPK model ..... A-38

A-6. Updated hierarchical structure for rat and human models ..... A-62

A-7. Comparison of best-fitting (out of 50,000 posterior samples) PBPK model prediction and Kim et al. (2009) TCA blood concentration data for mice gavaged with 2,140 mg/kg TCE ..... A-75

A-8. Comparison of best-fitting (out of 50,000 posterior samples) PBPK model prediction and Kim et al. (2009) DCVG blood concentration data for mice gavaged with 2,140 mg/kg TCE ..... A-76

A-9. PBPK model predictions for the fraction of intake undergoing GSH conjugation in mice continuously exposed orally to TCE ..... A-77

A-10. PBPK model predictions for the fraction of intake undergoing GSH conjugation in mice continuously exposed via inhalation to TCE ..... A-78

*This document is a draft for review purposes only and does not constitute Agency policy.*

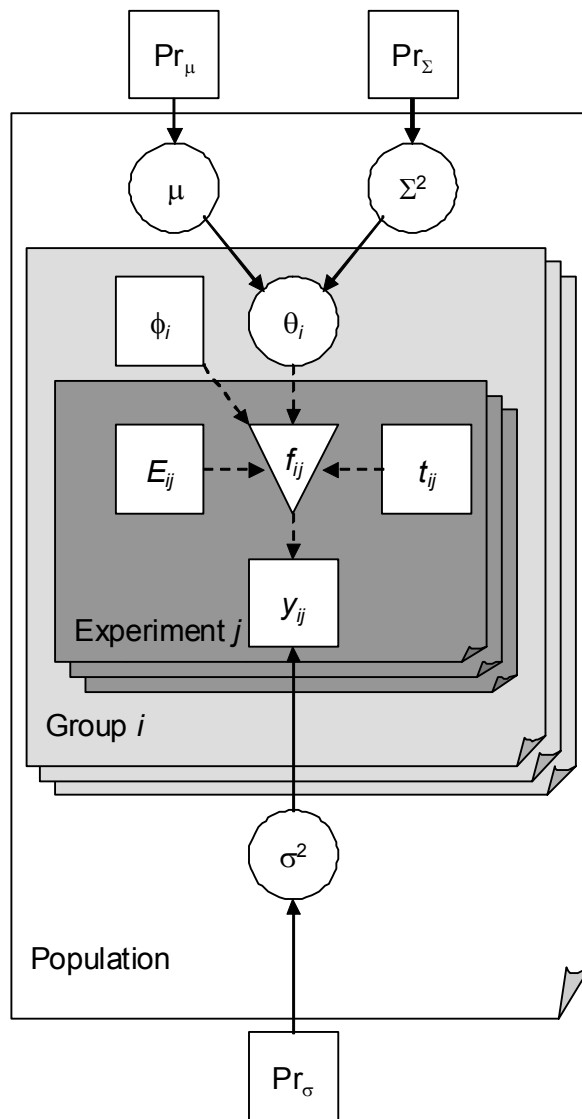
1 **APPENDIX A. PBPK MODELING OF TCE AND METABOLITES—DETAILED**  
2 **METHODS AND RESULTS**

3  
4  
5 **A.1. THE HIERARCHICAL BAYESIAN APPROACH TO CHARACTERIZING**  
6 **PHYSIOLOGICALLY BASED PHARMACOKINETIC (PBPK) MODEL**  
7 **UNCERTAINTY AND VARIABILITY**

8 The Bayesian approach for characterizing uncertainty and variability in PBPK model  
9 parameters, used previously for trichloroethylene (TCE) in Bois (2000a, b) and Hack et al.  
10 (2006), is briefly described here as background. Once a physiologically based pharmacokinetic  
11 (PBPK) model structure is specified, characterizing the model reduces to calibrating and making  
12 inferences about model parameters. The use of least-squares point estimators is limited by the  
13 large number of parameters and small amounts of data. The use of least-squares estimation is  
14 reported after imposing constraints for several parameters (Fisher, 2000; Clewell et al., 2000).  
15 This is reasonable for a first estimate, but it is important to follow-up with a more refined  
16 treatment. This is implemented by a Bayesian approach to estimate posterior distributions on the  
17 unknown parameters, a natural choice, and almost a compulsory consequence given the large  
18 number of parameters and relatively small amount of data, and given the difficulties of  
19 frequentist estimation in this setting.

20 As described by Gelman et al. (1996), the Bayesian approach to population PBPK  
21 modeling involves setting up the overall model in several stages. A nonlinear PBPK model, with  
22 predictions denoted  $f$ , describes the absorption, distribution, metabolism, and excretion of a  
23 compound and its metabolites in the body. This model depends on several, usually known,  
24 parameters such as measurement times  $t$ , exposure  $E$ , and measured covariates  $\varphi$ . Additionally,  
25 each subject  $i$  in a population has a set of unmeasured parameters  $\theta_i$ . A random effects model  
26 describes their population variability  $P(\theta_i | \mu, \Sigma^2)$ , and a prior distribution  $P(\mu, \Sigma^2)$  on the  
27 population mean  $\mu$  and covariance  $\Sigma^2$  (often assumed to be diagonal) incorporates existing  
28 scientific knowledge about them. Finally, a “measurement error” model  $P(y | f[\theta, \varphi, E, t], \sigma^2)$   
29 describes deviations (with variance  $\sigma^2$ ) between the data  $y$  and model predictions  $f$  (which of  
30 course depends on the unmeasured parameters  $\theta_i$  and the measured parameters  $t, E$ , and  $\varphi$ ). This  
31 “measurement error” level of the hierarchical model typically also encompasses intraindividual  
32 variability as well as model misspecification, but for notational convenience we refer to it here as  
33 “measurement error.” Because these other sources of variance are lumped into a single  
34 “measurement error,” a prior distribution of its variance  $\sigma^2$  must be specified even if the actual  
35 analytic measurement error is known. All these components are illustrated graphically in  
36 Figure A-1.

*This document is a draft for review purposes only and does not constitute Agency policy.*



1  
2 **Figure A-1. Hierarchical population statistical model for PBPK model**  
3 **parameter uncertainty and variability (see Gelman et al., 1996).** Square nodes  
4 denote fixed or observed quantities; circle notes represent uncertain or unobserved  
5 quantities, and the nonlinear model outputs are denoted by the inverted triangle.  
6 Solid arrows denote a stochastic relationship represented by a conditional  
7 distribution [ $A \rightarrow B$  means  $B \sim P(B|A)$ ], while dashed arrows represent a function  
8 relationship [ $B = f(A)$ ]. The population consists of groups (or subjects)  $i$ , each of  
9 which undergoes one or more experiments  $j$  with exposure parameters  $E_{ij}$  with  
10 data  $y_{ij}$  collected at times  $t_{ij}$ . The PBPK model produces outputs  $f_{ij}$  for comparison  
11 with the data  $y_{ij}$ . The difference between them (“measurement error”) has  
12 variance  $\sigma^2$ , with a fixed prior distribution  $Pr$ , which in this case is the same for  
13 the entire population. The PBPK model also depends on measured covariates  $\phi_i$   
14 (e.g., body weight) and unobserved model parameters  $\theta_i$  (e.g.,  $V_{MAX}$ ). The  
15 parameters  $\theta_i$  are drawn from a population with mean  $\mu$  and variance  $\Sigma^2$ , each of  
16 which is uncertain and has a prior distribution assigned to it.

*This document is a draft for review purposes only and does not constitute Agency policy.*

1 The posterior distribution for the unknown parameters is obtained in the usual manner by  
 2 multiplying (1) the prior distribution for the population mean and variance and the  
 3 “measurement” error  $P(\mu, \Sigma^2) P(\sigma^2)$ , (2) the population distribution for the individual parameters  
 4  $P(\theta | \mu, \Sigma^2)$ , and (3) the likelihood  $P(y | \theta, \sigma^2)$ , where for notational convenience, the dependence  
 5 on  $f$ ,  $\varphi$ ,  $E$ , and  $t$  (which are taken as fixed for a given dataset) is dropped:

$$6 \quad P(\theta, \mu, \Sigma^2, \sigma^2 | y) \propto P(\mu, \Sigma^2) P(\sigma^2) P(\theta | \mu, \Sigma^2) P(y | \theta, \sigma^2) \quad (\text{Eq. A-1})$$

8 Here, each subject’s parameters  $\theta_i$  have the same sampling distribution (i.e., they are  
 9 independently and identically distributed), so their joint prior distribution is

$$10 \quad P(\theta | \mu, \Sigma^2) = \prod_{i=1 \dots n} P(\theta_i | \mu, \Sigma^2) \quad (\text{Eq. A-2})$$

11  
 12 Different experiments  $j = 1 \dots n_j$  may have different exposure and different data collected and  
 13 different time points. In addition, different types of measurements  $k = 1 \dots n_k$  (e.g., TCE blood,  
 14 TCE breath, trichloroacetic acid [TCA] blood, etc.) may have different errors, but errors are  
 15 otherwise assumed to be iid. Since the individuals are treated as independent given  $\theta_{1 \dots n}$ , the  
 16 total likelihood function is simply

$$17 \quad P(y | \theta, \sigma^2) = \prod_{i=1 \dots n} \prod_{j=1 \dots n_{ij}} \prod_{k=1 \dots m} \prod_{l=1 \dots N_{ijk}} P(y_{ijkl} | \theta_i, \sigma_k^2, t_{ijkl}) \quad (\text{Eq. A-3})$$

18  
 19 where  $n$  is the number of subjects,  $n_{ij}$  is the number of experiments in that subject,  $m$  is the  
 20 number of different types of measurements,  $N_{ijk}$  is the number (possibly 0) of measurements  
 21 (e.g., time points) for subject  $i$  of type  $k$  in experiment  $j$ , and  $t_{ijkl}$  are the times at which  
 22 measurements for individual  $i$  of type  $k$  were made in experiment  $j$ .

23 Given the large number of parameters, complex likelihood functions, and nonlinear  
 24 PBPK model, Markov chain Monte Carlo (MCMC) simulation was used to generate samples  
 25 from the posterior distribution. An important practical advantage of MCMC sampling is the  
 26 ability to implement inference in nearly any probability model and the possibility to report  
 27 inference on any event of interest. MCMC simulation was introduced by Gelfand and Smith  
 28 (1990) as a generic tool for posterior inference. See Gilks et al. (1996) for a review. In addition,  
 29 because many parameters are allowed to vary simultaneously, the local parameter sensitivity  
 30 analyses often performed with PBPK models (in which the changes in model predictions are  
 31  
 32  
 33



1 assessed with each parameter varied by a small amount) are unnecessary.<sup>1</sup> In the context of  
2 PBPK models, the MCMC simulation can be carried out as described by Hack et al. (2006). The  
3 simulation program MCSim (version 5.0.0) was used to implement MCMC posterior simulation,  
4 with analysis of the results performed using the *R* statistical package. Simulation-based  
5 parameter estimation with MCMC posterior simulation gives rise to an additional source of  
6 uncertainty. For instance, averages computed from the MCMC simulation output represent the  
7 desired posterior means only asymptotically, in the limit as the number of iterations goes to  
8 infinity. Any implementation needs to include a convergence diagnostic to judge practical  
9 convergence. The potential scale-reduction-factor convergence diagnostic *R* of Gelman et al.  
10 (1996) was used here, as it was in Hack et al. (2006).

11

## 12 **A.2. EVALUATION OF THE HACK ET AL. (2006) PHYSIOLOGICALLY BASED** 13 **PHARMACOKINETIC (PBPK) MODEL**

14 U.S. Environmental Protection Agency (U.S. EPA) obtained the original model code for  
15 the version of the TCE PBPK model published in Hack et al. (2006) and conducted a detailed  
16 evaluation of the model, focusing on the following areas: convergence, posterior estimates for  
17 model parameters, and comparison of model predictions with *in vivo* data.

18

### 19 **A.2.1. Convergence**

20 As noted in Hack et al. (2006), the diagnostics for the MCMC simulations (3 chains of  
21 length 20,000–25,000 for each species) indicated that additional samples might further improve  
22 convergence. A recent analysis of tetrachloroethylene pharmacokinetics indicated the need to be  
23 especially careful in ensuring convergence (Chiu and Bois, 2006). Therefore, the number of  
24 MCMC samples per chain was increased to 75,000 for rats (first 25,000 discarded) and 175,000  
25 for mice and humans (first 75,000 discarded). Using these chain lengths, the vast majority of the  
26 parameters had potential scale reduction factors  $R \leq 1.01$ , and all population parameters had  
27  $R \leq 1.05$ , indicating that longer chains would be expected to reduce the standard deviation (or  
28 other measure of scale, such as a confidence interval) of the posterior distribution by less than  
29 this factor (Gelman et al., 2004).

---

<sup>1</sup> In particular, local sensitivity analyses are typically used to assess the impact of alternative parameter estimates on model predictions, inform experimental design, or assist prioritizing risk assessment research. Only the first purpose is relevant here; however, the full uncertainty and variability analysis allows for a more comprehensive assessment than can be done with sensitivity analyses. Separately, such analyses could be done to design experiments and prioritize research that would be most likely to help reduce the remaining uncertainties in TCE toxicokinetics, but that is beyond the scope of this assessment.

*This document is a draft for review purposes only and does not constitute Agency policy.*

1           In addition, analysis of autocorrelation within chains using the R-CODA package  
2 (Plumber et al., 2008) indicated that there was significant serial correlation, so additional  
3 “thinning” of the chains was performed in order to reduce serial correlations. In particular, for  
4 rats, for each of three chains, every 100<sup>th</sup> sample from the last 50,000 samples was used; and for  
5 mice and humans, for each of three chains, every 200<sup>th</sup> sample from the last 100,000 samples  
6 was used. This thinning resulted in a total of 1,500 samples for each species available for use for  
7 posterior inference.

8           Finally, an evaluation was made of the “convergence” of dose metric predictions—that is,  
9 the extent to which the standard deviation or confidence intervals for these predictions would be  
10 reduced with additional samples. This is analogous to a “sensitivity analysis” performed so that  
11 most effort is spent on parameters that are most influential in the result. In this case, the purpose  
12 is to evaluate whether one can sample chains only long enough to ensure convergence of  
13 predictions of interest, even if certain more poorly identified parameters take longer chains to  
14 converge. The motivation for this analysis is that for a more complex model, running chains  
15 until all parameters have  $R \leq 1.01$  or 1.05 may be infeasible given the available time and  
16 resource. In addition, as some of the model parameters had prior distributions derived from  
17 “visual fitting” to the same data, replacing those distributions with less informative distributions  
18 (in order to reduce bias from “using the same data twice”) may require even longer chains for  
19 convergence.

20           Indeed, it was found that  $R$ -values for dose metric predictions approached one more  
21 quickly than PBPK model input parameters. The most informative simulations were for mice,  
22 which converged the slowest and, thus, had the most potential for convergence-related error.  
23 Results for rats could not be assessed because the model converged so rapidly, and results for  
24 humans were similar to those in mice, though the deviations were all less because of the more  
25 rapid convergence. In the mouse model, after 25,000 iterations, many PBPK model parameters  
26 had  $R$ -values  $>2$ , with more than 25% greater than 1.2. However, all dose metric predictions had  
27  $R < 1.4$ , with the more than 96% of them  $<1.2$  and the majority of them  $<1.01$ . In addition, when  
28 compared to the results of the last 100,000 iterations (after the total of 175,000 iterations), more  
29 than 90% of the medians estimates shifted by less than 20%, with the largest shifts less than 40%  
30 (for glutathione [GSH] metabolism dose metrics, which had no relevant calibration data). Tail  
31 quantiles had somewhat larger shifts, which was expected given the limited number of samples  
32 in the tail, but still more than 90% of the 2.5 and 97.5 percentile quantiles had shifts of less than  
33 40%. Again, the largest shifts, on order of 2-fold, were for GSH-related dose metrics that had  
34 high uncertainty, so the relative impact of limited sample size is small.

*This document is a draft for review purposes only and does not constitute Agency policy.*

1           Therefore, the additional simulations performed in this evaluation, with 3- to 7-fold  
2 longer chains, did not result in much change in risk assessment predictions from the original  
3 Hack et al. (2006) results. Thus, assessing prediction convergence appears sufficient for  
4 assessing convergence of the TCE PBPK model for the purposes of risk assessment prediction.  
5

#### 6 **A.2.2. Evaluation of Posterior Distributions for Population Parameters**

7           Posterior distributions for the population parameters were first checked for whether they  
8 appeared reasonable given the prior distributions. Inconsistency between the prior and posterior  
9 distributions may indicate an insufficiently broad prior distribution (i.e., overconfidence in their  
10 specification), a mis-specification of the model structure, or an error in the data. Parameters that  
11 were flagged for further investigation were those for which the interquartile ranges (intervals  
12 bounded by the 25<sup>th</sup> and 75<sup>th</sup> percentiles) of the prior and posterior distributions did not overlap.  
13 In addition, lumped metabolism and clearance parameters for TCA, trichloroethanol (TCOH),  
14 and trichloroethanol-glucuronide conjugate (TCOG) were checked to make sure that they  
15 remained physiological—e.g., metabolic clearance was not more than hepatic blood flow and  
16 urinary clearance not more than kidney blood flow (constraints that were not present in the Hack  
17 et al., 2006 priors).

18           In mice, population mean parameters that had lack of overlap between priors and  
19 posteriors included the affinity of oxidative metabolism ( $\ln K_M$ ), the TCA plasma-blood  
20 concentration ratio ( $\ln TCAPlas$ ), the TCE stomach to duodenum transfer coefficient ( $\ln KTSD$ ),  
21 and the urinary excretion rates of TCA and TCOG ( $\ln k_{UrnTCA}$  and  $\ln k_{UrnTCOG}$ ). For  $K_M$ ,  
22 this is not unexpected, as previous investigators have noted inconsistency in the  $K_M$  values  
23 between *in vitro* values (upon which the prior distribution was based) and *in vivo* values derived  
24 from oral and inhalation exposures in mice (Abbas and Fisher, 1997; Greenberg et al., 1999).  
25 For the other mean parameters, the central estimates were based on visual fits, without any other  
26 *a priori* data, so it is reasonable to assume that the inconsistency is due to insufficiently broad  
27 prior distributions. In addition, the population variance for the TCE absorption coefficient from  
28 the duodenum ( $kAD$ ) was rather large compared to the prior distribution, likely due to the fact  
29 that oral studies included TCE in both oil and aqueous solutions, which are known to have very  
30 different absorption properties. Thus, the larger population variance was required to  
31 accommodate both of them. Finally, the estimated clearance rate for glucuronidation of TCOH  
32 was substantially greater than hepatic blood flow. This is an artifact of the one-compartment  
33 model used for TCOH and TCOG, and suggests that first pass effects are important for TCOH  
34 glucuronidation. Therefore, the model would benefit from the additional of a separate liver

*This document is a draft for review purposes only and does not constitute Agency policy.*

1 compartment so that first pass effects can be accounted for, particularly when comparing across  
2 dose-routes.

3 In rats, the only population mean or variance parameter for which the posterior  
4 distribution was somewhat inconsistent with the prior distribution was the population mean for  
5 the  $\ln K_M$ . While the interquartile regions did not overlap, the 95 percentile regions did, so the  
6 discordance was relatively minor. However, as with mice, the estimated clearance rate for  
7 glucuronidation of TCOH was substantially greater than hepatic blood flow.

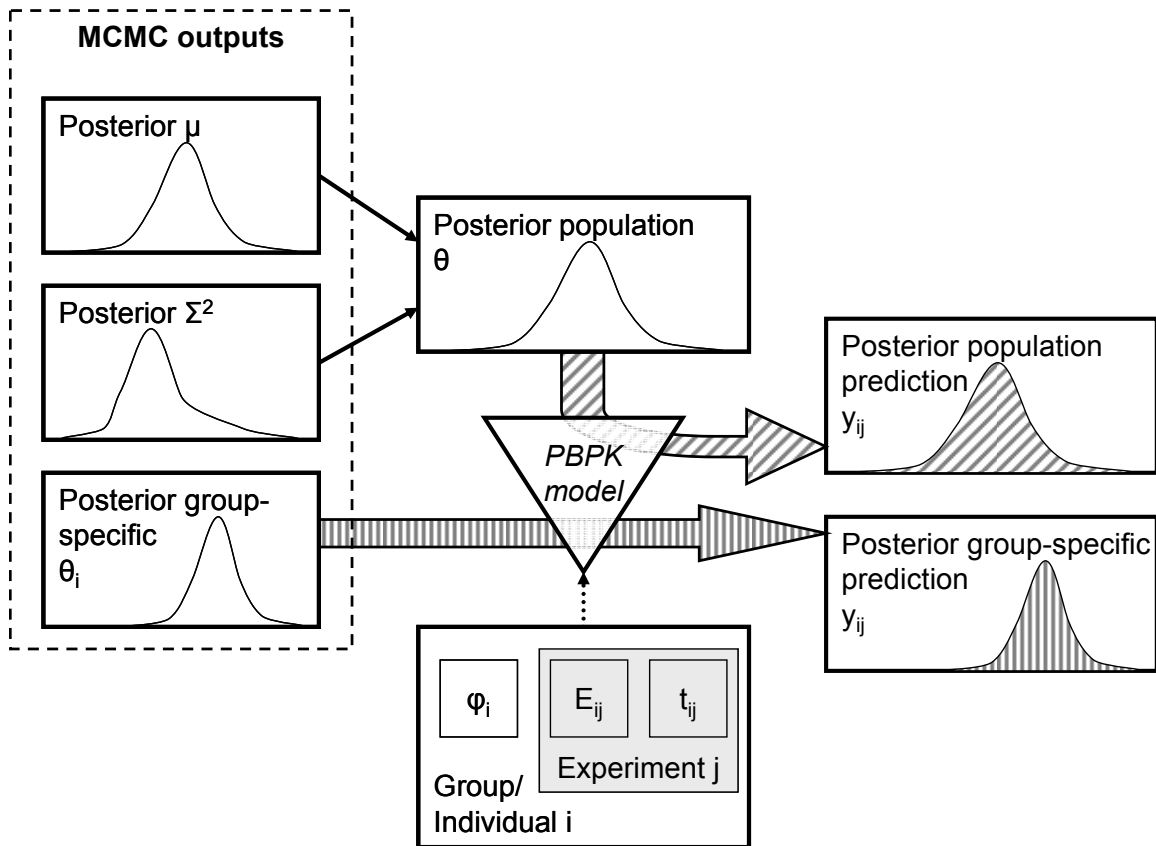
8 In humans, some of the chemical-specific parameters for which priors were established  
9 using visual fits had posterior distributions that were somewhat inconsistent, including the  
10 oxidative split between TCA and TCOH, biliary excretion of TCOG ( $\ln k_{BileC}$ ), and the TCOH  
11 distribution volume ( $V_{BodC}$ ). More concerning was the fact that the posterior distributions for  
12 several physiological volumes and flows were rather strongly discordant with the priors and/or  
13 near their truncation limits, including gut, liver, and slowly perfused blood flow, the volumes of  
14 the liver and rapidly perfused compartments. In addition, a number of tissue partition  
15 coefficients were somewhat inconsistent with their priors, including those for TCE in the gut,  
16 rapidly perfused, and slowly perfused tissues, and TCA in the body and liver. Finally, a number  
17 of population variances (for TCOH clearance [ $CITCOHC$ ], urinary excretion of TCOG  
18 [ $k_{UrnTCOGC}$ ], ventilation-perfusion ratio [ $VPR$ ], cardiac output [ $QCC$ ], fat blood flow and  
19 volume [ $Q_{FatC}$  and  $V_{FatC}$ ], and TCE blood-air partition coefficient [ $PB$ ]) were somewhat high  
20 compared to their prior distributions, indicating much greater population variability than  
21 expected.

### 22 23 **A.2.3. Comparison of Model Predictions With Data**

24 A schematic of the comparisons between model predictions and data are shown in  
25 Figure A-2. In the hierarchical population model, group-specific parameters were estimated for  
26 each dataset used in calibrating the model (posterior group-specific  $\theta_i$  in Figure A-2). Because  
27 these parameters are in a sense “optimized” to the experimental data themselves, the group-  
28 specific predictions (posterior group-specific  $y_{ij}$  in Figure A-2) using these parameters should be  
29 accurate by design. Poor fits to the data using these group-parameters may indicate a  
30 misspecification of the model structure, prior parameter distributions, or an error in the data. In  
31 addition, it is useful to generate “population-based” parameters (posterior population  $\theta$ ) using  
32 only the posterior distributions for the population means ( $\mu$ ) and variances ( $\Sigma^2$ ), instead of the  
33 estimated group-specific parameters. These population predictions provide a sense as to whether  
34 the model and the predicted degree of population uncertainty and variability adequately account  
35 for the range of heterogeneity in the experimental data. Furthermore, assuming the group-

1 specific predictions are accurate, the population-based predictions are useful to identify whether  
 2 one or more if the datasets are “outliers” with respect to the predicted population. In addition, a  
 3 substantial number of *in vivo* datasets was available in all three species that were not previously  
 4 used for calibration. Thus, it is informative to compare the population-based model predictions,  
 5 discussed above, to these additional “validation” data in order to assess the predictive power of  
 6 the PBPK model.

7



8

9

10

11

12

13

14

15

**Figure A-2. Schematic of how posterior predictions were generated for comparison with experimental data.** Two sets of posterior predictions were generated: population predictions (diagonal hashing) and group-specific predictions (vertical hashing).

16

17

18

19

### A.2.3.1. Mouse Model

**A.2.3.1.1. Group-specific and population-based predictions.** Initially, the sampled group-specific parameters were used to generate predictions for comparison to the calibration data. Because these parameters were “optimized” for each group, these “group-specific” predictions should be accurate by design. However, unlike for the rat (see below), this was not the case for

1 some experiments (this is partially responsible for the slower convergence). In particular, the  
2 predictions for TCE and TCOH concentrations for the Abbas and Fisher (1997) data were poor.  
3 In addition, TCE blood concentrations for the Greenberg et al. (1999) data were consistently  
4 overpredicted. These data are discussed further in Table A-1.

5 Next, only samples of the population parameters (means and variances) were used, and  
6 “new groups” were sampled from appropriate distributions using these population means and  
7 variances. These “new groups” then represent the predicted population distribution,  
8 incorporating both variability in the population as well as uncertainty in the population means  
9 and variances. These “population-based” predictions were then compared to both the data used  
10 in calibration, as well as the additional data identified that was not used in calibration. The  
11 PBPK model was modified to accommodate some of the different outputs (e.g., tissue  
12 concentrations) and exposure routes (TCE, TCA, and TCOH intravenous [i.v.]) used in the  
13 “noncalibration” data, but otherwise it is unchanged.

14  
15 **A.2.3.1.1.1. Group-specific predictions and calibration data.** [See  
16 [Appendix.linked.files\AppA.2.3.1.1.1.Hack.mouse.group.calib.TCE.DRAFT.pdf.](#)]

17  
18 **A.2.3.1.1.2. Population-based predictions and calibration and additional evaluation data.**  
19 [See [Appendix.linked.files\AppA.2.3.1.1.2.Hack.mouse.pop.calib.eval.TCE.DRAFT.pdf.](#)]

20  
21 **A.2.3.1.2. Conclusions regarding mouse model.**

22 **A.2.3.1.2.1. Trichloroethylene (TCE) concentrations in blood and tissues not well-predicted.**

23 The PBPK model for the parent compound does not appear to be robust. Even group-specific  
24 fits to datasets used for calibration were not always accurate. For oral dosing data, there is  
25 clearly high variability in oral uptake parameters, and the addition of uptake through the first  
26 (stomach) compartment should improve the fit. Unfortunately, inaccurate TCE uptake  
27 parameters may lead to inaccurately estimated kinetic parameters for metabolites TCA and  
28 TCOH, even if current fits are adequate.

**Table A-1. Evaluation of Hack et al. (2006) PBPK model predictions for *in vivo* data in mice**

Reference	Simulation #	Calibration data	Discussion
Abbas et al., 1997	41–42		These data are only published as an abstract. They consist of TCA and TCOH blood and urine data from TCA and TCOH i.v. dosing. Blood levels of TCA and TCOH are fairly accurately predicted. From TCOH dosing, urinary TCOG excretion is substantially overpredicted, and from TCA dosing, urinary TCA excretion is substantially overpredicted.
Abbas and Fisher, 1997	3–6	√	<p>Results for these data were mixed. TCA levels were the best fit. The calibration data included TCA blood and liver data, which were well predicted except at the earliest time-point. In addition, TCA concentrations in the kidney were fairly consistent with the surrogate TCA body concentrations predicted by the model. Urinary TCA was well predicted at the lower two and highest doses, but somewhat underpredicted (though still in the 95% confidence region) at 1,200 mg/kg.</p> <p>TCE levels were in general not well fit. Calibration data included blood, fat, and liver concentrations, which were predicted poorly particularly at early and late times. One reason for this is probably the representation of oral uptake. Although both the current model and the original Abbas and Fisher (1997) model had two-compartments representing oral absorption, in the current model uptake can only occur from the second compartment. By contrast, the Abbas and Fisher (1997) model had uptake from both compartments, with the majority occurring from the first compartment. Thus, the explanation for the poor fit, particularly of blood and liver concentrations, at early times is probably simply due to differences in modeling oral uptake. This is also supported by the fact that the oral uptake parameters tended to be among those that took the longest to converge.</p> <p>Group-specific blood TCOH predictions were poor, with under-prediction at early times and overprediction at late times. Population-based blood TCOH predictions tended to be underpredicted, though generally within the 95% confidence region. Group-specific urinary TCOG predictions were fairly accurate except at the highest dose. These predictions are also probably affected by the apparent misrepresentation of oral uptake. In addition, a problem as found in the calibration data in that data on free TCOH was calibrated against predictions of total TCOH (TCOH+TCOG).</p> <p>A number of TCOH and TCOG measurements were not included in the calibration—among them tissue concentrations of TCOH and tissue and blood concentrations of TCOG. Blood concentrations (the only available surrogate) were poor predictors of tissue concentrations of TCOH and TCOG (model generally under-predicted). For TCOG, this may be due in part to the model assumption that the distribution volume of TCOG is equal to that of TCOH.</p>

Table A-1. Evaluation of Hack et al. (2006) PBPK model predictions for *in vivo* data in mice (continued)

Reference	Simulation #	Calibration data	Discussion
Fisher et al., 1991	1–2 (open chamber)	√	Venous blood TCE concentrations were somewhat underpredicted (a common issue with inhalation exposures in mice—see discussion of Greenberg et al., 1999 below), but within the 95% confidence region of both group-specific and population-based predictions. Plasma TCA levels were well predicted, with most of the data near the interquartile region of both group-specific and population-based predictions (but with substantial scatter in the male mice). However, it should be noted that only a single exposure concentration for each sex was used in calibration, with 6 additional exposures (3 for each sex) not included (see simulations 21–26, below).
	7–16 (closed chamber)	√	Good posterior fits were obtained for these data—closed chamber data with initial concentrations from 300 to 10,000 ppm. Some variability in $V_{MAX}$ , however, was noted in the posterior distributions for that parameter. Using group-specific $V_{MAX}$ values resulted in better fits to these data. However, there appears to be a systematic trend of lower estimated apparent $V_{MAX}$ at higher exposures. Similarly, posterior estimates of cardiac output and the ventilation-perfusion ratio declined (slightly) with higher exposures. These could be related to documented physiological changes (e.g., reduced ventilation rate and body temperature) in mice when exposed to some volatile organics.
	21–26 (open chamber, additional exposures)		Data from three additional exposures for each sex were available for comparison to model predictions. Plasma TCA levels were generally well predicted, though the predictions for female mice data showed some systematic over-prediction, particularly at late times (i.e., data showed shorter apparent half-life). Blood TCE concentrations were consistently overpredicted, sometimes by almost an order of magnitude, except in the case of female mice at 236 ppm, for which predictions were fairly accurate.
Fisher and Allen, 1993	31–36		Predictions for these gavage data were generally fairly accurate. There was a slight tendency to overpredict TCA plasma concentrations, with predictions tending to be worse in the female mice. Blood levels of TCE were adequately predicted, though there was some systematic underprediction at 2–6 h after dosing.
Green and Prout, 1985	40		This datum consists of a single measurement of urinary excretion of TCA at 24 h as a fraction of dose, from TCA i.v. dosing. The model substantially over-predicts the amount excreted. Whereas Green and Prout (1985) measured 35% excreted at 24 h, the model predicts virtually complete excretion at 24 h.



**Table A-1. Evaluation of Hack et al. (2006) PBPK model predictions for *in vivo* data in mice (continued)**

Reference	Simulation #	Calibration data	Discussion
Greenberg et al., 1999	17–18	√	<p>The calibration data included blood TCE, TCOH, and TCA data. Fits to blood TCA and TCOH were adequate, but as with the Fisher et al. (1991) inhalation data, TCE levels were overpredicted (outside the 95% confidence region during and shortly after exposure).</p> <p>As with Abbas and Fisher (1997), there were additional data in the study that was not used in calibration, including blood levels of TCOG and tissue levels of TCE, TCA, TCOH, and TCOG. Tissue levels of TCE were somewhat overpredicted, but generally within the 95% confidence region. TCA levels were adequately predicted, and mostly in or near the interquartile region. TCOH levels were somewhat underpredicted, though within the 95% confidence region. TCOG levels, for which blood served as a surrogate for all tissues, were well predicted in blood and the lung, generally within the interquartile region. However, blood TCOG predictions underpredicted liver and kidney concentrations.</p>
Larson and Bull, 1992b	37–39		<p>Blood TCA predictions were fairly accurate for these data. However, TCE and TCOH blood concentrations were underpredicted by up to an order of magnitude (outside the 95% confidence region). Part of this may be due to uncertain oral dosing parameters. Urinary TCA and TCOG were also generally underpredicted, in some cases outside of the 95% confidence region.</p>
Prout et al., 1985	19	√	Fits to these data were generally adequate—within or near the interquartile region.
	27–30 (urinary excretion at different doses)		<p>These data consisted of mass balance studies of the amount excreted in urine and exhaled unchanged at doses from 10 to 2,000 mg/kg. TCA excretion was consistently overpredicted, except at the highest dose. TCOG excretion was generally well predicted—within the interquartile range. The amount exhaled was somewhat overpredicted, with a 4-fold difference (but still within 95% confidence) at the highest dose.</p>
Templin et al., 1993	20	√	<p>Blood TCA levels from these data were well predicted by the model. Blood TCE and TCOH levels were well predicted using group-specific parameters, but did not appear representative using population-derived parameters. However, this is probably a result of the group-specific oral absorption parameter, which was substantially different than the population mean.</p>

1 The TCE data from inhalation experiments also are not well estimated, particularly blood  
2 levels of TCE. While fractional uptake has been hypothesized, direct evidence for this is  
3 lacking. In addition, physiologic responses to TCE vapors (reduced ventilation rates, lowered  
4 body temperature) are a possibility. These are weakly supported by the closed chamber data, but  
5 the amount of the changes is not sufficient to account for the low blood levels of TCE observed  
6 in the open chamber experiments. It is also not clear what role presystemic elimination due to  
7 local metabolism in the lung may play. It is known that the mouse lung has a high capacity to  
8 metabolize TCE (Green et al., 1997). However, in the Hack et al. (2006) model, lung  
9 metabolism is limited by flow to the tracheobronchial region. An alternative formulation for  
10 lung metabolism in which TCE is available for metabolism directly from inhaled air (similar to  
11 that used for styrene, Sarangapani et al., 2003), may allow for greater presystemic elimination of  
12 TCE, as well as for evaluating the possibility of wash-in/wash-out effects. Furthermore, the  
13 potential impact of other extrahepatic metabolism has not been evaluated. Curiously, predictions  
14 for the tissue concentrations of TCE observed by Greenberg et al. (1999) were not as discrepant  
15 as those for blood. A number of these hypotheses could be tested; however, the existing data  
16 may not be sufficient to distinguish them. The Merdink et al. (1998) study, in which TCE was  
17 given by i.v. (thereby avoiding both first pass in the liver and any fractional uptake issue in the  
18 lung), may be somewhat helpful, but unfortunately only oxidative metabolite concentrations  
19 were reported, not TCE concentrations.

20  
21 **A.2.3.1.2.2. Trichloroacetic acid (TCA) blood concentrations well predicted following**  
22 **trichloroethylene (TCE) exposures, but TCA flux and disposition may not be accurate.** TCA  
23 blood and plasma concentrations following TCE exposure are consistently well predicted.  
24 However, the total flux of TCA may not be correct, as evidenced by the varying degrees of  
25 consistency with urinary excretion data. Of particular importance are TCA dosing studies, none  
26 of which were included in the calibration. In these studies, total recovery of urinary TCA was  
27 found to be substantially less than the administered dose. However, the current model assumes  
28 that urinary excretion is the only source of clearance of TCA, leading to overestimation of  
29 urinary excretion. This fact, combined with the observation that under TCE dosing, the model  
30 appears to give accurate predictions of TCA urinary excretion for several datasets, strongly  
31 suggests a discrepancy in the amount of TCA formed from TCE. That is, since the model  
32 appears to overpredict the fraction of TCA that appears in urine, it may be reducing TCA  
33 production to compensate. Inclusion of the TCA dosing studies (including some oral dosing  
34 studies), along with inclusion of a nonrenal clearance pathway, would probably be helpful in

1 reducing these discrepancies. Finally, improvements in the TCOH/TCOG submodel, below,  
2 should also help to ensure accurate estimates of TCA kinetics.

3  
4 **A.2.3.1.2.3. Trichloroethanol–trichloroethanol-glucuronide conjugate (TCOH/TCOG)**

5 **submodel requires revision and recalibration.** Blood levels of TCOH and TCOG were  
6 inconsistently predicted. Part of this is due to the problems with oral uptake, as discussed above.  
7 In addition, the problems identified with the use of the Abbas and Fisher (1997) data (i.e., free  
8 TCOH vs. total TCOH), mean that this submodel is not likely to be robust.

9 An additional concern is the over-prediction of urinary TCOG from the Abbas et al.  
10 (1997) TCOH i.v. data. Like the case of TCA, this indicates that some other source of TCOH  
11 clearance (not to TCA or urine—e.g., to dichloroacetic acid [DCA] or some other untracked  
12 metabolite) is possible. This pathway can be considered for inclusion, and limits can be placed  
13 on it using the available data.

14 Also, like for TCA, the fact that blood and urine are relatively well predicted from TCE  
15 dosing strongly suggests a discrepancy in the amount of TCOH formed from TCE. That is, since  
16 the model appears to overpredict the fraction of TCOH that appears in urine, it may be reducing  
17 TCOH production to compensate. Including the TCOH dosing data would likely be helpful in  
18 reducing these discrepancies.

19 Finally, as with the rat, the model needs to ensure that any first pass effect is accounted  
20 for appropriately. Importantly, the estimated clearance rate for glucuronidation of TCOH is  
21 substantially greater than hepatic blood flow. As was shown in Okino et al. (2005), in such a  
22 situation, the use of a single compartment model across dose routes will be misleading because it  
23 implies a substantial first-pass effect in the liver that cannot be modeled in a single compartment  
24 model. That is, since TCOH is formed in the liver from TCE, and TCOH is also glucuronidated  
25 in the liver to TCOG, a substantial portion of the TCOH may be glucuronidated before reaching  
26 systemic circulation. This suggests that a liver compartment for TCOH is necessary.  
27 Furthermore, because substantial TCOG can be excreted in bile from the liver prior to systemic  
28 circulation, a liver compartment for TCOG may also be necessary to address that first pass  
29 effect.

30 The addition of the liver compartment will necessitate several changes to model  
31 parameters. The distribution volume for TCOH will be replaced by two parameters: the  
32 liver:blood and body:blood partition coefficients. Similarly for TCOG, liver:blood and  
33 body:blood partition coefficients will need to be added. Clearance of TCOH to TCA and TCOG  
34 can be redefined as occurring in the liver, and urinary clearance can be redefined as coming from  
35 the rest of the body. Fortunately, there are substantial data on circulating TCOG that has not

*This document is a draft for review purposes only and does not constitute Agency policy.*

1 been included in the calibration. These data should be extremely informative in better estimating  
2 the TCOH/TCOG submodel parameters.

3  
4 **A.2.3.1.2.4. *Uncertainty in estimates of total metabolism.*** Closed chamber data are generally  
5 thought to provide a good indicator of total metabolism. Both group-specific and population-  
6 based predictions of the only available closed chamber data (Fisher et al., 1991) were fairly  
7 accurate. Unfortunately, no additional closed chamber data were available. In addition, the  
8 discrepancies in observed and predicted TCE blood concentrations following inhalation  
9 exposures remain unresolved. Hypothesized explanations such as fractional uptake or  
10 pre-systemic elimination could have a substantial impact on estimates of total metabolism.

11 In addition, no data are directly informative as to the fraction of total metabolism in the  
12 lung, the amount of “untracked” hepatic oxidative metabolism (parameterized as “FracDCA”), or  
13 any other extrahepatic metabolism. The lung metabolism as currently modeled could just as well  
14 be located in other extrahepatic tissues, with little change in calibration. In addition, it is  
15 difficult to distinguish between untracked hepatic oxidative metabolism and GSH conjugation,  
16 particularly at low doses.

#### 17 **A.2.3.2. *Rat Model***

18 **A.2.3.2.1. *Group-specific and population-based predictions.*** As with the mouse mode,  
19 initially, the sampled group-specific parameters were used to generate predictions for  
20 comparison to the calibration data. Because these parameters were “optimized” for each group,  
21 these “group-specific” predictions should be accurate by design, and indeed they were, as  
22 discussed in more detail in Table A-2.

23 Next, as with the mouse, only samples of the population parameters (means and  
24 variances) were used, and “new groups” were sampled from appropriate distribution using these  
25 population means and variances. These “new groups” then represent the predicted population  
26 distribution, incorporating both variability in the population as well as uncertainty in the  
27 population means and variances. These “population-based” predictions were then compared to  
28 both the data used in calibration, as well as the additional data identified that was not used in  
29 calibration. The Hack et al. (2006) PBPK model used for prediction was modified to  
30 accommodate some of the different outputs (e.g., tissue concentrations) and exposure routes (i.v.,  
31 intra-arterial [i.a.], and intraperivenous [p.v.]) used in the “noncalibration” data, but otherwise  
32 unchanged.

**Table A-2. Evaluation of Hack et al. (2006) PBPK model predictions for *in vivo* data in rats**

Reference	Simulation #	Calibration data	Discussion
Andersen et al., 1987	7–11	√	Good posterior fits were obtained for these data—closed chamber data with initial concentrations from 100 to 4,640 ppm.
Barton et al., 1995	17–20		It was assumed that the closed chamber volume was the same as for Andersen et al. (1987). However, the initial chamber concentrations are not clear in the paper. The values that were used in the simulations do not appear to be correct, since in many cases the time-course is inaccurately predicted even at the earliest time-points. Conclusions as to these data need to await definitive values for the initial chamber concentrations, which were not available.
Bernauer et al., 1996	1–3	√	<p>Urinary time-course data (Fig 6-7) for TCA, TCOG, and NAcDCVC was given in concentration units (mg/mg creat-h), whereas total excretion at 48 h (Table 2) was given in molar units (mmol excreted). In the original calibration files, the conversion from concentration to cumulative excretion was not consistent—i.e., the amount excreted at 48 h was different. The data were revised using a conversion that forced consistency. One concern, however, is that this conversion amounts to 6.2 mg creatinine over 48 h, or 1.14 micromol/h. This seems very low for rats; Trevisan et al. (2001), in samples from 195 male control rats, found a median value of 4.95 micromol/h, a mean of 5.39 micromol/h, and a 1–99 percentile range of 2.56–10.46 micromol/h.</p> <p>In addition, the NAcDCVC data were revised to include both 1,2- and 2,2-isomers, since the goal of the GSH pathway is primarily to constrain the total flux. Furthermore, because of the extensive interorgan processing of GSH conjugates, and the fact that excretion was still ongoing at the end of the study (48 h), the amount of NAcDCVC recovered can only be a lower bound on the amount ultimately excreted in urine. However, the model does not attempt to represent the excretion time-course of GSH conjugates—it merely models the total flux. This is evinced by the fact that the model predicts complete excretion by the first time point of 12 h, whereas in the data, there is still substantial excretion occurring at 48 h.</p> <p>Posterior fits to these data were poor in all cases except urinary TCA at the highest dose. In all other cases, TCOH/TCOG and TCA excretion was substantially overpredicted, though this is due to the revision of the data (i.e., the different assumptions about creatinine excretion). Unfortunately, of the original calibration data, this is the only one with TCA and TCOH/TCOG urinary excretion. Therefore, that part of the model is poorly calibrated. On the other hand, NAcDCVC was underpredicted for a number of reasons, as noted above.</p> <p>Because of the incomplete capture of NAcDCVC in urine, unless the model can accurately portray the time-course of NAcDCVC in urine, it should probably not be used for calibration of the GSH pathway, except perhaps as a lower bound.</p>

Table A-2. Evaluation of Hack et al. (2006) PBPK model predictions for *in vivo* data in rats (continued)

Reference	Simulation #	Calibration data	Discussion
Birner et al., 1993	21–22		These data only showed urine concentrations, so a conversion was made to cumulative excretion based on an assumed urine flow rate of 22.5 mL/d. Based on this, urinary NAcDCVC was underestimated by 100- to 1,000-fold. Urinary TCA was underestimated by about 2-fold in females (barely within the 95% confidence interval), and was accurately estimated in males. Note that data on urinary flow rate from Trevisan et al. (2001) in samples from 195 male control rats showed high variability, with a geometric standard deviation of 1.75, so this may explain the discrepancy in urinary TCA. However, the underestimation of urinary NAcDCVC cannot be explained this way.
Dallas et al., 1991	23–24		At the lower (50 ppm) exposure, arterial blood concentrations were consistently overpredicted by about 2.5-fold, while at the higher (500 ppm) exposure, arterial blood was overpredicted by 1.5- to 2-fold, but within the range of variability. Exhaled breath concentrations were in the middle of the predicted range of variability at both exposure levels. The ratio of exhaled breath and arterial blood should depend largely on the blood-air partition coefficient, with minor dependence on the assumed dead space. This suggests the possibility of some unaccounted-for variability in the partition coefficient (e.g., posterior mean estimated to be 15.7; <i>in vitro</i> measured values from the literature are as follows: 25.82 [Sato et al., 1977], 21.9 [Gargas et al., 1989], 25.8 [Koizumi, 1989], 13.2 [Fisher et al., 1989], posterior). Alternatively, there may be a systematic error in these data, since, as discussed below, the fit of the model to the arterial blood data of Keys et al. (2003) was highly accurate.
Fisher et al., 1989	25–28		Good posterior fits were obtained for these data (in females)—closed chamber data with initial concentrations from 300 to 5,100 ppm. There was some slight overprediction of chamber concentrations (i.e., data showed more uptake/metabolism) at the lower doses, but still within the 95% confidence interval.
Fisher et al., 1991	4–6	√	Good posterior fits were obtained from these data—plasma levels of TCA and venous blood levels of TCE.
Green and Prout, 1985	29–30		In naive rats at 500 mg/kg, urinary excretion of TCOH/TCOG and TCA at 24 h was underpredicted (2-fold), although within the 95% confidence interval. With bile-cannulated rats at the same dose, the amount of TCOG in bile was well within the 95% confidence interval. Urinary TCOH/TCOG was still underpredicted by about 2-fold, but again still within the 95% confidence interval.
Jakobson et al., 1986	31		The only data from the experiment (500 ppm in female rats) were venous blood concentrations during exposure. There were somewhat overpredicted at early times (outside of 95% confidence interval for first 30 min) but was well predicted at the termination of exposure. This suggests some discrepancies in uptake to tissues that reach equilibrium quickly—the model approaches the peak concentration at a faster rate than the data suggest.

**Table A-2. Evaluation of Hack et al. (2006) PBPK model predictions for *in vivo* data in rats (continued)**

Reference	Simulation #	Calibration data	Discussion
Kaneko et al., 1994	32–35		<p>In these inhalation experiments (50–1,000 ppm), urinary excretion of TCOH/TCOG and TCA are consistently overpredicted, particularly at lower doses. The discrepancy decreases systematically as dose increases, with TCA excretion accurately predicted at 1,000 ppm (TCOH/TCOG excretion slightly below near the lower 95% confidence interval at this dose). This suggests a discrepancy in the dose-dependence of TCOH, TCOG, and TCA formation and excretion.</p> <p>On the other hand, venous blood TCE concentrations postexposure are well predicted. TCE blood concentrations right at the end of the exposure are overpredicted; however, concentrations are rapidly declining at this point, so even a few minutes delay in obtaining the blood sample could explain the discrepancy.</p>
Keys et al., 2003	36–39		<p>These experiments collected extensive data on TCE in blood and tissues following i.a., oral, and inhalation exposures. For the i.a. exposure, blood and tissue concentrations were very well predicted by the model, even with the use of the rapidly perfused tissue concentration as a surrogate for brain, heart, kidney, liver, lung, and spleen concentrations. Similarly accurate predictions were found with the higher (500 ppm) inhalation exposure. At the lower inhalation exposure (50 ppm), there was some minor overprediction of concentrations (2-fold), particularly in fat, but values were still within the 95% confidence intervals.</p> <p>For oral exposure, the GI absorption parameters needed to be revised substantially to obtain a good fit. When the values reported by Keys et al. (2003) were used, the model generally had accurate predictions. Two exceptions were the values in the gut and fat in the first 30 min after exposure. In addition, the liver concentration was over-predicted in the first 30 min, and under-predicted at 2–4 h, but still within the 95% confidence interval during the entire period.</p>
Kimmerle and Eben, 1973a	40–44		<p>In these inhalation experiments (49 to 3,160 ppm), urinary excretion of TCOH/TCOG was systematically overpredicted (&gt;2-fold; outside 95% confidence interval), while excretion of TCA was accurately predicted. In addition, elimination by exhaled breath was substantially overpredicted at the lowest exposure. Blood TCOH levels were accurately predicted, but blood TCE levels were overpredicted at the 55 ppm. Part of the discrepancies may be due to limited analytic sensitivities at the lower exposures.</p>
Larson and Bull, 1992b	12–14	√	<p>The digitization in the calibration file did not appear to be accurate, as there was a 10-fold discrepancy with the original paper in the TCOH data. The data were replaced with those used by Clewell et al. (2000) and Bois (2000b). Except for the TCOH data, differences between the digitizations were 20% or less. Adequate posterior predictions were obtained for these data (oral dosing from 200 mg/kg to 3,000 mg/kg). All predictions were within the 95% confidence interval of posterior predictions. Better fits were obtained using group-specific posterior parameters, for which gut absorption and TCA urinary excretion parameters were more highly identified.</p>

**Table A-2. Evaluation of Hack et al. (2006) PBPK model predictions for *in vivo* data in rats (continued)**

Reference	Simulation #	Calibration data	Discussion
Lash et al., 2006	45–46		In these corn-oil gavage experiments, almost all of the measurements appeared to be systematically low, sometimes by many orders of magnitude. For example, at the lowest dose (263 mg/kg), urinary excretion of TCOH/TCOG and TCA, and blood concentrations of TCOH were overpredicted by the model by around $>10^5$ -fold. TCE concentrations in blood and tissues at 2, 4, and 8 h were underpredicted by $10^3$ - to $10^4$ -fold. Many studies, including those using the corn oil gavage (Green and Prout, 1985; Hissink et al., 2002), with similar ranges of oral doses show good agreement with the model, it seems likely that these data are aberrant.
Lee et al., 1996	47–61		<p>This extensive set of experiments involved multiroute administration of TCE (oral, i.v., i.a., or portal vein), with serial measurements of arterial blood concentrations. For the oral route (8 mg/kg–64 mg/kg), the GI absorption parameters had to be modified. The values from Keys et al. (2003) were used, and the resulting predictions were quite accurate, albeit a more prominent peak was predicted. Predictions <math>&gt;30</math> min after dosing were highly accurate.</p> <p>For the i.v. route (0.71 mg/kg–64 mg/kg), predictions were also highly accurate in almost all cases. At the lower doses (0.71 mg/kg and 2 mg/kg), there was slight overprediction in the first 30 min after dosing. At highest dose (64 mg/kg), there was slight underprediction between 1 and 2 h after dosing. In all cases, the values were within the 95% confidence interval.</p> <p>For the i.a. route (0.71 mg/kg–16 mg/kg), all predictions were very accurate.</p> <p>For the p.v. route (0.71 mg/kg–64 mg/kg), predictions still remained in the 95% confidence interval, although there was more variation. At the lowest dose, there was overprediction in the first 30 min after dosing. At the highest two doses (16 mg/kg and 64 mg/kg), there was slight underprediction between 1 and 5 h after dosing. This may in part be because a pharmacodynamic change in metabolism (e.g., via direct solvent injury proposed by Lee et al., 2000).</p>
Lee et al., 2000	62–69		In the p.v. and i.v. exposures, blood and liver concentrations were accurately predicted. For oral exposures, the GI absorption parameters needed to be changed. While the values from Keys et al. (2003) led to accurate predictions for lower doses (2 mg/kg–16 mg/kg), at the higher doses (48 mg/kg–432 mg/kg), much slower absorption was evident. Comparisons at these higher dose are not meaningful without calibration of absorption parameters.
Prout et al., 1985	15	√	Adequate posterior fits were obtained for these data—rat dosing at 1,000 mg/kg in corn oil. All predictions were within the 95% confidence interval of posterior predictions. Better fits were obtained using group-specific posterior parameters, for which gut absorption and TCA urinary excretion parameters were more highly identified.



**Table A-2. Evaluation of Hack et al. (2006) PBPK model predictions for *in vivo* data in rats (continued)**

Reference	Simulation #	Calibration data	Discussion
Stenner et al., 1997	70		<p>As with other oral exposures, different GI absorption parameters were necessary. Again, the values from Keys et al. (2003) were used, with some success. Blood TCA levels were accurately predicted, while TCOH blood levels were systematically under-predicted (up to 10-fold).</p> <p>Additional data with TCOH and TCA dosing, including naive and bile-cannulated rats, can be added when those exposure routes are added to the model. These could be useful in better calibrating the enterohepatic recirculation parameters.</p>
Templin et al., 1995	16	√	<p>Adequate posterior fits were obtained for blood TCA from these data—oral dosing at 100 mg/kg in Tween. Blood levels of TCOH were underpredicted, while the time-course of TCE in blood exhibited an earlier peak. Better fits were obtained using group-specific posterior parameters, for which gut absorption and TCA urinary excretion parameters (and to a lesser extent glucuronidation of TCOH and biliary excretion of TCOG) were more highly identified.</p>

GI = gastrointestinal, NAc-1,2-DCVC = N-acetyl-S-(1,2-dichlorovinyl)-L-cysteine, NAc-2,2-DCVC = N-acetyl-S-(2,2-dichlorovinyl)-L-cysteine, NAcDCVC = NAc-1,2-DCVC and NAc-2,2-DCVC.

1 **A.2.3.2.1.1. Group-specific predictions and calibration data.** [See  
2 [Appendix.linked.files\AppA.2.3.2.1.1.Hack.rat.group.calib.TCE.DRAFT.pdf.](#)]

3  
4 **A.2.3.2.1.2. Population-based predictions and calibration and additional evaluation data.**  
5 [See [Appendix.linked.files\AppA.2.3.2.1.2.Hack.rat.pop.calib.eval.TCE.DRAFT.pdf.](#)]

6  
7 **A.2.3.2.2. Conclusions regarding rat model.**

8 **A.2.3.2.2.1. Trichloroethylene (TCE) concentrations in blood and tissues generally well-**  
9 **predicted.** The PBPK model for the parent compound appears to be robust. Multiple datasets  
10 not used for calibration with TCE measurements in blood and tissues were simulated, and overall  
11 the model gave very accurate predictions. A few datasets seemed somewhat anomalous—Dallas  
12 et al. (1991), Kimmerle and Eben (1973a), Lash et al. (2006). However, data from Kaneko et al.  
13 (1994), Keys et al. (2003), and Lee et al. (1996, 2000) were all well simulated, and corroborated  
14 the data used for calibration (Fisher et al., 1991; Larson and Bull, 1992b; Prout et al., 1985;  
15 Templin et al., 1995). Particularly important is the fact that tissue concentrations from  
16 Keys et al. (2003) were well simulated.

17  
18 **A.2.3.2.2.2. Total metabolism probably well simulated, but ultimate disposition is less certain.**  
19 Closed chamber data are generally thought to provide a good indicator of total metabolism. Two  
20 closed chamber studies not used for calibration were available—Barton et al. (1995) and Fisher  
21 et al. (1989). Additional experimental information is required to analyze the Barton et al. (1995)  
22 data, but the predictions for the Fisher et al. (1989) data were quite accurate.

23 However, the ultimate disposition of metabolized TCE is much less certain. Clearly, the  
24 flux through the GSH pathway is not well constrained, with apparent discrepancies between the  
25 N-acetyl-S-(1,2-dichlorovinyl)-L-cysteine (NAc-1,2-DCVC) data of Bernauer et al. (1996) and  
26 Birner et al. (1993). Moreover, each of these data has limitations—in particular, the Bernauer et  
27 al. (1996) data show that excretion is still substantial at the end of the reporting period, so that  
28 the total flux of mercapturates has not been collected. Moreover, there is some question as to the  
29 consistency of the Bernauer et al. (1996) data (Table 2 vs. Figures 6 and 7), since a direct  
30 comparison seems to imply a very low creatinine excretion rate. The Birner et al. (1993) data  
31 only report concentrations—not total excretion—so a urinary flow rate needs to be assumed.

32 In addition, no data are directly informative as to the fraction of total metabolism in the  
33 lung or the amount of “untracked” hepatic oxidative metabolism (parameterized as “FracDCA”).  
34 The lung metabolism could just as well be located in other extrahepatic tissues, with little change

1 in calibration. In addition, there is a degeneracy between untracked hepatic oxidative  
2 metabolism and GSH conjugation, particularly at low doses.

3 The ultimate disposition of TCE as excreted TCOH/TCOG or TCA is also poorly  
4 estimated in some cases, as discussed in more detail below.

5  
6 **A.2.3.2.2.3. Trichloroethanol–trichlorethanol-glucuronide conjugate (TCOH/TCOG)**  
7 **submodel requires revision and recalibration.** TCOH blood levels of TCOH were  
8 inconsistently predicted in noncalibration datasets (well predicted for Larson and Bull [1992b];  
9 Kimmerle and Eben [1973a]; but not Stenner et al. [1997] or Lash et al. [2006]), and the amount  
10 of TCE ultimately excreted as TCOG/TCOH also appeared to be poorly predicted. The model  
11 generally underpredicted TCOG/TCOH urinary excretion (underpredicted Green and Prout  
12 [1985], overpredicted Kaneko et al. [1994], Kimmerle and Eben [1973a], and Lash et al. [2006]).  
13 This may in part be due to discrepancies in the Bernauer et al. (1996) data as to the conversion of  
14 excretion relative to creatinine.

15 Moreover, there are relatively sparse data on TCOH in combination with a relatively  
16 complex model, so the identifiability of various pathways—conversion to TCA, enterohepatic  
17 recirculation, and excretion in urine—is questionable.

18 This could be improved by the ability to incorporate TCOH dosing data from Merdink et  
19 al. (1999) and Stenner et al. (1997), the latter of which included bile duct cannulation to better  
20 estimate enterohepatic recirculation parameters. However, the TCOH dosing in these studies is  
21 by the intravenous route, whereas with TCE dosing, TCOH first appears in the liver. Thus, the  
22 model needs to ensure that any first pass effect is accounted for appropriately. Importantly, the  
23 estimated clearance rate for glucuronidation of TCOH is substantially greater than hepatic blood  
24 flow. That is, since TCOH is formed in the liver from TCE, and TCOH is also glucuronidated in  
25 the liver to TCOG, a substantial portion of the TCOH may be glucuronidated before reaching  
26 systemic circulation. Thus, suggests that a liver compartment for TCOH is necessary.  
27 Furthermore, because substantial TCOG can be excreted in bile from the liver prior to systemic  
28 circulation, a liver compartment for TCOG may also be necessary to address that first pass  
29 effect.

30 The addition of the liver compartment will necessitate several changes to model  
31 parameters. The distribution volume for TCOH will be replaced by two parameters: the  
32 liver:blood and body:blood partition coefficients. Similarly for TCOG, liver:blood and  
33 body:blood partition coefficients will need to be added. Clearance of TCOH to TCA and TCOG  
34 can be redefined as occurring in the liver, and urinary clearance can be redefined as coming from  
35 the rest of the body.

*This document is a draft for review purposes only and does not constitute Agency policy.*

1 Finally, additional clearance of TCOH (not to TCA or urine—e.g., to DCA or some other  
2 untracked metabolite) is possible. This may in part explain the discrepancy between the accurate  
3 predictions to blood data along with poor predictions to urinary excretion (i.e., there is a missing  
4 pathway). This pathway can be considered for inclusion, and limits can be placed on it using the  
5 available data.

6  
7 **A.2.3.2.2.4. Trichloroacetic acid (TCA) submodel would benefit from revised**  
8 **trichloroethanol/trichloroethanol-glucuronide conjugate (TCOH/TCOG) submodel and**  
9 **incorporating TCA dosing studies.** While blood levels of TCA were well predicted in the one  
10 noncalibration dataset (Stenner et al., 1997), the urinary excretion of TCA was inconsistently  
11 predicted (underpredicted in Green and Prout [1985]; overpredicted in Kaneko et al. [1994] and  
12 Lash et al. [2006]; accurately predicted in Kimmerle and Eben [1973a]). Because TCA is in part  
13 derived from TCOH, a more accurate TCOH/TCOG submodel would probably improve the TCA  
14 submodel.

15 In addition, there are a number of TCA dosing studies that could be used to isolate the  
16 TCA kinetics from the complexities of TCE and TCOH. These could be readily incorporated  
17 into the TCA submodel.

18 Finally, as with TCOH, additional clearance of TCA (not to urine—e.g., to DCA or some  
19 other untracked metabolite) is possible. This may in part explain the discrepancy between the  
20 accurate predictions to blood data along with poor predictions to urinary excretion (i.e., there is a  
21 missing pathway). As with TCOH, this pathway can be considered for inclusion, and limits can  
22 be placed on it using the available data.

### 23 24 **A.2.3.3. Human model.**

25 **A.2.3.3.1. Individual-specific and population-based predictions.** As with the mouse and rat  
26 models, initially, the sampled individual-specific parameters (the term “individual” instead of  
27 “group” is used since human variability was at the individual level) were used to generate  
28 predictions for comparison to the calibration data. Because these parameters were “optimized”  
29 for each individual, these “individual-specific” predictions should be accurate by design.  
30 However, unlike for the rat, this was not the case for some experiments (this is partially  
31 responsible for the slower convergence), although the inaccuracies were generally less than those  
32 in the mouse. For example, alveolar air concentrations were systematically overpredicted for  
33 several datasets. There was also variability in the ability to predict the precise time-course of  
34 TCA and TCOH blood levels, with a few datasets more difficult for the model to accommodate.  
35 These data are discussed further in Table A-3.

Table A-3. Evaluation of Hack et al. (2006) PBPK model predictions for *in vivo* data in humans

Reference	Simulation #	Calibration data	Discussion
Bartonicek, 1962	38–45		<p>The measured minute-volume was multiplied by a factor of 0.7 to obtain an estimate for alveolar ventilation rate, which was fixed for each individual. These data are difficult to interpret because they consist of many single data points. It is easiest to go through the measurements one at a time:</p> <p><i>Alveolar retention</i> (1—exhaled dose/inhaled dose during exposure) and <i>Retained dose</i> (inhaled dose—exhaled dose during exposure): Curiously, retention was generally under-predicted, which in many cases retained dose was accurately predicted. However, alveolar retention was an adjustment of the observed total retention:</p> $\text{TotRet} = (\text{CInh} - \text{CExh})/\text{CInh} = \text{QAlv} \times (\text{CInh} - \text{CAlv})/(\text{MV} \times \text{CInh}), \text{ so that}$ $\text{AlvRet} = \text{TotRet} \times (\text{QAlv}/\text{MV}), \text{ with QAlv/MV assumed to be 0.7}$ <p>Because retained dose is the more relevant quantity, and is less sensitive to assumptions about QAlv/MV, then this is the better quantity to use for calibration.</p> <p><i>Urinary TCOG</i>: This was generally underpredicted, although generally within the 95% confidence interval. Thus, these data will be informative as to interindividual variability.</p> <p><i>Urinary TCA</i>: Total collection (at 528 h) was accurately predicted, although the amount collected at 72 h was generally under-predicted, sometimes substantially so.</p> <p><i>Plasma TCA</i>: Generally well predicted.</p>
Bernauer et al., 1996	1–3	√	<p>Individual-specific predictions were good for the time-courses of urinary TCOG and TCA, but poor for total urinary TCOG+TCA and for urinary NAc-1,2-DCVC. One reason for the discrepancy in urinary excretion of TCA and TCOG is that the urinary time-course data (see Figures 4-5 in the manuscript) for TCA, TCOG, and NAc-1,2-DCVC was given in concentration units (mg/mg creat-h), whereas total excretion at 48 h (Table 2 in the manuscript) was given in molar units (mmol excreted). In the original calibration files, the conversion from concentration to cumulative excretion was not consistent—i.e., the amount excreted at 48 h was different. For population-based predictions, the data were revised using a conversion that forced consistency. One concern, however, is that this conversion amounts to 400–500 mg creatinine over 48 h, or 200–250 mg/d, which seems rather low. For instance, Araki (1978) reported creatinine excretion of 11.5+/-1.8 mmol/24 h (mean +/- SD) in 9 individuals, corresponding to 1,300 +/- 200 mg/d.</p> <p>In addition, for population-based predictions, the data were revised include both the NAc-1,2-DCVC and the N acetyl-S-(2,2-dichlorovinyl)-L-cysteine isomer (the combination denoted NAcDCVC), since the goal of the GSH pathway is primarily to constrain the total flux. Furthermore, because of the extensive interorgan processing of GSH conjugates, and the fact that excretion was still ongoing at the end of the study (48 h), the amount of NAcDCVC recovered can only be a lower bound on the amount ultimately excreted in urine. However, the model does not attempt to represent the excretion time-course of GSH conjugates—it merely models the total flux. This is evinced by the fact that the model predicts complete excretion by the first time point of 12 h, whereas in the data, there is still substantial excretion occurring at 48 h.</p>

**Table A-3. Evaluation of Hack et al. (2006) PBPK model predictions for *in vivo* data in humans (continued)**

Reference	Simulation #	Calibration data	Discussion
Bernauer et al., 1996 (continued)	1–3 (continued)		Population-based posterior fits to these data were quite good for urinary TCA and TCOH, but not for NAcDCVC in urine. Because of the incomplete capture of NAcDCVC in urine, unless the model can accurately portray the time-course of NAcDCVC in urine, it should probably not be used for calibration of the GSH pathway, except perhaps as a lower bound.
Bloemen et al., 2001	72–75		Like Bartonicek (1962), these data are more difficult to interpret due to their being single data points for each individual and exposure. However, in general, posterior population-based estimates of retained dose, urinary TCOG, and urinary TCA were fairly accurate, staying within the 95% confidence interval, and mostly inside the interquartile range. The data on GSH mercapturates are limited—first they are all nondetects. In addition, because of the 48–56 h collection period, excretion of GSH mercapturates is probably incomplete, as noted above in the discussion of Bernauer et al. (1996).
Chiu et al., 2007	66–71		<p>The measured minute-volume was multiplied by a factor of 0.7 to obtain an estimate for alveolar ventilation rate, which was fixed for each individual. Alveolar air concentrations of TCE were generally well predicted, especially during the exposure period. Postexposure, the initial drop in TCE concentration was generally further than predicted, but the slope of the terminal phase was similar. Blood concentrations of TCE were consistently overpredicted for all subjects and occasions.</p> <p>Blood concentrations of TCA were consistently over-predicted, though mostly staying in the lower 95% confidence region. Blood TCOH (free) levels were generally over-predicted, in many cases falling below the 95% confidence region, though in some cases the predictions were accurate. On the other hand, total TCOH (free+glucuronidated) was well predicted (or even under-predicted) in most cases—in the cases where free TCOH was accurately predicted, total TCOH was underpredicted. The free and total TCOH data reflect the higher fraction of TCOH as TCOG than previously reported (e.g., Fisher et al. [1998] reported no detectable TCOG in blood).</p> <p>Data on urinary TCA and TCOG were complicated by some measurements being saturated, as well as the intermittent nature of urine collection after Day 3. Thus, only the nonsaturated measurements for which the time since the last voiding was known were included for direct comparison to the model predictions. Saturated measurements were kept track of separately for comparison, but were considered only rough lower bounds. TCA excretion was generally over-predicted, whether looking at unsaturated or saturated measurements (the latter, would of course, be expected). Urinary excretion of TCOG generally stayed within the 95% confidence range.</p>
Fernandez et al., 1977			Alveolar air concentrations are somewhat overestimated. Other measurements are fairly well predicted.

**Table A-3. Evaluation of Hack et al. (2006) PBPK model predictions for *in vivo* data in humans (continued)**

Reference	Simulation #	Calibration data	Discussion
Fisher et al., 1998	13–33	√	<p>The majority of the data used in the calibration (both in terms of experiments and data points) came from this study. In general, the individual-specific fits to these data were good, with the exception of alveolar air concentrations, which were consistently over-predicted. In addition, for some individuals, the shape of the TCOH time-course deviated from the predictions (#14, #24, #29, and #30)—the predicted peak was too “sharp,” with underprediction at early times. Simulation #23 showed the most deviation from predictions, with substantial inaccuracies in blood TCA, TCOH, and urinary TCA.</p> <p>Interestingly, in the population-based predictions, in some cases the predictions were not very accurate—indicating that the full range of population variability is not accounted for in the posterior simulations. This is particularly the case with venous blood TCE concentrations, which are generally under-predicted in population estimates (although in some cases the predictions are accurate).</p> <p>One issue with the way in which these data were utilized in the calibration is that in some cases, the same individual was exposed to two different concentrations, but in the calibration, they were treated as separate “individuals.” Thus, parameters were allowed to vary between exposures, mixing interindividual and interoccasion variability. It is recommended that in subsequent calibrations, the different occasions with the same individual be modeled together. This will also allow identification of any dose-related changes in parameters (e.g., saturation).</p>
Kimmerle and Eben, 1973b	46–57		<p>Blood TCE levels are generally over-predicted for both single and multiexposure experiments. However, levels at the end of exposure are rapidly changing, so some of those values may be better predicted if the “exact” time after cessation of exposure were known.</p> <p>Blood TCOH levels are fairly accurately predicted, although in some individuals in single exposure experiments, there is a tendency to overpredict at early times and underpredict at late times. In multiexposure experiments, the decline after the last exposure was somewhat steeper than predicted. Urinary excretion of TCA and TCOH was well predicted.</p> <p>Only grouped data on alveolar air concentrations were available, so they were not used.</p>
Laparé et al., 1995	34	√	<p>Predictions for these data were not accurate. However, there was an error in some of the exposure concentrations used in the original calibration. In addition, the last exposure “occasion” in these experiments involved exercise/workload, and so should be excluded. Finally, individual data are available for these experiments.</p>
	62–65 (individual data)		<p>Taking into account these changes, population-based predictions were somewhat more accurate. However, alveolar air concentrations and venous blood TCE concentrations were still over-predicted.</p>

**Table A-3. Evaluation of Hack et al. (2006) PBPK model predictions for *in vivo* data in humans (continued)**

Reference	Simulation #	Calibration data	Discussion
Monster et al., 1976	5–6 (summary data)	√	<p>Individual-specific predictions were quite good, except that for blood TCA concentrations exhibited a higher peak than predicted. However, TCOH values were entered as free TCOH, whereas the TCOH data were actually total (free+glucuronidated) TCOH. Therefore, for population-based predictions, this change was made. In addition, as with the Monster et al. (1979) data, minute-volume and exhaled air concentrations were measured and incorporated for population-based predictions. Finally, individual-specific data are available, so in those data should replace the grouped data in any revised calibration. These individual data also included estimates of retained dose based on complete inhaled and exhaled air samples during exposure.</p> <p>For population-based predictions, as with the Monster et al. (1979) data, grouped urinary and blood TCOH/TCOG was somewhat under-predicted in the population-based predictions, and grouped alveolar and blood TCE concentrations were somewhat over-predicted.</p>
	58–61 (individual data)		<p>The results for the individual data were similar, but exhibited substantially greater variability than predicted. For instance, in subject A, blood TCOH levels were generally greater than the 95% confidence interval at both 70 and 140 ppm, whereas predictions for blood TCOH in subject D were quite good. In another example, for blood TCE levels, predictions for subject B were quite good, but those for subject D were poor (substantially over-predicted). Thus, it is anticipated that adding these individual data will be substantially informative as to interindividual variability, especially since all 4 individuals were exposed at 2 different doses.</p>
Monster et al., 1979	4	√	<p>Individual-specific predictions for these data were quite good. However, TCA values were entered as plasma, whereas the TCA data were actually in whole blood. Therefore, for population-based predictions, this change was made. In addition, two additional time-courses were available that were not used in calibration: exhaled air concentrations and total TCOH blood concentrations. These were added for population-based predictions.</p> <p>In addition, the original article had data on ventilation rate, which was incorporated into the model. The minute volume needed to be converted to alveolar ventilation rate for the model, but this required adjustment for an extra dead space volume of 0.15 L due to use of a mask, as suggested in the article. The measured mean minute volume was 11 L/min, and with a breathing rate of 14 breaths/min (assumed in the article), this corresponding to a total volume of 0.79 L. Subtracting the 0.15 L of mask dead space and 0.15 L of physiological dead space (suggested in the article) gives 0.49 L of total physiological dead space. Thus, the minute volume of 11 L/min was adjusted by the factor 0.49/0.79 to give an alveolar ventilation rate of 6.8 L/min, which is a reasonably typical value at rest.</p> <p>Due to extra nonphysiological dead space issue, some adjustment to the exhaled air predictions also needed to be made. The alveolar air concentration <math>CA_{lv}</math> was, therefore, estimated based on the formula</p>



**Table A-3. Evaluation of Hack et al. (2006) PBPK model predictions for *in vivo* data in humans (continued)**

Reference	Simulation #	Calibration data	Discussion
Monster et al., 1979 (continued)	4 (continued)		$CA_{lv} = (CE_{exh} \times VT_{tot} - C_{inh} \times VD_s) / VA_{lv}$ where $CE_{exh}$ is the measured exhaled air concentration, $VT_{tot}$ is the total volume (alveolar space $VA_{lv}$ of 0.49 L, physiological dead space of 0.15 L, and mask dead space of 0.15 L), $VD_s$ is the total dead space of 0.3 L, and $C_{inh}$ is the inhaled concentration. Population-based predictions for these data lead to slight underestimation urinary TCOG and blood TCOH levels, as well as some over-prediction of alveolar air and venous blood concentrations by factors of 3~10-fold.
Muller et al., 1972, 1974, 1975	7-10	√	Individual-specific predictions for these data were good, except for alveolar air concentrations. However, several problems were found with these data as utilized in the original calibration: <ul style="list-style-type: none"> <li>• Digitization problems, particular with the time axis in the multiday exposure study (Simulation 9) that led to measurements taken prior to an exposure modeled as occurring during the exposure. The original digitization from Bois (2000b) and Clewell et al. (2000) was used for population-based estimates.</li> <li>• Original article showed TCA as measured in plasma, not blood as was assumed in the calibration.</li> <li>• Blood was taken from the earlobe, which is thought to be indicative of arterial blood concentrations, rather than venous blood concentrations.</li> <li>• TCOH in blood was free, not total, as Ertle et al. (1972 [cited in Methods]) had no use of beta-glucuronidase in analyzing blood samples. Separate free and total measurements were done in plasma (not whole blood), but these data were not included.</li> <li>• Simulation 9, contiguous data on urinary excretion were only available out to 6 d, so only that data should be included.</li> <li>• Simulation 10, is actually the same as the first day of simulation 9, from Muller et al. (1972, 1975) (the data were reported in both papers), and, thus, should be deleted.</li> </ul> These were corrected in the population-based estimates. Alveolar air concentration measurements remained over-predicted, while the change to arterial blood led to over-prediction of those measurements during exposure (but postexposure predictions were accurate).

**Table A-3. Evaluation of Hack et al. (2006) PBPK model predictions for *in vivo* data in humans (continued)**

Reference	Simulation #	Calibration data	Discussion
Muller et al., 1974	81–82 (TCA and TCOH dosing)		The experiment with TCA showed somewhat more rapid decline in plasma levels than predicted, but still well within the 95% confidence range. Urinary excretion was well predicted, but only accounted for 60% of the administered dose—this is not consistent with the rapid decline in TCA plasma levels (10-fold lower than peak at the end of exposure), which would seem to suggest the majority of TCA has been eliminated. With TCOH dosing, blood levels of TCOH were over-predicted in the first 5 hours, perhaps due to slower oral absorption (the augmented model used instantaneous and complete absorption). TCA plasma and urinary excretion levels were fairly well predicted. However, urinary excretion of TCOG was near the bottom of the 95% confidence interval; while, in the same individuals with TCE dosing (Simulation 7), urinary excretion of TCOG was substantially greater (near slightly above the interquartile region). Furthermore, total TCA and TCOG urinary excretion accounted for <40% of the administered dose.
Paycok and Powell, 1945	35–37		Population-based fits were good, within the inner quartile region.
Sato et al., 1977	76		Both alveolar air and blood concentrations are over-predicted in this model. Urinary TCA and TCOG, on the other hand, are well predicted.
Stewart et al., 1970	11	√	<p>Individual-specific predictions for these data were good, except for some alveolar air concentrations. However, a couple of problems were found with these data as utilized in the original calibration:</p> <ul style="list-style-type: none"> <li>• The original article noted that individual took a lunch break during which there was no exposure. This was not accounted for in the calibration runs, which assumed a continuous 7-h exposure. The exposures were, therefore, revised with a 3-h morning exposure (9–12), a 1 hour lunch break (12–1), and 4-h afternoon exposure (1–5), to mimic a typical workday. The times of the measurements had to be revised as well, since the article gave “relative” rather than “absolute” times (e.g., x hours postexposure).</li> <li>• Contiguous data on urinary excretion were only available out to 11 d, so only that data should be included (Table 2).</li> </ul> <p>With these changes, population-based predictions of urinary TCA and TCOG were still accurate, but alveolar air concentrations were over-predicted.</p>
Triebig et al., 1976	12	√	Only two data points are available for alveolar air, and blood TCA and TCOH. Only one data point is available on blood TCE. Alveolar air was underpredicted at 24 h. Blood TCA and TCOH were within the 95% confidence ranges. Blood TCE was over-predicted substantially (outside 95% confidence range).

SD = standard deviation.

1 Next, only samples of the population parameters (means and variances) were used, and  
2 “new individuals” were sampled from appropriate distribution using these population means and  
3 variances. These “new individuals” then represent the predicted population distribution,  
4 incorporating both variability as well as uncertainty in the population means and variances.  
5 These “population-based” predictions were then compared to both the data used in calibration, as  
6 well as the additional data identified that was not used in calibration. The Hack et al. (2006)  
7 PBPK model was modified to accommodate some of the different outputs (e.g., arterial blood,  
8 intermittently collected urine, retained dose) and exposure routes (TCA i.v., oral TCA, and  
9 TCOH) used in the “noncalibration” data, but otherwise unchanged.

10  
11 **A.2.3.3.1.1. Individual-specific predictions and calibration data.** [See  
12 [Appendix.linked.files\AppA.2.3.3.1.1.Hack.human.indiv.calib.TCE.DRAFT.pdf.](#)]

13  
14 **A.2.3.3.1.2. Population-based predictions and calibration and additional evaluation data.**  
15 [See [Appendix.linked.files\AppA.2.3.3.1.2.Hack.human.pop.calib.eval.TCE.DRAFT.pdf.](#)]

16  
17 **A.2.3.3.2. Conclusions regarding human model.**

18 **A.2.3.3.2.1. Trichloroethylene (TCE) concentrations in blood and air are often not well-**  
19 **predicted.** Except for the Chiu et al. (2007) during exposure, TCE alveolar air levels were  
20 consistently overpredicted. Even in Chiu et al. (2007), TCE levels postexposure were over-  
21 predicted, as the drop-off after the end of exposure was further than predicted. Because  
22 predictions for retained dose appear to be fairly accurate, this implies that less clearance is  
23 occurring via exhalation than predicted by the model. This could be the result of additional  
24 metabolism or storage not accounted for by the model.

25 Except for the Fisher et al. (1998) data, TCE blood levels were consistently  
26 overpredicted. Because the majority of the data used for calibration was from Fisher et al.  
27 (1998), this implies that the Fisher et al. (1998) data had blood concentrations that were  
28 consistently higher than the other studies. This could be due to differences in metabolism and/or  
29 distribution among studies.

30 Interestingly, the mouse inhalation data also exhibited inaccurate prediction of blood  
31 TCE levels. Hypotheses such as fractional uptake or presystemic elimination due to local  
32 metabolism in the lung have not been tested experimentally, nor is it clear that they can explain  
33 the discrepancies.

1 Due to the difficulty in accurately predicted blood and air concentrations, there may be  
2 substantial uncertainty in tissue concentrations of TCE. However, such potential model errors  
3 can be characterized estimated and estimated as part of a revised calibration.

4  
5 **A.2.3.3.2.2. Trichloroacetic acid (TCA) blood concentrations well predicted following**  
6 **trichloroethylene (TCE) exposures, but some uncertainty in TCA flux and disposition.** TCA  
7 blood and plasma concentrations and urinary excretion, following TCE exposure, are generally  
8 well predicted. Even though the model's central estimates over-predicted the Chiu et al. (2007)  
9 TCA data, the confidence intervals were still wide enough to encompass those data.

10 However, the total flux of TCA may not be correct, as evidenced by TCA dosing studies,  
11 none of which were included in the calibration. In these studies, total recovery of urinary TCA  
12 was found to be substantially less than the administered dose. However, the current model  
13 assumes that urinary excretion is the only source of clearance of TCA. This leads to  
14 overestimation of urinary excretion. This fact, combined with the observation that under TCE  
15 dosing, the model appears to give accurate predictions of TCA urinary excretion for several  
16 datasets, strongly suggests a discrepancy in the amount of TCA formed from TCE. That is, since  
17 the model appears to overpredict the fraction of TCA that appears in urine, it may be reducing  
18 TCA production to compensate. Inclusion of the TCA dosing studies, along with inclusion of a  
19 nonrenal clearance pathway, would probably be helpful in reducing these discrepancies. Finally,  
20 improvements in the TCOH/TCOG submodel, below, should also help to insure accurate  
21 estimates of TCA kinetics.

22  
23 **A.2.3.3.2.3. Trichloroethanol–trichlorethanol-glucuronide conjugate (TCOH/TCOG)**  
24 **submodel requires revision and recalibration.** Blood levels of TCOH and urinary excretion of  
25 TCOG were generally well predicted. Additional individual data show substantial  
26 interindividual variability than can be incorporated into the calibration. Several errors as to the  
27 measurement of free or total TCOH in blood need to be corrected.

28 A few inconsistencies with noncalibration datasets stand out. The presence of substantial  
29 TCOG in blood in the Chiu et al. (2007) data are not predicted by the model. Interestingly, only  
30 two studies that included measurements of TCOG in blood (rather than just total TCOH or just  
31 free TCOH)—Muller et al. (1975), which found about 17% of total TCOH to be TCOG, and  
32 Fisher et al. (1998), who could not detect TCOG. Both of these studies had exposures at  
33 100 ppm. Interestingly Muller et al. (1975) reported increased TCOG (as fraction of total  
34 TCOH) with ethanol consumption, hypothesizing the inhibition of a glucuronyl transferase that

1 slowed glucuronidation. This also would result in a greater half-life for TCOH in blood with  
2 ethanol consumptions, which was observed.

3 An additional concern is the over-prediction of urinary TCOG following TCOH  
4 administration from the Muller et al. (1974) data. Like the case of TCA, this indicates that some  
5 other source of TCOH clearance (not to TCA or urine—e.g., to DCA or some other untracked  
6 metabolite) is possible. This pathway can be considered for inclusion, and limits can be placed  
7 on it using the available data.

8 Also, as for TCA, the fact that blood and urine are relatively well predicted from TCE  
9 dosing strongly suggests a discrepancy in the amount of TCOH formed from TCE. That is, since  
10 the model appears to overpredict the fraction of TCOH that appears in urine, it may be reducing  
11 TCOH production to compensate.

12 Finally, as with the rat and mice, the model needs to ensure that any first pass effect is  
13 accounted for appropriately. Particularly for the Chiu et al. (2007) data, in which substantial  
14 TCOG appears in blood, since TCOH is formed in the liver from TCE, and TCOH is also  
15 glucuronidated in the liver to TCOG, a substantial portion of the TCOH may be glucuronidated  
16 before reaching systemic circulation. Thus, suggests that a liver compartment for TCOH is  
17 necessary. Furthermore, because substantial TCOG can be excreted in bile from the liver prior  
18 to systemic circulation, a liver compartment for TCOG may also be necessary to address that  
19 first pass effect. In addition, in light of the Chiu et al. (2007) data, it may be useful to expand the  
20 prior range for the  $K_M$  of TCOH glucuronidation.

21 The addition of the liver compartment will necessitate several changes to model  
22 parameters. The distribution volume for TCOH will be replaced by two parameters: the  
23 liver:blood and body:blood partition coefficients. Similarly for TCOG, liver:blood and  
24 body:blood partition coefficients will need to be added. Clearance of TCOH to TCA and TCOG  
25 can be redefined as occurring in the liver, and urinary clearance can be redefined as coming from  
26 the rest of the body. Fortunately, there are *in vitro* partition coefficients for TCOH. It may be  
27 important to incorporate the fact that Fisher et al. (1998) found no TCOG in blood. This can be  
28 included by having the TCOH data be used for both free and total TCOH (particularly since that  
29 is how the estimation of TCOG was made—by taking the difference between total and free).

30  
31 **A.2.3.3.2.4. *Uncertainty in estimates of total metabolism.*** Estimates of total recovery after  
32 TCE exposure (TCE in exhaled air, TCA and TCOG in urine) have been found to be only  
33 60–70% (Monster et al., 1976, 1979; Chiu et al., 2007). Even estimates of total recovery after  
34 TCA and TCOH dosing have found 25–50% unaccounted for in urinary excretion (Paycok and  
35 Powell, 1945; Muller et al., 1974). Bartonicek found some TCOH and TCA in feces, but this

1 was about 10-fold less than that found in urine, so this cannot account for the discrepancy.  
2 Therefore, it is likely that additional metabolism of TCE, TCOH, and/or TCA are occurring.  
3 Additional metabolism of TCE could account for the consistent overestimation of TCE in blood  
4 and exhaled breath found in many studies. However, no data are *directly* informative as to the  
5 fraction of total metabolism in the lung, the amount of “untracked” hepatic oxidative metabolism  
6 (parameterized as “FracDCA”), or any other extrahepatic metabolism. The lung (TB)  
7 metabolism as currently modeled could just as well be located in other extrahepatic tissues, with  
8 little change in calibration. In addition, it is difficult to distinguish between untracked hepatic  
9 oxidative metabolism and GSH conjugation, particularly at low doses.

### 11 **A.3. PRELIMINARY ANALYSIS OF MOUSE GAS UPTAKE DATA: MOTIVATION** 12 **FOR MODIFICATION OF RESPIRATORY METABOLISM**

13 Potential different model structures can be investigated using the core PBPK model  
14 containing averaged input parameters, since this approach saves computational time and is more  
15 efficient when testing different structural hypotheses. This approach is particularly helpful for  
16 quick comparisons of data with model predictions. During the calibration process, this approach  
17 was used for different routes of exposure and across all three species. For both mice and rats, the  
18 closed chamber inhalation data resulted in fits that were considered not optimal when visually  
19 examined. Although closed chamber inhalation usually combines multiple animals per  
20 experiment, and may not be as useful in differentiating between individual and experimental  
21 uncertainty (Hack et al., 2006), closed chamber data do describe *in vivo* metabolism and have  
22 been historically used to quantify averaged *in vivo* Michaelis-Menten kinetics in rodents.

23 There are several assumptions used when combining PBPK modeling and closed  
24 chamber data to estimate metabolism via regression. The key experimental principles require a  
25 tight, sealed, or air-closed system where all chamber variables are controlled to known set points  
26 or monitored, that is all except for metabolism. For example, the inhalation chamber is  
27 calibrated without an animal, to determine normal absorption to the empty system. This empty  
28 chamber calibration is then followed with a dead animal experiment, identical in every way to  
29 the *in vivo* exposure, and is meant to account for every factor other than metabolism, which is  
30 zero in the dead animal. When the live animal(s) are placed in the chamber, oxygen is provided  
31 for, and carbon dioxide accumulated during breathing is removed by absorption with a chemical  
32 scrubber. A bolus injection of the parent chemical, TCE, is given and this injection time starts  
33 the inhalation exposure. The chemical inside the chamber will decrease with time, as it is  
34 absorbed by the system and the metabolic process inside the rodent. Since all known processes

*This document is a draft for review purposes only and does not constitute Agency policy.*

1 contributing to the decline are quantified, except for metabolism, the metabolic parameters can  
2 be extracted from the total chamber concentration decline using regression techniques.

3 The basic structure for the PBPK model that is linked to closed chamber inhalation data  
4 has the same basic structure as described before. The one major difference is the inclusion of  
5 one additional equation that accounts for mass balance changes inside the inhalation chamber or  
6 system, and connects the chamber with the inhaled and exhaled concentrations breathed in and  
7 out by the animal:

$$\frac{dA_{Ch}}{dt} = RATS(Q_P)(C_X - \frac{A_{Ch}}{V_{Ch}}) - K_{LOSS}A_{Ch} \quad (\text{Eq. A-4})$$

10 where

11	$RATS$	= number of animals in the chamber
12	$Q_P$	= alveolar ventilation rate
13	$C_X$	= exhaled concentration
14	$A_{Ch}$	= net amount of chemical inside chamber
15	$V_{Ch}$	= volume of chamber
16	$K_{LOSS}$	= loss rate constant to glassware.

17  
18  
19 An updated model was developed that included updated physiological and chemical-  
20 specific parameters as well as GSH metabolism in the liver and kidney, as discussed in  
21 Chapter 3. The PBPK model code was translated from MCSim to use in Matlab<sup>®</sup> (version  
22 7.2.0.232, R2006a, Natick, MA) using their m language. This PBPK model made use of fixed or  
23 constant, averaged values for physiological, chemical and other input parameters; there were no  
24 statistical distributions attached to each average value. As an additional step in quality control,  
25 mass balance was checked for the MCSim code, and comparisons across both sets of code were  
26 made to ensure that both sets of predictions were the same.

27 The resulting simulations were compared to mice gas uptake data (Fisher et al., 1991)  
28 after some adjustments of the fat compartment volumes and flows based on visual fits, and  
29 limited least-squares optimization of just  $V_{MAX}$  (different for males and females) and  $K_M$  (same  
30 for males and females). The results are shown in the top panels of Figures A-3–A-4, which  
31 showed poor fits particularly at lower chamber concentrations. In particular, metabolism is  
32 observed to be faster than predicted by simulation. This is directly related to metabolism of TCE  
33 being limited by hepatic blood flow at these exposures. Indeed, Fisher et al. (1991) was able to  
34 obtain adequate fits to these data by using cardiac output and ventilation rates that were about  
35 2-fold higher than is typical for mice. Although their later publication reporting inhalation  
36 experiments (Greenberg et al., 1999) used the lower values from Brown et al. (1997) for these

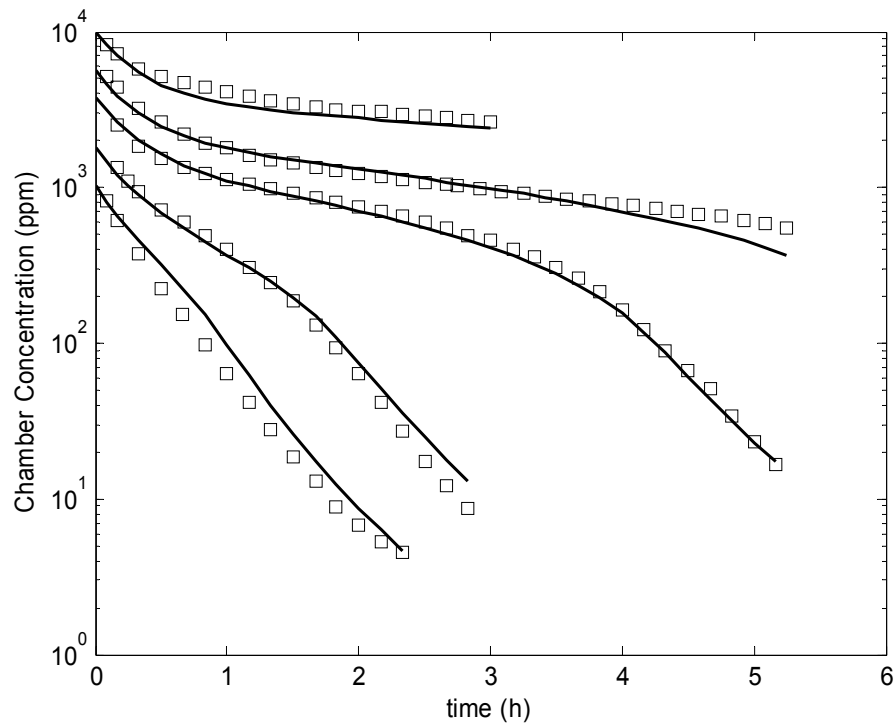
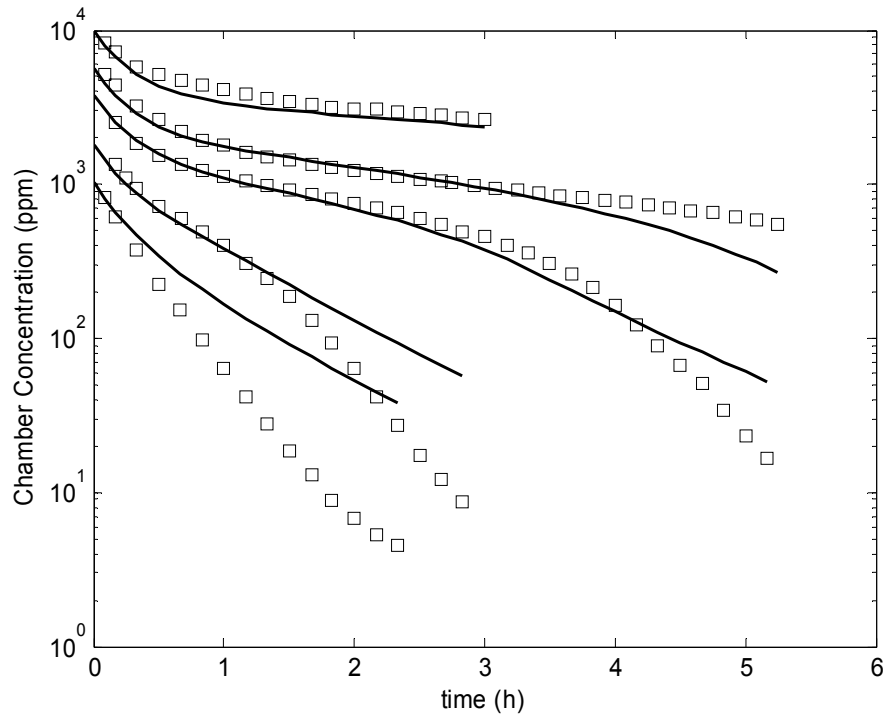
*This document is a draft for review purposes only and does not constitute Agency policy.*

1 parameters, they did not revisit the Fisher et al. (1991) data with the updated model. In addition,  
2 the Hack et al. (2006) model estimated the cardiac output and ventilation rate and for these  
3 experiments to be about 2-fold higher than typical. However, it seems unlikely that cardiac  
4 output and ventilation rate were really as high as used in these models, since TCE and other  
5 solvents typically have central nervous system-depressing effects. In the mouse, after the liver,  
6 the lung has the highest rate of oxidative metabolism, as assessed by *in vitro* methods (see  
7 footnote in Section 3.5.4.2 for a discussion of why kidney oxidative metabolism is likely to be  
8 minor quantitatively). In addition, TCE administered via inhalation is available to the lung  
9 directly, as well as through blood flow. Therefore, it was hypothesized that a more refined  
10 treatment of respiratory metabolism may be necessary to account for the additional metabolism.

11 The structure of the updated respiratory metabolism model is shown in Figure A-5, with  
12 the mathematical formulation shown in the model code in Section A.6, where the “D” is the  
13 diffusion rate, “concentrations” and “amounts” are related by the compartment volume, and the  
14 other symbols have their standard meanings in the context of PBPK modeling. In brief, this is a  
15 more highly “lumped” version of the Sarangapani et al. (2003) respiratory metabolism model for  
16 styrene combined with a “continuous breathing” model to account for a possible wash-in/wash-  
17 out effect. In brief, upon inhalation (at a rate equal to the full minute volume, not just the  
18 alveolar ventilation), TCE can either (1) diffuse between the respiratory tract lumen and the  
19 respiratory tract tissue; (2) remain in the dead space, or (3) enter the gas exchange region. In the  
20 respiratory tract tissue, TCE can either be “stored” temporarily until exhalation, during which it  
21 diffuses to the “exhalation” respiratory tract lumen, or be metabolized. In the dead space, TCE is  
22 transferred directly to the “exhalation” respiratory tract lumen at a rate equal to the minute-  
23 volume minus the alveolar ventilation rate, where it mixes with the other sources. In the gas  
24 exchange region, it undergoes transfer to and from blood, as is standard for PBPK models of  
25 volatile organics. Therefore, if respiratory metabolism is absent ( $V_{MAXClara} = 0$ ), then the  
26 model reduces to a wash-in/wash-out effect where TCE is temporarily adsorbed to the  
27 respiratory tract tissue, the amount of which depends on the diffusion rate, the volume of the  
28 tissue, and the partition coefficients.

29 The results of the same limited optimization, now with additional parameters  $V_{MAXClara}$ ,  
30  $K_{MClara}$ , and  $D$  being estimated simultaneously with the hepatic  $V_{MAX}$  and  $K_M$ , are shown in the  
31 bottom panels of Figures A-2 and A-3. The improvement in the model fits is obvious, and these  
32 results served as a motivation to include this respiratory metabolism model for analysis by the  
33 more formal Bayesian methods.



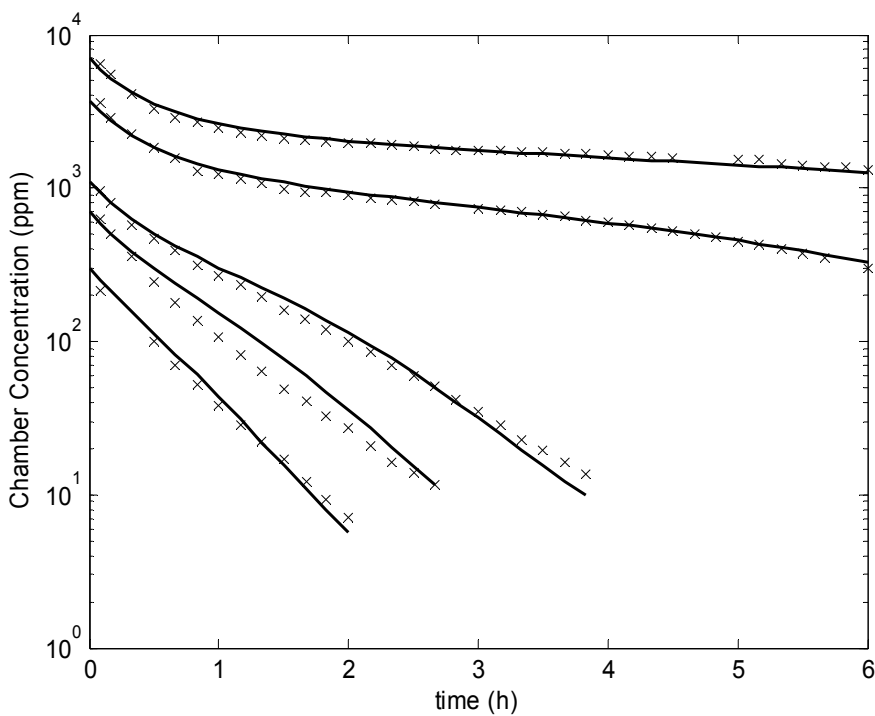
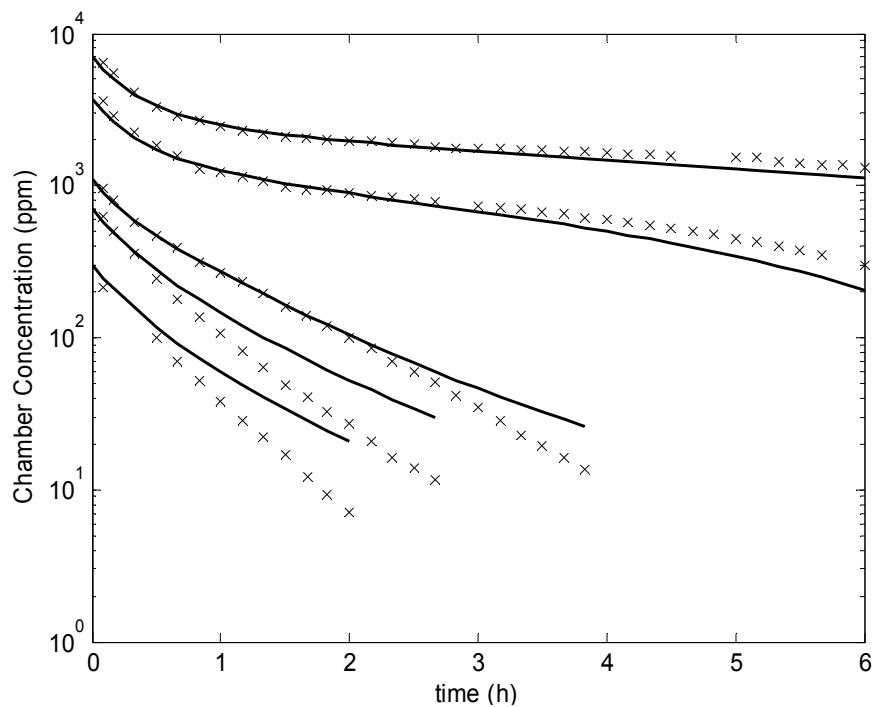


1

2

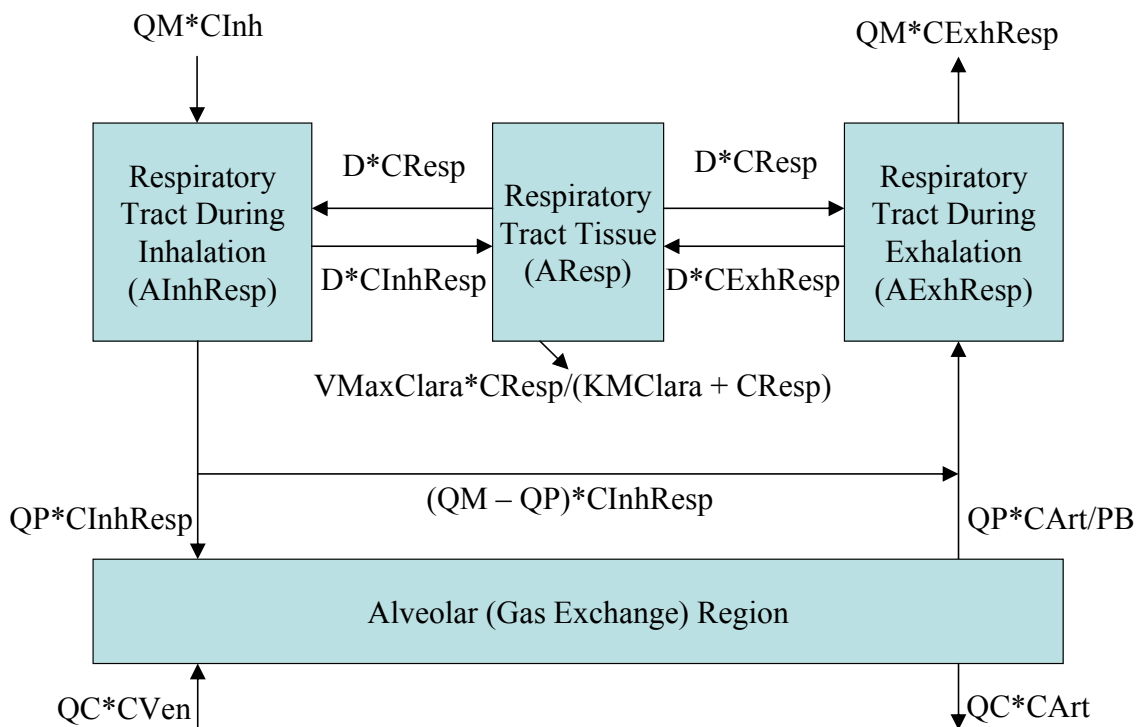
3

**Figure A-3. Limited optimization results for male closed chamber data from Fisher et al. (1991) without (top) and with (bottom) respiratory metabolism.**



1  
2  
3  
4

**Figure A-4. Limited optimization results for female closed chamber data from Fisher et al. (1991) without (top) and with (bottom) respiratory metabolism.**



1  
2 **Figure A-5. Respiratory metabolism model for updated PBPK model.**  
3  
4

5 **A.4. DETAILS OF THE UPDATED PHYSIOLOGICALLY BASED**  
6 **PHARMACOKINETIC (PBPK) MODEL FOR TRICHLOROETHYLENE (TCE)**  
7 **AND ITS METABOLITES**

8 The structure of the updated PBPK model and the statistical population model are shown  
9 graphically in Chapter 3, with the model code shown below in Section A.6. Details as to its  
10 parameter values and their prior distributions are given below.

11  
12 **A.4.1. Model Parameters and Baseline Values**

13 The multipage Table A-4 below describes all the parameters of the updated PBPK model,  
14 their baseline values (which are used as central estimates in the prior distributions for the  
15 Bayesian analysis), and any scaling relationship used in their calculation. More detailed notes  
16 are included in the comments of the model code (see Section A.6).

Table A-4. PBPK model parameters, baseline values, and scaling relationships

Model parameter	Abbreviation	Baseline value (if applicable)				Scaling (Sampled) Parameter	Additional scaling (if any)	Notes/ source
		Mouse	Rat	Human				
				Female (or both)	Male			
Body weight (kg)	<b>BW</b>	0.03	0.3	60	70			a
<b>Flows</b>								
Cardiac output (L/h)	<b>QC</b>	11.6	13.3	16		<b>InQCC</b>	BW <sup>3/4</sup>	b
Alveolar ventilation (L/h)	<b>QP</b>	2.5	1.9	0.96		<b>InVPRC</b>	QC	c
Respiratory lumen:tissue diffusion flow rate (L/h)	<b>DResp</b>					<b>InDRespC</b>	QP	d
<b>Physiological blood flows to tissues</b>								
Fat blood flow	<b>QFat</b>	0.07	0.07	0.085	0.05	<b>QFatC</b>	QC	e
Gut blood flow (portal vein)	<b>QGut</b>	0.141	0.153	0.21	0.19	<b>QGutC</b>	QC	e
Liver blood flow (hepatic artery)	<b>QLiv</b>	0.02	0.021	0.065		<b>QLivC</b>	QC	e
Slowly perfused blood flow	<b>QSlw</b>	0.217	0.336	0.17	0.22	<b>QSlwC</b>	QC	e
Kidney blood flow	<b>QKid</b>	0.091	0.141	0.17	0.19	<b>QKidC</b>	QC	e
Rapidly perfused blood flow	<b>QRap</b>							e
Fraction of blood that is plasma	<b>FracPlas</b>	0.52	0.53	0.615	0.567	<b>FracPlasC</b>		f
<b>Physiological volumes</b>								
Fat compartment volume (L)	<b>VFat</b>	0.07	0.07	0.317	0.199	<b>VFatC</b>	BW	g
Gut compartment volume (L)	<b>VGut</b>	0.049	0.032	0.022	0.02	<b>VGutC</b>	BW	g
Liver compartment volume (L)	<b>VLiv</b>	0.055	0.034	0.023	0.025	<b>VLivC</b>	BW	g
Rapidly perfused compartment volume (L)	<b>VRap</b>	0.1	0.088	0.093	0.088	<b>VRapC</b>	BW	g
Volume of respiratory lumen (L air)	<b>VRespLum</b>	0.004667	0.004667	0.002386		<b>VRespLumC</b>	BW	g
Effective volume for respiratory tissue (L air)	<b>VRespEff</b>	0.0007	0.0005	0.00018	0.00018	<b>VRespEffC</b>	BW x PResp x PB	g
Kidney compartment volume (L)	<b>VKid</b>	0.017	0.007	0.0046	0.0043	<b>VKidC</b>	BW	g
Blood compartment volume (L)	<b>VBld</b>	0.049	0.074	0.068	0.077	<b>VBldC</b>	BW	g
Total perfused volume (L)	<b>VPerf</b>	0.8897	0.8995	0.85778	0.8560		BW	g

Table A-4. PBPK model parameters, baseline values, and scaling relationships (continued)

Model parameter	Abbreviation	Baseline value (if applicable)				Scaling (Sampled) Parameter	Additional scaling (if any)	Notes/ source
		Mouse	Rat	Human				
				Female (or both)	Male			
Slowly perfused compartment volume (L)	<b>VSlw</b>							g
Plasma compartment volume (L)	<b>VPlas</b>							h
TCA body compartment volume (L)	<b>VBod</b>							i
TCOH/G body compartment volume (L)	<b>VBodTCOH</b>							j
<b>TCE distribution/partitioning</b>								
TCE blood/air partition coefficient	<b>PB</b>	15	22	9.5		<b>InPBC</b>		k
TCE fat/blood partition coefficient	<b>PFat</b>	36	27	67		<b>InPFatC</b>		l
TCE gut/blood partition coefficient	<b>PGut</b>	1.9	1.4	2.6		<b>InPGutC</b>		m
TCE liver/blood partition coefficient	<b>PLiv</b>	1.7	1.5	4.1		<b>InPLivC</b>		n
TCE rapidly perfused/blood partition coefficient	<b>PRap</b>	1.9	1.3	2.6		<b>InPRapC</b>		o
TCE respiratory tissue:air partition coefficient	<b>PResp</b>	2.6	1	1.3		<b>InPRespC</b>		p
TCE kidney/blood partition coefficient	<b>PKid</b>	2.1	1.3	1.6		<b>InPKidC</b>		q
TCE slowly perfused/blood partition coefficient	<b>PSlw</b>	2.4	0.58	2.1		<b>InPSlwC</b>		r
<b>TCA distribution/partitioning</b>								
TCA blood/plasma concentration ratio	<b>TCAPlas</b>	0.5	0.5	0.5		<b>InPRBCPlasTCAC</b>	See note	s
Free TCA body/blood plasma partition coefficient	<b>PBodTCA</b>	0.88	0.88	0.52		<b>InPBodTCAC</b>		t
Free TCA liver/blood plasma partition coefficient	<b>PLivTCA</b>	1.18	1.18	0.66		<b>InPLivTCAC</b>		t
<b>TCA plasma binding</b>								
Protein/TCA dissociation constant (μmol/L)	<b>kDissoc</b>	107	275	182		<b>InkDissocC</b>		u
Protein concentration (umole/L)	<b>BMax</b>	0.88	1.22	4.62		<b>InBMaxkDC</b>		u

Table A-4. PBPK model parameters, baseline values, and scaling relationships (continued)

Model parameter	Abbreviation	Baseline value (if applicable)				Scaling (Sampled) Parameter	Additional scaling (if any)	Notes/ source
		Mouse	Rat	Human				
				Female (or both)	Male			
<b>TCOH and TCOG distribution/partitioning</b>								
TCOH body/blood partition coefficient	<b>PBodTCOH</b>	1.11	1.11	0.91		<b>InPBodTCOHC</b>		v
TCOH liver/body partition coefficient	<b>PLivTCOH</b>	1.3	1.3	0.59		<b>InPLivTCOHC</b>		v
TCOG body/blood partition coefficient	<b>PBodTCOG</b>	1.11	1.11	0.91		<b>InPBodTCOGC</b>		w
TCOG liver/body partition coefficient	<b>PLivTCOG</b>	1.3	1.3	0.59		<b>InPLivTCOGC</b>		w
<b>DCVG distribution/partitioning</b>								
DCVG effective volume of distribution	<b>VDCVG</b>					<b>InPeffDCVG</b>	See note	x
<b>TCE metabolism</b>								
$V_{MAX}$ for hepatic TCE oxidation (mg/h)	<b><math>V_{MAX}</math></b>	2,700	600	255		<b>In<math>V_{MAX}C</math></b>	$V_{Liv}$	y
$K_M$ for hepatic TCE oxidation (mg/L)	<b><math>K_M</math></b>	36	21			<b>In<math>K_M C</math></b>		y
				66		<b>In<math>CIC</math></b>	See note	y
Fraction of hepatic TCE oxidation not to TCA+TCOH	<b>FracOther</b>					<b>InFracOtherC</b>	See note	z
Fraction of hepatic TCE oxidation to TCA	<b>FracTCA</b>	0.32	0.32	0.32		<b>InFracTCAC</b>	See note	aa
$V_{MAX}$ for hepatic TCE GSH conjugation (mg/h)	<b><math>V_{MAX}DCVG</math></b>	300	66			<b>In<math>V_{MAX}DCVGC</math></b>	$V_{Liv}$	bb
		1.53	0.25	19		<b>In<math>CIDCVGC</math></b>		bb
$K_M$ for hepatic TCE GSH conjugation (mg/L)	<b><math>K_MDCVG</math></b>			2.9		<b>In<math>K_MDCVGC</math></b>		bb
$V_{MAX}$ for renal TCE GSH conjugation (mg/h)	<b><math>V_{MAX}KidDCVG</math></b>	60	6			<b>In<math>V_{MAX}KidDCVGC</math></b>	$V_{Kid}$	bb
		0.34	0.026	230		<b>In<math>CIKidDCVGC</math></b>		bb
$K_M$ for renal TCE GSH conjugation (mg/L)	<b><math>K_MKidDCVG</math></b>			2.7		<b>In<math>K_MKidDCVGC</math></b>		bb
<b>TCE metabolism (respiratory tract)</b>								
$V_{MAX}$ for tracheo-bronchial TCE oxidation (mg/h)	<b><math>V_{MAX}Clara</math></b>	0.070102	0.014347	0.027273	0.025253	<b>In<math>V_{MAX}LungLivC</math></b>	$V_{MAX}$	cc
$K_M$ for tracheo-bronchial TCE oxidation (mg/L air)	<b><math>K_MClara</math></b>					<b>In<math>K_MClara</math></b>		cc

Table A-4. PBPK model parameters, baseline values, and scaling relationships (continued)

Model parameter	Abbreviation	Baseline value (if applicable)				Scaling (Sampled) Parameter	Additional scaling (if any)	Notes/ source
		Mouse	Rat	Human				
				Female (or both)	Male			
Fraction of respiratory oxidation entering systemic circulation	<b>FracLungSys</b>					<b>InFracLungSysC</b>	See note	dd
<b>TCOH metabolism</b>								
$V_{MAX}$ for hepatic TCOH->TCA (mg/h)	<b><math>V_{MAX}TCOH</math></b>					<b>In<math>V_{MAX}TCOHC</math></b>	$BW^{3/4}$	
						<b>InCITCOHC</b>	$BW^{3/4}$	
$K_M$ for hepatic TCOH->TCA (mg/L)	<b><math>K_MTCOH</math></b>					<b>In<math>K_MTCOH</math></b>		
$V_{MAX}$ for hepatic TCOH->TCOG (mg/h)	<b><math>V_{MAX}Gluc</math></b>					<b>In<math>V_{MAX}GlucC</math></b>	$BW^{3/4}$	
						<b>InCIGlucC</b>	$BW^{3/4}$	
$K_M$ for hepatic TCOH->TCOG (mg/L)	<b><math>K_MGluc</math></b>					<b>In<math>K_MGluc</math></b>		
Rate constant for hepatic TCOH->other (/h)	<b>kMetTCOH</b>					<b>InkMetTCOHC</b>	$BW^{-1/4}$	
<b>TCA metabolism/clearance</b>								
Rate constant for TCA plasma->urine (/h)	<b>kUrnTCA</b>	0.6	0.522	0.108		<b>InkUrnTCAC</b>	$VPlas^{-1}$	ee
Rate constant for hepatic TCA->other (/h)	<b>kMetTCA</b>					<b>InkMetTCAC</b>	$BW^{-1/4}$	
<b>TCOG metabolism/clearance</b>								
Rate constant for TCOG liver->bile (/h)	<b>kBile</b>					<b>InkBileC</b>	$BW^{-1/4}$	
Lumped rate constant for TCOG bile->TCOH liver (/h)	<b>KEHR</b>					<b>InkEHRC</b>	$BW^{-1/4}$	
Rate constant for TCOG->urine (/h)	<b>kUrnTCOG</b>	0.6	0.522	0.108		<b>InkUrnTCOGC</b>	$VBl d^{-1}$	ee
<b>DCVG metabolism</b>								
Rate constant for hepatic DCVG->DCVC (/h)	<b>kDCVG</b>					<b>InkDCVGC</b>	$BW^{-1/4}$	ff

**Table A-4. PBPK model parameters, baseline values, and scaling relationships (continued)**

Model parameter	Abbreviation	Baseline value (if applicable)				Scaling (Sampled) Parameter	Additional scaling (if any)	Notes/ source
		Mouse	Rat	Human				
				Female (or both)	Male			
<b>DCVC metabolism/clearance</b>								
Lumped rate constant for DCVC->Urinary NAcDCVC (/h)	<b>kNAT</b>					<b>InkNATC</b>	BW <sup>-1/4</sup>	gg
Rate constant for DCVC bioactivation (/h)	<b>kKidBioact</b>					<b>InkKidBioactC</b>	BW <sup>-1/4</sup>	gg
<b>Oral uptake/transfer coefficients</b>								
TCE Stomach-duodenum transfer coefficient (/h)	<b>kTSD</b>					<b>InkTSD</b>		hh
TCE stomach absorption coefficient (/h)	<b>kAS</b>					<b>InkAS</b>		hh
TCE duodenum absorption coefficient (/h)	<b>kAD</b>					<b>InkAD</b>		hh
TCA stomach absorption coefficient (/h)	<b>kASTCA</b>					<b>InkASTCA</b>		hh
TCOH stomach absorption coefficient (/h)	<b>kASTCOH</b>					<b>InkASTCOH</b>		hh

**Explanatory note.** Unless otherwise noted, the model parameter is obtained by multiplying (1) the “baseline value” (equals 1 if not specified) times (2) the scaling parameter [or for those beginning with “ln,” which are natural-log transformed, exp(lnXX)] times (3) any additional scaling as noted in the second to last column. Unless otherwise noted, all log-transformed scaling parameters have baseline value of 0 [i.e., exp(lnXX) has baseline value of 1] and all other scaling parameters have baseline parameters of 1.

<sup>a</sup>Use measured value if available.

<sup>b</sup>If QP is measured, then scale by QP using VPR. Baseline values are from Brown et al. (1997) (mouse and rat) and ICRP (International Commission on Radiological Protection) Publication 89 (2003) (human).

<sup>c</sup>Use measured QP, if available; otherwise scale by QC using alveolar VPR. Baseline values are from Brown et al. (1997) (mouse and rat) and ICRP Publication 89 (2003) (human).

<sup>d</sup>Scaling parameter is relative to alveolar ventilation rate.

<sup>e</sup>Fat represents adipose tissue only. Gut is the gastro-intestinal tract, pancreas, and spleen (all drain to the portal vein). Slowly perfused tissue is the muscle and skin. Rapidly perfused tissue is the rest of the organs, plus the bone marrow and lymph nodes, the blood flow for which is calculated as the difference between QC and the sum of the other blood flows. Baseline values are from Brown et al. (1997) (mouse and rat) and ICRP Publication 89 (2003) (human).

<sup>f</sup>This is equal to 1 minus the hematocrit (measured value used if available). Baseline values from control animals in Hejtmancik et al. (2002) (mouse and rat) and ICRP Publication 89 (2003) (human).



**Table A-4. PBPK model parameters, baseline values, and scaling relationships (continued)**

- <sup>e</sup>Fat represents adipose tissue only, and the measured value is used, if available. Gut is the gastro-intestinal tract, pancreas, and spleen (all drain to the portal vein). Rapidly perfused tissue is the rest of the organs, plus the bone marrow and lymph nodes, minus the tracheobronchial region. The respiratory tissue volume is tracheobronchial region, with an effective air volume given by multiplying by its tissue:air partition coefficient (= tissue:blood times blood:air). The slowly perfused tissue is the muscle and skin. This leaves a small (10–15% of body weight [BW]) unperfused volume that consists mostly of bone (minus marrow) and the gastro-intestinal tract contents. Baseline values are from Brown et al. (1997) (mouse and rat) and ICRP Publication 89 (2003) (human), except for volumes of the respiratory lumen, which are from Sarangapani et al. (2003).
- <sup>b</sup>Derived from blood volume using FracPlas.
- <sup>i</sup>Sum of all compartments except the blood and liver.
- <sup>j</sup>Sum of all compartments except the liver.
- <sup>k</sup>Mouse value is from pooling Abbas and Fisher (1997) and Fisher et al. (1991). Rat value is from pooling Sato et al. (1977), Gargas et al. (1989), Barton et al. (1995), Simmons et al. (2002), Koizumi (1989), and Fisher et al. (1989). Human value is from pooling Sato and Nakajima (1979), Sato et al. (1977), Gargas et al. (1989), Fiserova-Bergerova et al. (1984), Fisher et al. (1998), and Koizumi (1989).
- <sup>l</sup>Mouse value is from Abbas and Fisher (1997). Rat value is from pooling Barton et al. (1995), Sato et al. (1977), and Fisher et al. (1989). Human value is from pooling Fiserova-Bergerova et al. (1984), Fisher et al. (1998), and Sato et al. (1977).
- <sup>m</sup>Value is the geometric mean of liver and kidney (relatively high uncertainty) values.
- <sup>n</sup>Mouse value is from Fisher et al. (1991). Rat value is from pooling Barton et al. (1995), Sato et al. (1977), and Fisher et al. (1989). Human value is from pooling Fiserova-Bergerova et al. (1984) and Fisher et al. (1998).
- <sup>o</sup>Mouse value is geometric mean of liver and kidney values. Rat value is the brain value from Sato et al. (1977). Human value is the brain value from Fiserova-Bergerova et al. (1984).
- <sup>p</sup>Mouse value is the lung value from Abbas and Fisher (1997). Rat value is the lung value from Sato et al. (1977). Human value is from pooling lung values from Fiserova-Bergerova et al. (1984) and Fisher et al. (1998).
- <sup>q</sup>Mouse value is from Abbas and Fisher (1997). Rat value is from pooling Barton et al. (1995) and Sato et al. (1977). Human value is from pooling Fiserova-Bergerova et al. (1984) and Fisher et al. (1998).
- <sup>r</sup>Mouse value is the muscle value from Abbas and Fisher (1997). Rat value is the muscle value from pooling Barton et al. (1995), Sato et al. (1977), and Fisher et al. (1989). Human value is the muscle value from pooling Fiserova-Bergerova et al. (1984) and Fisher et al. (1998).
- <sup>s</sup>Scaling parameter is the effective partition coefficient between red blood cells and plasma. Thus, the TCA blood-plasma concentration ratio depends on the plasma fraction. Baseline value is based on the blood-plasma concentration ratio of 0.76 in rats (Schultz et al., 1999).
- <sup>t</sup>*In vitro* partition coefficients were determined at high concentration, when plasma binding is saturated, so should reflect the free blood:tissue partition coefficient. To get the plasma partition coefficient, the partition coefficient is multiplied by the blood:plasma concentration ratio (TCAPlas). *In vitro* values were from Abbas and Fisher (1997) in the mouse (used for both mouse and rat) and from Fisher et al. (1998). Body values based on measurements in muscle.
- <sup>u</sup>Values are based on the geometric mean of estimates based on data from Lumpkin et al. (2003), Schultz et al. (1999), Templin et al. (1993, 1995), and Yu et al. (2000). Scaling parameter for  $B_{MAX}$  is actually the ratio of  $B_{MAX}/kD$ , which determines the binding at low concentrations.
- <sup>v</sup>Data are from Abbas and Fisher (1997) in the mouse (used for the mouse and rat) and Fisher et al. (1998) (human).
- <sup>w</sup>Used *in vitro* measurements in TCOH as a proxy, but higher uncertainty is noted.
- <sup>x</sup>The scaling parameter (only used in the human model) is the effective partition coefficient for the “body” (nonblood) compartment, so that the distribution volume VDCVG is given by  $V_{Bld} + \exp(\ln P_{effDCVG}) \times (V_{Bod} + V_{Liv})$ .

**Table A-4. PBPK model parameters, baseline values, and scaling relationships (continued)**

- <sup>y</sup>Baseline values have the following units: for  $V_{\text{Max}}$ , mg/hour/kg liver; for  $K_{\text{M}}$ , mg/L blood; and for clearance (Cl), L/hour/kg liver (in humans,  $K_{\text{M}}$  is calculated from  $K_{\text{M}} = V_{\text{Max}} / (\exp(\ln \text{ClC}) \times V_{\text{liv}})$ . Values are based on *in vitro* (microsomal and hepatocellular preparations) from Elfarra et al. (1998), Lipscomb et al. (1997, 1998a, b). Scaling from *in vitro* data based on 32 mg microsomal protein/g liver and  $99 \times 10^6$  hepatocytes/g liver (Barter et al., 2007). Scaling of  $K_{\text{M}}$  from microsomes were based on two methods: (1) assuming microsomal concentrations equal to liver tissue concentrations and (2) using the measured microsome:air partition coefficient and a central estimate of the blood:air partition coefficient. For  $K_{\text{M}}$  from human hepatocyte preparations, the measured hepatocyte:air partition coefficient and a central estimate of the blood:air partition coefficient was used.
- <sup>z</sup>Scaling parameter is ratio of “DCA” to “non-DCA” oxidative pathway (where DCA is a proxy for oxidative metabolism not producing TCA or TCOH). Fraction of “other” oxidation is  $\exp(\ln \text{FracOtherC}) / (1 + \exp[\ln \text{FracOtherC}])$ .
- <sup>aa</sup>Scaling parameter is ratio of TCA to TCOH pathways. Baseline value based on geometric mean of Lipscomb et al. (1998b) using fresh hepatocytes and Bronley-DeLancey et al. (2006) using cryogenically-preserved hepatocytes. Fraction of oxidation to TCA is  $(1 - \text{FracOther}) \times \exp(\ln \text{FracTCAC}) / (1 + \exp[\ln \text{FracTCAC}])$ .
- <sup>bb</sup>Baseline values are based on *in vitro* data. In the mouse and rat, the only *in vitro* data are at 1 or 2 mM (Lash et al., 1995, 1998). In most cases, rates at 2 mM were increased over the same sex/species at 1 mM, indicating  $V_{\text{Max}}$  has not yet been reached. These data therefore put lower bounds on both  $V_{\text{Max}}$  (in units of mg/hour/kg tissue) and clearance (in units of L/hour/kg tissue), so those are the scaling parameters used, with those bounds used as baseline values. For humans, data from Lash et al. (1999a) in the liver (hepatocytes) and the kidney (cytosol) and Green et al. (1997) (liver cytosol) was used to estimate the clearance in units of L/hour/kg tissue and  $K_{\text{M}}$  in units of mg/L in blood.
- <sup>cc</sup>Scaling parameter is the ratio of the lung to liver  $V_{\text{Max}}$  (each in units of mg/hour), with baseline values based on microsomal preparations (mg/hour/mg protein) assayed at ~1 mM (Green et al., 1997), further adjusted by the ratio of lung to liver tissue masses (Brown et al., 1997; ICRP Publication 89 [2003]).
- <sup>dd</sup>Scaling parameter is the ratio of respiratory oxidation entering systemic circulation (translocated to the liver) to that locally cleared in the lung. Fraction of respiratory oxidation entering systemic circulation is  $\exp(\ln \text{FracLungSysC}) / (1 + \exp[\ln \text{FracLungSysC}])$ .
- <sup>ee</sup>Baseline parameters for urinary clearance (L/hour) were based on glomerular filtration rate per unit body weight (L/hour/kg BW) from Lin (1995), multiplied by the body weights cited in the study. For TCA, these were scaled by plasma volume to obtain the rate constant (/hour), since the model clears TCA from plasma. For TCOG, these were scaled by the effective distribution volume of the body ( $V_{\text{BodTCOH}} \times P_{\text{BodTCOG}}$ ) to obtain the rate constant (/hour), since the model clears TCOG from the body compartment.
- <sup>ff</sup>Human model only.
- <sup>gg</sup>Rat and human models only.
- <sup>hh</sup>Baseline value for oral absorption scaling parameter are as follows:  $k_{\text{TSD}}$  and  $k_{\text{AS}}$ , 1.4/hour, based on human stomach half time of 0.5 hour;  $k_{\text{AD}}$ ,  $k_{\text{ASTCA}}$ , and  $k_{\text{ASTCOH}}$ , 0.75/hour, based on human small intestine transit time of 4 hours (ICRP Publication 89, 2003). These are noted to have very high uncertainty.

DCVG = S-dichlorovinyl glutathione.

1 **A.4.2. Statistical Distributions for Parameter Uncertainty and Variability**

2 **A.4.2.1. Initial Prior Uncertainty in Population Mean Parameters**

3 The following multipage Table A-5 describes the initial prior distributions for the  
4 population mean of the PBPK model parameters. For selected parameters, rat prior distributions  
5 were subsequently updated using the mouse posterior distributions, and human prior distributions  
6 were then updated using mouse and rat posterior distributions (see Section A.4.2.2).

7  
8 **A.4.2.2. Interspecies Scaling to Update Selected Prior Distributions in the Rat and Human**

9 As shown in Table A-5, for several parameters, there is little or no *in vitro* or other prior  
10 information available to develop informative prior distributions, so many parameters had  
11 lognormal or log-uniform priors that spanned a wide range. Initially, the PBPK model for each  
12 species was run with the initial prior distributions in Table A-5, but, in the time available for  
13 analysis (up to about 100,000 iterations), only for the mouse did all these parameters achieve  
14 adequate convergence. Additional preliminary runs indicated replacing the log-uniform priors  
15 with lognormal priors and/or requiring more consistency between species could lead to adequate  
16 convergence. However, an objective method of “centering” the lognormal distributions that did  
17 not rely on the *in vivo* data (e.g., via visual fitting or limited optimization) being calibrated  
18 against was necessary in order to minimize potential bias.

19 Therefore, the approach taken was to consider three species sequentially, from mouse to  
20 rat to human, and to use a model for interspecies scaling to update the prior distributions across  
21 species (the original prior distributions define the prior bounds). This sequence was chosen  
22 because the models are essentially “nested” in this order—the rat model adds to the mouse model  
23 the “downstream” GSH conjugation pathways, and the human model adds to the rat model the  
24 intermediary S-dichlorovinyl glutathione (DCVG) compartment. Therefore, for those  
25 parameters with little or no independent data *only*, the mouse posteriors were used to update the  
26 rat priors, and both the mouse and rat posteriors were used to update the human priors. A list of  
27 the parameters for which this scaling was used to update prior distributions is contained in  
28 Table A-6, with the updated prior distributions. The correspondence between the “scaling  
29 parameters” and the physical parameters generally follows standard practice, and were explicitly  
30 described in Table A-4. For instance,  $V_{MAX}$  and clearance rates are scaled by body weight to the  
31  $3/4$  power, whereas  $K_M$  values are assumed to have no scaling, and rate constants (inverse time  
32 units) are scaled by body weight to the  $-1/4$  power.

33

*This document is a draft for review purposes only and does not constitute Agency policy.*

**Table A-5. Uncertainty distributions for the population mean of the PBPK model parameters**

Scaling (sampled) parameter	Mouse			Rat			Human			Notes/Source
	Distribution <sup>a</sup>	SD or Min	Truncation ( $\pm n \times SD$ ) or Max	Distribution	SD or Min	Truncation ( $\pm n \times SD$ ) or Max	Distribution	SD or Min	Truncation ( $\pm n \times SD$ ) or Max	
<b>Flows</b>										
<b>InQCC</b>	TruncNormal	0.2	4	TruncNormal	0.14	4	TruncNormal	0.2	4	a
<b>InVPRC</b>	TruncNormal	0.2	4	TruncNormal	0.3	4	TruncNormal	0.2	4	a
<b>InDRespC</b>	Uniform	-11.513	2.303	Uniform	-11.513	2.303	Uniform	-11.513	2.303	b
<b>Physiological blood flows to tissues</b>										
<b>QFatC</b>	TruncNormal	0.46	2	TruncNormal	0.46	2	TruncNormal	0.46	2	a
<b>QGutC</b>	TruncNormal	0.17	2	TruncNormal	0.17	2	TruncNormal	0.18	2	a
<b>QLivC</b>	TruncNormal	0.17	2	TruncNormal	0.17	2	TruncNormal	0.45	2	a
<b>QSIwC</b>	TruncNormal	0.29	2	TruncNormal	0.3	2	TruncNormal	0.32	2	a
<b>QKidC</b>	TruncNormal	0.32	2	TruncNormal	0.13	2	TruncNormal	0.12	2	a
<b>FracPlasC</b>	TruncNormal	0.2	3	TruncNormal	0.2	3	TruncNormal	0.05	3	c
<b>Physiological volumes</b>										
<b>VFatC</b>	TruncNormal	0.45	2	TruncNormal	0.45	2	TruncNormal	0.45	2	a
<b>VGutC</b>	TruncNormal	0.13	2	TruncNormal	0.13	2	TruncNormal	0.08	2	a
<b>VLivC</b>	TruncNormal	0.24	2	TruncNormal	0.18	2	TruncNormal	0.23	2	a
<b>VRapC</b>	TruncNormal	0.1	2	TruncNormal	0.12	2	TruncNormal	0.08	2	a
<b>VRespLumC</b>	TruncNormal	0.11	2	TruncNormal	0.18	2	TruncNormal	0.2	2	a
<b>VRespEffC</b>	TruncNormal	0.11	2	TruncNormal	0.18	2	TruncNormal	0.2	2	a
<b>VKidC</b>	TruncNormal	0.1	2	TruncNormal	0.15	2	TruncNormal	0.17	2	a
<b>VBldC</b>	TruncNormal	0.12	2	TruncNormal	0.12	2	TruncNormal	0.12	2	a

Table A-5. Uncertainty distributions for the population mean of the PBPK model parameters (continued)

Scaling (sampled) parameter	Mouse			Rat			Human			Notes/Source
	Distribution <sup>a</sup>	SD or Min	Truncation ( $\pm n \times SD$ ) or Max	Distribution	SD or Min	Truncation ( $\pm n \times SD$ ) or Max	Distribution	SD or Min	Truncation ( $\pm n \times SD$ ) or Max	
<b>TCE distribution/partitioning</b>										
InPBC	TruncNormal	0.25	3	TruncNormal	0.25	3	TruncNormal	0.2	3	d
InPFatC	TruncNormal	0.3	3	TruncNormal	0.3	3	TruncNormal	0.2	3	
InPGutC	TruncNormal	0.4	3	TruncNormal	0.4	3	TruncNormal	0.4	3	
InPLivC	TruncNormal	0.4	3	TruncNormal	0.15	3	TruncNormal	0.4	3	
InPRapC	TruncNormal	0.4	3	TruncNormal	0.4	3	TruncNormal	0.4	3	
InPRespC	TruncNormal	0.4	3	TruncNormal	0.4	3	TruncNormal	0.4	3	
InPKidC	TruncNormal	0.4	3	TruncNormal	0.3	3	TruncNormal	0.2	3	
InPSIwC	TruncNormal	0.4	3	TruncNormal	0.3	3	TruncNormal	0.3	3	
<b>TCA distribution/partitioning</b>										
InPRBCPlasTCAC	Uniform	-4.605	4.605	TruncNormal	0.336	3	Uniform	-4.605	4.605	e
InPBodTCAC	TruncNormal	0.336	3	TruncNormal	0.693	3	TruncNormal	0.336	3	f
InPLivTCAC	TruncNormal	0.336	3	TruncNormal	0.693	3	TruncNormal	0.336	3	
<b>TCA plasma binding</b>										
InkDissocC	TruncNormal	1.191	3	TruncNormal	0.61	3	TruncNormal	0.06	3	g
InBMaxkDC	TruncNormal	0.495	3	TruncNormal	0.47	3	TruncNormal	0.182	3	
<b>TCOH and TCOG distribution/partitioning</b>										
InPBodTCOHC	TruncNormal	0.336	3	TruncNormal	0.693	3	TruncNormal	0.336	3	
InPLivTCOHC	TruncNormal	0.336	3	TruncNormal	0.693	3	TruncNormal	0.336	3	
InPBodTCOGC	Uniform	-4.605	4.605	Uniform	-4.605	4.605	Uniform	-4.605	4.605	
InPLivTCOGC	Uniform	-4.605	4.605	Uniform	-4.605	4.605	Uniform	-4.605	4.605	

Table A-5. Uncertainty distributions for the population mean of the PBPk model parameters (continued)

Scaling (sampled) parameter	Mouse			Rat			Human			Notes/Source
	Distribution <sup>a</sup>	SD or Min	Truncation ( $\pm n \times SD$ ) or Max	Distribution	SD or Min	Truncation ( $\pm n \times SD$ ) or Max	Distribution	SD or Min	Truncation ( $\pm n \times SD$ ) or Max	
<b>DCVG distribution/partitioning</b>										
InPeffDCVG	Uniform	-6.908	6.908	Uniform	-6.908	6.908	Uniform	-6.908	6.908	h
<b>TCE Metabolism</b>										
InV <sub>MAX</sub> C	TruncNormal	0.693	3	TruncNormal	0.693	3	TruncNormal	0.693	3	i
InK <sub>M</sub> C	TruncNormal	1.386	3	TruncNormal	1.386	3				i
InCIC							TruncNormal	1.386	3	i
InFracOtherC	Uniform	-6.908	6.908	Uniform	-6.908	6.908	Uniform	-6.908	6.908	h
InFracTCAC	TruncNormal	1.163	3	TruncNormal	1.163	3	TruncNormal	1.163	3	j
InV <sub>MAX</sub> DCVGC	Uniform	-4.605	9.21	Uniform	-4.605	9.21				k
InCIDCVGC	Uniform	-4.605	9.21	Uniform	-4.605	9.21	TruncNormal	4.605	3	k
InK <sub>M</sub> DCVGC							TruncNormal	1.386	3	k
InV <sub>MAX</sub> KidDCVGC	Uniform	-4.605	9.21	Uniform	-4.605	9.21				k
InCIKidDCVGC	Uniform	-4.605	9.21	Uniform	-4.605	9.21	TruncNormal	4.605	3	k
InK <sub>M</sub> KidDCVGC							TruncNormal	1.386	3	k
InV <sub>MAX</sub> LungLivC	TruncNormal	1.099	3	TruncNormal	1.099	3	TruncNormal	1.099	3	l
InK <sub>M</sub> Clara	Uniform	-6.908	6.908	Uniform	-6.908	6.908	Uniform	-6.908	6.908	h
InFracLungSysC	Uniform	-6.908	6.908	Uniform	-6.908	6.908	Uniform	-6.908	6.908	h
<b>TCOH metabolism</b>										
InV <sub>MAX</sub> TCOHC	Uniform	-9.21	9.21	Uniform	-9.21	9.21				h
InCITCOHC							Uniform	-11.513	6.908	
InK <sub>M</sub> TCOH	Uniform	-9.21	9.21	Uniform	-9.21	9.21	Uniform	-9.21	9.21	
InV <sub>MAX</sub> GlucC	Uniform	-9.21	9.21	Uniform	-9.21	9.21				
InCIGlucC							Uniform	-9.21	4.605	
InK <sub>M</sub> Gluc	Uniform	-6.908	6.908	Uniform	-6.908	6.908	Uniform	-6.908	6.908	h
InkMetTCOHC	Uniform	-11.513	6.908	Uniform	-11.513	6.908	Uniform	-11.513	6.908	

10/20/09

This document is a draft for review purposes only and does not constitute Agency policy.

A-49

DRAFT: DO NOT CITE OR QUOTE

Table A-5. Uncertainty distributions for the population mean of the PBPK model parameters (continued)

Scaling (sampled) parameter	Mouse			Rat			Human			Notes/Source
	Distribution <sup>a</sup>	SD or Min	Truncation ( $\pm n \times SD$ ) or Max	Distribution	SD or Min	Truncation ( $\pm n \times SD$ ) or Max	Distribution	SD or Min	Truncation ( $\pm n \times SD$ ) or Max	
<b>TCA metabolism/clearance</b>										
InkUrnTCAC	Uniform	-4.605	4.605	Uniform	-4.605	4.605	Uniform	-4.605	4.605	h
InkMetTCAC	Uniform	-9.21	4.605	Uniform	-9.21	4.605	Uniform	-9.21	4.605	
<b>TCOG metabolism/clearance</b>										
InkBileC	Uniform	-9.21	4.605	Uniform	-9.21	4.605	Uniform	-9.21	4.605	h
InkEHRC	Uniform	-9.21	4.605	Uniform	-9.21	4.605	Uniform	-9.21	4.605	
InkUrnTCOGC	Uniform	-6.908	6.908	Uniform	-6.908	6.908	Uniform	-6.908	6.908	
<b>DCVG metabolism</b>										
InFracKidDCVCC	Uniform	-6.908	6.908	Uniform	-6.908	6.908	Uniform	-6.908	6.908	h
InkDCVGC	Uniform	-9.21	4.605	Uniform	-9.21	4.605	Uniform	-9.21	4.605	
<b>DCVC metabolism/clearance</b>										
InkNATC	Uniform	-9.21	4.605	Uniform	-9.21	4.605	Uniform	-9.21	4.605	h
InkKidBioactC	Uniform	-9.21	4.605	Uniform	-9.21	4.605	Uniform	-9.21	4.605	
<b>Oral uptake/transfer coefficients</b>										
InkTSD	Uniform	-4.269	4.942	Uniform	-4.269	4.942	Uniform	-4.269	4.942	h
InkAS	Uniform	-6.571	7.244	Uniform	-6.571	7.244	Uniform	-6.571	7.244	
InkTD	Uniform	-4.605	0	Uniform	-4.605	0	Uniform	-4.605	0	
InkAD	Uniform	-7.195	6.62	Uniform	-7.195	6.62	Uniform	-7.195	6.62	
InkASTCA	Uniform	-7.195	6.62	Uniform	-7.195	6.62	Uniform	-7.195	6.62	h
InkASTCOH	Uniform	-7.195	6.62	Uniform	-7.195	6.62	Uniform	-7.195	6.62	

**Explanatory note.** All population mean parameters have either truncated normal (TruncNormal) or uniform distributions. For those with TruncNormal distributions, the mean for the population mean is 0 for natural-log transformed parameters (parameter name starting with “ln”) and 1 for untransformed parameters, with the truncation at the specified number ( $n$ ) of standard deviations (SD). All uniformly distributed parameters are natural-log transformed, so their untransformed minimum and maximum are  $\exp(\text{Min})$  and  $\exp(\text{Max})$ , respectively.

**Table A-5. Uncertainty distributions for the population mean of the PBPK model parameters (continued)**

- <sup>a</sup>Uncertainty based on CV or range of values in Brown et al. (1997) (mouse and rat) and a comparison of values from ICRP Publication 89 (2003), Brown et al. (1997), and Price et al. (2003) (human).
- <sup>b</sup>Noninformative prior distribution intended to span a wide range of possibilities because no independent data are available on these parameters. These priors for the rat and human were subsequently updated (see Section A.4.2.2).
- <sup>c</sup>Because of potential strain differences, uncertainty in mice and rat assumed to be 20%. In humans, Price et al. (2003) reported variability of about 5%, and this is also used for the uncertainty in the mean.
- <sup>d</sup>For partition coefficients, it is not clear whether interstudy variability is due to interindividual or assay variability, so uncertainty in the mean is based on interstudy variability among *in vitro* measurements. For single measurements, uncertainty SD of 0.3 was used for fat (mouse) and 0.4 for other tissues was used. In addition, where measurements were from a surrogate tissue (e.g., gut was based on liver and kidney), an uncertainty SD 0.4 was used.
- <sup>e</sup>Single *in vitro* data point available in rats, so a geometric standard deviation (GSD) of 1.4 was used. In mice and humans, where no *in vitro* data was available, a noninformative prior was used.
- <sup>f</sup>Single *in vitro* data points available in mice and humans, so a GSD of 1.4 was used. In rats, where the mouse data was used as a surrogate, a GSD of 2.0 was used, based on the difference between mice and rats *in vitro*.
- <sup>g</sup>GSD for uncertainty based on different estimates from different *in vitro* studies.
- <sup>h</sup>Noninformative prior distribution.
- <sup>i</sup>Assume 2-fold uncertainty GSD in  $V_{Max}$ , based on observed variability and uncertainties of *in vitro*-to-*in vivo* scaling. For  $K_M$  and CIC, the uncertainty is assumed to be 4-fold, due to the different methods for scaling of concentrations from TCE in the *in vitro* medium to TCE in blood.
- <sup>j</sup>Uncertainty GSD of 3.2-fold reflects difference between *in vitro* measurements from Lipscomb et al. (1998b) and Bronley-DeLancey et al. (2006).
- <sup>k</sup>In mice and rats, the baseline values are notional lower-limits on  $V_{Max}$  and clearance, however, the lower bound of the prior distribution is set to 100-fold less because of uncertainty in *in vitro-in vivo* extrapolation, and because Green et al. (1997) reported values 100-fold smaller than Lash et al. (1995, 1998). In humans, the uncertainty GSD in clearance is assumed to be 100-fold, due to the difference between Lash et al. (1998) and Green et al. (1997). For  $K_M$ , the uncertainty GSD of 4-fold is based on differences between concentrations in cells and cytosol.
- <sup>l</sup>Uncertainty GSD of 3-fold was assumed due to possible differences in microsomal protein content, the fact that measurements were at a single concentration, and the fact that the human baseline values was based on the limit of detection.

DCVG = S-dichlorovinyl glutathione, SD = standard deviation.



1  
2  
3

**Table A-6. Updated prior distributions for selected parameters in the rat and human**

Scaling parameter	Initial prior bounds		Updated rat prior		Updated human prior	
	exp(min)	exp(max)	exp( $\mu$ )	exp( $\sigma$ )	exp( $\mu$ )	exp( $\sigma$ )
InDRespC	1.00E-05	1.00E+01	1.22	5.21	1.84	4.18
InPBodTCOGC	1.00E-02	1.00E+02	0.42	5.47	0.81	5.10
InPLivTCOGC	1.00E-02	1.00E+02	1.01	5.31	2.92	4.31
InFracOtherC	1.00E-03	1.00E+03	0.02	6.82	0.14	4.76
InV <sub>MAX</sub> DCVGC	1.00E-02	1.00E+04	2.61	42.52		
InCIDCVGC	1.00E-02	1.00E+04	0.36	15.03		
InV <sub>MAX</sub> KidDCVGC	1.00E-02	1.00E+04	2.56	22.65		
InCIKidDCVGC	1.00E-02	1.00E+04	1.22	15.03		
InV <sub>MAX</sub> LungLivC	3.70E-02	2.70E+01	2.77	6.17	2.80	4.71
InK <sub>M</sub> Clara	1.00E-03	1.00E+03	0.01	6.69	0.02	4.85
InFracLungSysC	1.00E-03	1.00E+03	4.39	11.13	3.10	8.08
InV <sub>MAX</sub> TCOHC	1.00E-04	1.00E+04	1.65	5.42		
InCITCOHC	1.00E-05	1.00E+03			0.37	4.44
InK <sub>M</sub> TCOH	1.00E-04	1.00E+04	0.93	5.64	4.81	4.53
InV <sub>MAX</sub> GlucC	1.00E-04	1.00E+04	69.41	5.58		
InCIGlucC	1.00E-04	1.00E+02			3.39	4.35
InK <sub>M</sub> Gluc	1.00E-03	1.00E+03	30.57	6.11	11.13	4.57
InkMetTCOHC	1.00E-05	1.00E+03	3.35	5.87	2.39	4.62
InkUrnTCAC	1.00E-02	1.00E+02	0.11	5.42	0.09	4.22
InkMetTCAC	1.00E-04	1.00E+02	0.61	5.37	0.45	4.26
InkBileC	1.00E-04	1.00E+02	1.01	5.70	3.39	4.44
InkEHRC	1.00E-04	1.00E+02	0.01	6.62	0.22	4.71
InkUrnTCOGC	1.00E-03	1.00E+03	8.58	6.05	16.12	4.81
InkNATC	1.00E-04	1.00E+02			0.00	6.11
InkKidBioactC	1.00E-04	1.00E+02			0.01	6.49

4  
5  
6  
7  
8  
9

Notes: updated rat prior is based on the mouse posterior; and the updated human priors are based on combining the mouse and rat posteriors, except in the case of InkNATC and InkKidBioactC, which are unidentified in the mouse model. Columns labeled exp(min) and exp(max) are the exponentiated prior bounds; columns labeled exp( $\mu$ ) and exp( $\sigma$ ) are the exponentiated mean and standard deviation of the updated prior distributions, which are normal distributions truncated at the prior bounds.

10  
11  
12  
13  
14  
15  
16

The scaling model is given explicitly as follows. If  $\theta_i$  are the “scaling” parameters (usually also natural-log-transformed) that are actually estimated, and A is the “universal” (species-independent) parameter, then  $\theta_i = A + \varepsilon_i$ , where  $\varepsilon_i$  is the species-specific “departure” from the scaling relationship, assumed to be normally distributed with variance  $\sigma_\varepsilon^2$ . This “scatter” in the interspecies scaling relationship is assumed to have a standard deviation of

1 1.15 = ln(3.16), so that the un-logarithmically transformed 95% confidence interval spans about  
 2 100-fold (i.e.,  $\exp(2\sigma) = 10$ ). This implies that 95% of the time, the species-specific scaling  
 3 parameter is assumed be within 10-fold higher or lower than the “species-independent” value.  
 4 However, the prior bounds, which generally span a wider range, are maintained so that if the data  
 5 strongly imply an extreme species-specific value, it can be accommodated.

6 Therefore, the mouse model gives an initial estimate of “A,” which is used to update the  
 7 prior distribution for  $\theta_r = A + \varepsilon_r$  in the rat (alternatively, since there is only one species at this  
 8 stage, one could think of this as estimating the rat parameter using the mouse parameter, but with  
 9 a cross-species variance is twice the allometric scatter variance). The rat and mouse together  
 10 then give a “better” estimate of A, which is used to update the prior distribution for  $\theta_h = A + \varepsilon_h$  in  
 11 the human, with the assumed distribution for  $\varepsilon_h$ . This approach is implemented by  
 12 approximating the posterior distributions by normal distributions, deriving heuristic “data” for  
 13 the specific-specific parameters, and then using these pseudo-data to derive updated prior  
 14 distributions for the other species parameters. Specifically, the procedure is as follows:

- 15
- 16 1. Run the mouse model.
- 17 2. Use the mouse posterior to derive the mouse “pseudo-data”  $D_m$  (equal to the posterior  
 18 mean) and its uncertainty  $\sigma_m^2$  (equal to the posterior variance).
- 19 3. Use the  $D_m$  as the prior mean for the rat. The prior variance for the rat is  $2\sigma_\varepsilon^2 + \sigma_m^2$ ,  
 20 which accounts for two components of species-specific departure from “species-  
 21 independence” (one each for mouse and rat), and the mouse posterior uncertainty.
- 22 4. Match the rat posterior mean and variance to the values derived from the normal  
 23 approximation (posterior mean =  $\{D_m/(2\sigma_\varepsilon^2 + \sigma_m^2) + D_r/\sigma_r^2\}/\{1/(2\sigma_\varepsilon^2 + \sigma_m^2) + 1/\sigma_r^2\}$ ;  
 24 posterior variance =  $\{1/(2\sigma_\varepsilon^2 + \sigma_m^2) + 1/\sigma_r^2\}^{-1}$ ), and solve for the rat “data”  $D_r$  and its  
 25 uncertainty  $\sigma_r^2$ .
- 26 5. Use,  $\sigma_m^2$ , and  $\sigma_r^2$  to derive the updated prior mean and variance for the human model.  
 27 For the mean ( $=\{D_m/(\sigma_\varepsilon^2 + \sigma_m^2) + D_r/(\sigma_\varepsilon^2 + \sigma_r^2)\}/\{1/(\sigma_\varepsilon^2 + \sigma_m^2) + 1/(\sigma_\varepsilon^2 + \sigma_r^2)\}$ ), it is the  
 28 weighted average of the mouse and rat, with each weight including both posterior  
 29 uncertainty and departure from “species-independence.” For the variance ( $=\{1/(\sigma_\varepsilon^2 + \sigma_m^2) + 1/(\sigma_\varepsilon^2 + \sigma_r^2)\}^{-1} + \sigma_\varepsilon^2$ ), it is the variance in the weighted average of the mouse and  
 30 rat plus an additional component of species-specific departure from “species-  
 31 independence.”  
 32

33

34 Formally, then, the probability of  $\theta_i$  given A can be written as

$$35 \quad P(\theta_i | A) = \phi(\theta_i - A, \sigma_\varepsilon^2) \quad (\text{Eq. A-5})$$

1 where  $\varphi(x, \sigma^2)$  is the normal density centered on 0 with variance  $\sigma^2$ . Let  $D_i$  be a heuristic  
 2 “datum” for species  $i$ , so the likelihood given  $\theta_i$  is adequately approximated by

$$3 \quad P(D_i | \theta_i) = \varphi(D_i - \theta_i, \sigma_i^2) \quad (\text{Eq. A-6})$$

4  
 5  
 6 Therefore, considering  $A$  to have a uniform prior distribution, then running the mouse model  
 7 gives a posterior of the form

$$8 \quad P(A, \theta_m | D_m) \propto P(A) P(\theta_m | A) P(D_m | \theta_m) \propto \varphi(\theta_m - A, \sigma_\varepsilon^2) \varphi(D_m - \theta_m, \sigma_m^2) \quad (\text{Eq. A-7})$$

9  
 10  
 11 From the MCMC posterior, the values of  $D_m$  and  $\sigma_m^2$  are simply the mean and variance of the  
 12 scaled parameter  $\theta_m$ .

13  
 14 Now, adding the rat data gives

$$15 \quad P(A, \theta_m, \theta_r | D_m, D_r) \propto P(A) P(\theta_m | A) P(D_m | \theta_m) P(\theta_r | A) P(D_r | \theta_r) \quad (\text{Eq. A-8})$$

$$16 \quad \propto \varphi(\theta_m - A, \sigma_\varepsilon^2) \varphi(D_m - \theta_m, \sigma_m^2) \varphi(\theta_r - A, \sigma_\varepsilon^2) \varphi(D_r - \theta_r, \sigma_r^2) \quad (\text{Eq. A-9})$$

17  
 18  
 19  $D_r$  and  $\sigma_r^2$  can be derived by marginalizing first over  $\theta_m$  and then over  $A$ :

$$20 \quad \int P(A, \theta_m, \theta_r | D_m, D_r) d\theta_m dA$$

$$21 \quad \propto \left[ \int P(A) \left\{ \int P(\theta_m | A) P(D_m | \theta_m) d\theta_m \right\} P(\theta_r | A) dA \right] P(D_r | \theta_r) \quad (\text{Eq. A-10})$$

$$22 \quad = \left[ \int P(A) P(D_m | A) P(\theta_r | A) dA \right] P(D_r | \theta_r) \quad (\text{Eq. A-11})$$

$$23 \quad \propto \left[ \int P(A | D_m) P(\theta_r | A) dA \right] P(D_r | \theta_r) \quad (\text{Eq. A-12})$$

$$24 \quad = P(\theta_r | D_m) P(D_r | \theta_r) \quad (\text{Eq. A-13})$$

25  
 26  
 27 So  $P(\theta_r | D_m)$  can be identified as the prior for  $\theta_r$  based on the mouse data, and  $P(D_r | \theta_r)$  as the  
 28 rat-specific likelihood. The updated prior for the rats is then

$$29 \quad P(\theta_r | D_m) \propto \int \varphi(\theta_m - A, \sigma_\varepsilon^2) \varphi(D_m - \theta_m, \sigma_m^2) \varphi(\theta_r - A, \sigma_\varepsilon^2) d\theta_m dA \quad (\text{Eq. A-14})$$

$$30 \quad = \int \varphi(D_m - A, \sigma_\varepsilon^2 + \sigma_m^2) \varphi(\theta_r - A, \sigma_\varepsilon^2) dA \quad (\text{Eq. A-15})$$

$$31 \quad = \varphi(D_m - \theta_r, 2\sigma_\varepsilon^2 + \sigma_m^2) \quad (\text{Eq. A-16})$$

32  
 33  
 34 Therefore, for the “mouse-based” prior, use the mean  $D_m$  from the mouse, and then the variance  
 35 from the mouse  $\sigma_m^2$  plus twice the “allometric scatter” variance  $\sigma_\varepsilon^2$ .

*This document is a draft for review purposes only and does not constitute Agency policy.*

1 The rat “data” and variance, assuming conditional independence of the rat and mouse “pseudo-  
2 data,” is thus

$$3 P(\theta_r | D_m, D_r) \propto P(\theta_r | D_m) P(D_r | \theta_r) \quad (\text{Eq. A-17})$$

$$4 \propto \varphi(D_m - \theta_r, 2\sigma_\varepsilon^2 + \sigma_m^2) \varphi(D_r - \theta_r, \sigma_r^2) \quad (\text{Eq. A-18})$$

6 This distribution is also normal with

$$7 E(\theta_r) = \{D_m/(2\sigma_\varepsilon^2 + \sigma_m^2) + D_r/\sigma_r^2\} / \{1/(2\sigma_\varepsilon^2 + \sigma_m^2) + 1/\sigma_r^2\} = \text{weighted mean of } D_r \quad (\text{Eq. A-19})$$

$$8 \text{VAR}(\theta_r) = \{1/(2\sigma_\varepsilon^2 + \sigma_m^2) + 1/\sigma_r^2\}^{-1} = \text{harmonic mean of variances} \quad (\text{Eq. A-20})$$

9 Thus, using the mean and variance of the posterior distribution from the MCMC analysis,  
10  $D_r$  and  $\sigma_r^2$  can be derived.

11 Now,  $D_m$ ,  $\sigma_m^2$ ,  $D_r$ , and  $\sigma_r^2$  are known, so the analogous “mouse+rat” based prior used in  
12 the human model can be derived. As with the rat prior, the human prior is based on a normal  
13 approximation of the posterior for  $A$ , and then incorporates a random term for cross-species  
14 variation (allometric scatter).

$$15 P(A, \theta_m, \theta_r, \theta_h | D_m, D_r, D_h)$$

$$16 \propto P(A) P(\theta_m | A) P(D_m | \theta_m) P(\theta_r | A) P(D_r | \theta_r) P(\theta_h | A) P(D_h | \theta_h) \quad (\text{Eq. A-21})$$

$$17 \propto \varphi(\theta_m - A, \sigma_\varepsilon^2) \varphi(D_m - \theta_m, \sigma_m^2) \varphi(\theta_r - A, \sigma_\varepsilon^2) \varphi(D_r - \theta_r, \sigma_r^2) \quad (\text{Eq. A-22})$$

$$18 \varphi(\theta_h - A, \sigma_\varepsilon^2) \varphi(D_h - \theta_h, \sigma_h^2)$$

19 Consider marginalizing first over  $\theta_m$ , then over  $\theta_r$ , and then over  $A$ :

$$20 \int P(A, \theta_m, \theta_r, \theta_h | D_m, D_r, D_h) d\theta_m d\theta_r dA$$

$$21 \propto \left[ \int P(A) \{ \int P(\theta_m | A) P(D_m | \theta_m) d\theta_m \} \{ \int P(\theta_r | A) P(D_r | \theta_r) d\theta_r \} P(\theta_h | A) dA \right] P(D_h | \theta_h) \quad (\text{Eq. A-23})$$

$$22 = \left[ \int P(A) P(D_m | A) P(D_r | A) P(\theta_h | A) dA \right] P(D_h | \theta_h) \quad (\text{Eq. A-24})$$

$$23 \propto \left[ \int P(A | D_m D_r) P(\theta_h | A) dA \right] P(D_h | \theta_h) \quad (\text{Eq. A-25})$$

$$24 = P(\theta_h | D_m D_r) P(D_h | \theta_h) \quad (\text{Eq. A-26})$$

25 So  $P(\theta_h | D_m D_r)$  is the prior for  $\theta_h$  based on the mouse and rat data, and  $P(D_h | \theta_h)$  as the  
26 human-specific likelihood. The prior is used in the MCMC analysis for the humans, and it is  
27 derived to be

28 *This document is a draft for review purposes only and does not constitute Agency policy.*

$$P(\theta_h | D_m D_r) \propto \int \varphi(\theta_m - A, \sigma_\varepsilon^2) \varphi(D_m - \theta_m, \sigma_m^2) \varphi(\theta_r - A, \sigma_\varepsilon^2) \varphi(D_r - \theta_r, \sigma_r^2) \quad (\text{Eq. A-27})$$

$$\varphi(\theta_h - A, \sigma_\varepsilon^2) d\theta_m d\theta_r dA$$

$$= \int [\varphi(D_m - A, \sigma_\varepsilon^2 + \sigma_m^2) \varphi(D_r - A, \sigma_\varepsilon^2 + \sigma_r^2)] \varphi(\theta_h - A, \sigma_\varepsilon^2) dA \quad (\text{Eq. A-28})$$

$$\propto \int \varphi(D_{m+r} - A, \sigma_{m+r}^2) \varphi(\theta_h - A, \sigma_\varepsilon^2) dA \quad (\text{Eq. A-29})$$

$$= \varphi(D_{m+r} - \theta_h, \sigma_{m+r}^2 + \sigma_\varepsilon^2) \quad (\text{Eq. A-30})$$

where  $D_{m+r}$  and  $\sigma_{m+r}^2$  are the weighted mean and variances of  $A$  under the density

$$[\varphi(D_m - A, \sigma_\varepsilon^2 + \sigma_m^2) \varphi(D_r - A, \sigma_\varepsilon^2 + \sigma_r^2)] \quad (\text{Eq. A-31})$$

which is given by

$$D_{m+r} = E(A | D_m D_r) = \{D_m/(\sigma_\varepsilon^2 + \sigma_m^2) + D_r/(\sigma_\varepsilon^2 + \sigma_r^2)\} / \{1/(\sigma_\varepsilon^2 + \sigma_m^2) + 1/(\sigma_\varepsilon^2 + \sigma_r^2)\}$$

$$= \text{weighted mean of } D_m \text{ and } D_r \quad (\text{Eq. A-32})$$

$$\sigma_{m+r}^2 = \text{VAR}(A | D_m D_r) = \{1/(\sigma_\varepsilon^2 + \sigma_m^2) + 1/(\sigma_\varepsilon^2 + \sigma_r^2)\}^{-1} \quad (\text{Eq. A-33})$$

= harmonic mean of variances

At this point, these values are used in the normal approximation of the combined rodent posterior, which will be incorporated into the cross-species extrapolation as described in Step 5 above.

The results of these calculations for the updated prior distributions, are shown in Table A-6. With this methodology for updating the prior distributions, adequate convergence was achieved for the rat and human after 110,000~140,000 iterations.

#### A.4.2.3. Population Variance: Prior Central Estimates and Uncertainty

The following multipage Table A-7 describes the uncertainty distributions used for the population variability in the PBPK model parameters.

1  
2  
3

**Table A-7. Uncertainty distributions for the population variance of the PBPK model parameters**

Scaling (sampled) parameter	Mouse		Rat		Human		Notes/ source
	CV	CU	CV	CU	CV	CU	
<b>Flows</b>							
InQCC	0.2	2	0.14	2	0.2	2	a
InVPRC	0.2	2	0.3	2	0.2	2	
InDRespC	0.2	0.5	0.2	0.5	0.2	0.5	
<b>Physiological blood flows to tissues</b>							
QFatC	0.46	0.5	0.46	0.5	0.46	0.5	a
QGutC	0.17	0.5	0.17	0.5	0.18	0.5	
QLivC	0.17	0.5	0.17	0.5	0.45	0.5	
QSIwC	0.29	0.5	0.3	0.5	0.32	0.5	
QKidC	0.32	0.5	0.13	0.5	0.12	0.5	
FracPlasC	0.2	0.5	0.2	0.5	0.05	0.5	
<b>Physiological volumes</b>							
VFatC	0.45	0.5	0.45	0.5	0.45	0.5	a
VGutC	0.13	0.5	0.13	0.5	0.08	0.5	
VLivC	0.24	0.5	0.18	0.5	0.23	0.5	
VRapC	0.1	0.5	0.12	0.5	0.08	0.5	
VRespLumC	0.11	0.5	0.18	0.5	0.2	0.5	
VRespEffC	0.11	0.5	0.18	0.5	0.2	0.5	
VKidC	0.1	0.5	0.15	0.5	0.17	0.5	
VBldC	0.12	0.5	0.12	0.5	0.12	0.5	
<b>TCE distribution/partitioning</b>							
InPBC	0.25	2	0.25	0.333	0.185	0.333	b
InPFatC	0.3	2	0.3	0.333	0.2	1	
InPGutC	0.4	2	0.4	2	0.4	2	
InPLivC	0.4	2	0.15	0.333	0.4	1.414	
InPRapC	0.4	2	0.4	2	0.4	2	
InPRespC	0.4	2	0.4	2	0.4	2	
InPKidC	0.4	2	0.3	0.577	0.2	1.414	
InPSIwC	0.4	2	0.3	0.333	0.3	1.414	
<b>TCA distribution/partitioning</b>							
InPRBCPlasTCAC	0.336	2	0.336	2	0.336	2	c
InPBodTCAC	0.336	2	0.693	2	0.336	2	b
InPLivTCAC	0.336	2	0.693	2	0.336	2	
<b>TCA plasma binding</b>							
InkDissocC	1.191	2	0.61	2	0.06	2	b
InBMaxkDC	0.495	2	0.47	2	0.182	2	

*This document is a draft for review purposes only and does not constitute Agency policy.*

**Table A-7. Uncertainty distributions for the population variance of the PBPK model parameters (continued)**

Scaling (sampled) parameter	Mouse		Rat		Human		Notes/ source
	CV	CU	CV	CU	CV	CU	
<b>TCOH and TCOG distribution/partitioning</b>							
InPBodTCOHC	0.336	2	0.693	2	0.336	2	b
InPLivTCOHC	0.336	2	0.693	2	0.336	2	b
InPBodTCOGC	0.4	2	0.4	2	0.4	2	d
InPLivTCOGC	0.4	2	0.4	2	0.4	2	d
<b>DCVG distribution/partitioning</b>							
InPeffDCVG	0.4	2	0.4	2	0.4	2	b
<b>TCE metabolism</b>							
InV <sub>MAX</sub> C	0.824	1	0.806	1	0.708	0.26	e
InK <sub>M</sub> C	0.270	1	1.200	1			
InCIC					0.944	1.41	
InFracOtherC	0.5	2	0.5	2	0.5	2	f
InFracTCAC	0.5	2	0.5	2	1.8	2	g
InV <sub>MAX</sub> DCVGC	0.5	2	0.5	2			f
InCIDCVGC	0.5	2	0.5	2	0.5	2	
InK <sub>M</sub> DCVGC					0.5	2	
InV <sub>MAX</sub> KidDCVGC	0.5	2	0.5	2			
InCIKidDCVGC	0.5	2	0.5	2	0.5	2	
InK <sub>M</sub> KidDCVGC					0.5	2	
InV <sub>MAX</sub> LungLivC	0.5	2	0.5	2	0.5	2	
InK <sub>M</sub> Clara	0.5	2	0.5	2	0.5	2	
InFracLungSysC	0.5	2	0.5	2	0.5	2	
<b>TCOH metabolism</b>							
InV <sub>MAX</sub> TCOHC	0.5	2	0.5	2			f
InCITCOHC					0.5	2	
InK <sub>M</sub> TCOH	0.5	2	0.5	2	0.5	2	
InV <sub>MAX</sub> GlucC	0.5	2	0.5	2			
InCIGlucC					0.5	2	
InK <sub>M</sub> Gluc	0.5	2	0.5	2	0.5	2	
InkMetTCOHC	0.5	2	0.5	2	0.5	2	
<b>TCA metabolism/clearance</b>							
InkUrnTCAC	0.5	2	0.5	2	0.5	2	f
InkMetTCAC	0.5	2	0.5	2	0.5	2	
<b>TCOG metabolism/clearance</b>							
InkBileC	0.5	2	0.5	2	0.5	2	f
InkEHRC	0.5	2	0.5	2	0.5	2	

*This document is a draft for review purposes only and does not constitute Agency policy.*

**Table A-7. Uncertainty distributions for the population variance of the PBPK model parameters (continued)**

Scaling (sampled) parameter	Mouse		Rat		Human		Notes/ source
	CV	CU	CV	CU	CV	CU	
InkUrnTCOGC	0.5	2	0.5	2	0.5	2	<sup>f</sup>
<b>DCVG metabolism/clearance</b>							
InFracKidDCVCC	0.5	2	0.5	2	0.5	2	<sup>f</sup>
InkDCVGC	0.5	2	0.5	2	0.5	2	
<b>DCVC metabolism/clearance</b>							
InkNATC	0.5	2	0.5	2	0.5	2	<sup>f</sup>
InkKidBioactC	0.5	2	0.5	2	0.5	2	
<b>Oral uptake/transfer coefficients</b>							
InkTSD	2	2	2	2	2	2	<sup>h</sup>
InkAS	2	2	2	2	2	2	
InkTD	2	2	2	2	2	2	
InkAD	2	2	2	2	2	2	
InkASTCA	2	2	2	2	2	2	
InkASTCOH	2	2	2	2	2	2	

**Explanatory note.** All population variance parameters (V\_pname, for parameter “pname”) have Inverse-Gamma distributions, with the expected value given by CV and coefficient of uncertainty given by CU (i.e., standard deviation of V\_pname divided by expected value of V\_pname) (notation the same as Hack et al. [2006]). Under these conditions, the Inverse-Gamma distribution has a shape parameter is given by  $\alpha = 2 + 1/CU^2$  and scale parameter  $\beta = (\alpha - 1) CV^2$ . In addition, it should be noted that, under a normal distribution and a uniform prior distribution on the population variance, the posterior distribution for the variance given  $n$  data points with a sample variance  $s^2$  is given by and Inverse-Gamma distribution with  $\alpha = (n - 1)/2$  and  $\beta = \alpha s^2$ . Therefore, the “effective” number of data points is given by  $n = 5 + 2/CU^2$  and the “effective” sample variance is  $s^2 = CV^2 \alpha / (\alpha - 1)$ .

<sup>a</sup>For physiological parameters, CV values generally taken to be equal to the uncertainty SD in the population mean, most of which were based on variability between studies (i.e., not clear whether variability represents uncertainty or variability). Given this uncertainty, CU of 2 assigned to cardiac output and ventilation-perfusion, while CU of 0.5 assigned to the remaining physiological parameters.

<sup>b</sup>As discussed above, it is not clear whether interstudy variability is due to interindividual or assay variability, so the same central were assigned to the uncertainty in the population mean as to the central estimate of the population variance. In the cases were direct measurements were available, the CU for the uncertainty in the population variance is based on the actual sample  $n$ , with the derivation discussed in the notes preceding this table.

Otherwise, a CU of 2 was assigned, reflecting high uncertainty.

<sup>c</sup>Used value from uncertainty in population in mean in rats for all species with high uncertainty.

<sup>d</sup>No data, so assumed CV of 0.4 with high uncertainty.

<sup>e</sup>For mice and rats, based on variability in results from Lipscomb et al. (1998a) and Elfarra et al. (1998) in microsomes. Since only pooled or mean values are available, CU of 1 was assigned (moderate uncertainty). For humans, based on variability in *individual* samples from Lipscomb et al. (1997) (microsomes), Elfarra et al. (1998) (microsomes) and Lipscomb et al. (1998a) (freshly isolated hepatocytes). High uncertainty in clearance (InkCIC) reflects two different methods for scaling concentrations in microsomal preparations to blood concentrations: (1) assuming microsomal concentration equals liver concentration and then using the measured liver: blood partition coefficient to convert to blood and (2) using the measured microsomes: air partition coefficient and then using the measured blood: air partition coefficient to convert to blood.

<sup>f</sup>No data on variability, so a CV of 0.5 was assigned, with a CU of 2.

*This document is a draft for review purposes only and does not constitute Agency policy.*



1 **Table A-7. Uncertainty distributions for the population variance of the**  
2 **BPBK model parameters (continued)**  
3

4 <sup>§</sup>For mice and rats, no data on variability, so a CV of 0.5 was assigned, with a CU of 2. For humans, 6-fold  
5 variability based on *in vitro* data from Bronley-DeLancy et al. (2006), but with high uncertainty.

6 <sup>h</sup>No data on variability, so a CV of 2 was assigned (larger than assumed for metabolism due to possible vehicle  
7 effects), with a CU of 2.  
8  
9

10 **A.4.2.4. Prior distributions for Residual Error Estimates**

11 In all cases except one, the likelihood was assumed to be lognormal, which requires  
12 specification of the variance of the “residual error.” This error may include variability due to  
13 measurement error, intraindividual and intrastudy heterogeneity, as well as model  
14 misspecification. The available *in vivo* measurements to which the model was calibrated are  
15 listed in Table A-8. The variances for each of the corresponding residual errors were given log-  
16 uniform distributions. For all measurements, the bounds on the log-uniform distribution was  
17 0.01 and 3.3, corresponding to geometric standard deviations bounded by 1.11 and 6.15. The  
18 lower bound was set to prevent “over-fitting,” as was done in Bois (2000a) and Hack et al.  
19 (2006).

20 Nondetects of DCVG from Lash et al. (1999b) were also included in the data, at it was  
21 found that these data were needed to place constraints on the clearance rate of DCVG from  
22 blood. The detection limit reported in the study was  $LD = 0.05 \text{ pmol/mL} = 5 \times 10^{-5} \text{ mmol/L}$ . It  
23 was assumed, as is standard in analytical chemistry, that the detection limit represents a response  
24 from a blank sample at 3-standard deviations. Because detector responses near the detection  
25 limit are generally normally distributed, the likelihood for observing a nondetect given a model-  
26 predicted value of  $y_p$  is equal to  $P(\text{ND}|y_p) = \Phi(3 \times \{1 - y_p/LD\})$ , where  $\Phi(y)$  is the cumulative  
27 standard normal distribution.

28 The rat and human models differed from mouse model in terms of the hierarchical  
29 structure of the residual errors. In the mouse model, all the studies were assumed to have the  
30 same residual error, as shown in Figure A-1. This appeared reasonable because there were fewer  
31 studies, and there appeared to be less variation between studies. In the rat and human models,  
32 each of which used a much larger database of *in vivo* studies, residual errors were assumed to be  
33 the same within a study, but may differ between studies. The updated hierarchical structures are  
34 shown in Figure A-6. Initial attempts to use a single set of residual errors led to large residual  
35 errors for some measurements, even though fits to many studies appeared reasonable. Residual  
36 errors were generally reduced when study-specific errors were used, except for some datasets  
37 that appeared to be outliers (discussed below).  
38

*This document is a draft for review purposes only and does not constitute Agency policy.*

1  
2

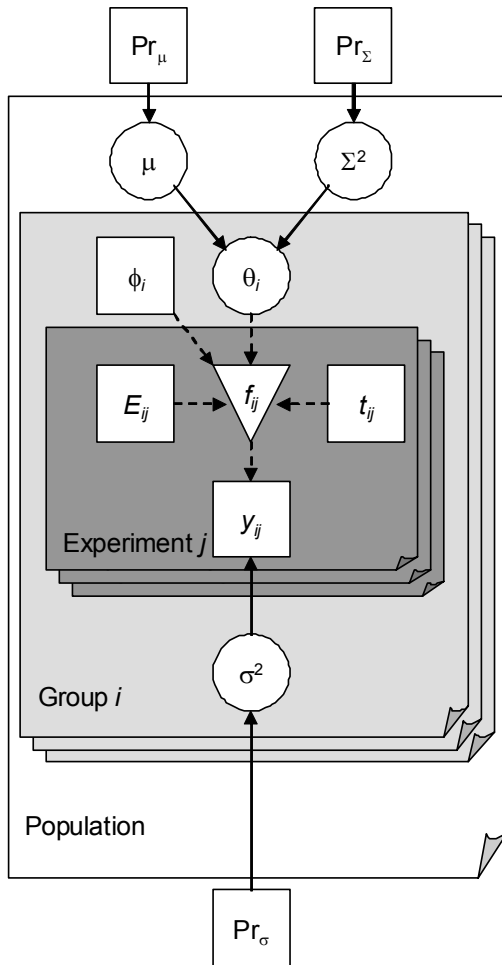
**Table A-8. Measurements used for calibration**

Measurement abbreviation	Mouse	Rat	Human	Measurement description
RetDose			√	Retained TCE dose (mg)
CAIvPPM			√	TCE concentration in alveolar air (ppm)
CIInhPPM	√	√		TCE concentration in closed chamber (ppm)
CArt		√		TCE concentration in arterial blood (mg/L)
CVen	√	√	√	TCE concentration in venous blood (mg/L)
CBldMix	√	√		TCE concentration in mixed arterial and venous blood (mg/L)
CFat	√	√		TCE concentration in fat (mg/L)
CGut		√		TCE concentration in gut (mg/L)
CKid	√	√		TCE concentration in kidney (mg/L)
CLiv	√	√		TCE concentration in liver (mg/L)
CMus		√		TCE concentration in muscle (mg/L)
AExhpost	√	√		Amount of TCE exhaled postexposure (mg)
CTCOH	√	√	√	Free TCOH concentration in blood (mg/L)
CLivTCOH	√			Free TCOH concentration in liver (mg/L)
CPlasTCA	√	√	√	TCA concentration in plasma (mg/L)
CBldTCA	√	√	√	TCA concentration in blood (mg/L)
CLivTCA	√	√		TCA concentration in liver (mg/L)
AUrnTCA	√	√	√	Cumulative amount of TCA excreted in urine (mg)
AUrnTCA_collect			√	Cumulative amount of TCA collected in urine (noncontinuous sampling) (mg)
ABileTCOG		√		Cumulative amount of bound TCOH excreted in bile (mg)
CTCOG		√		Bound TCOH concentration in blood (mg/L)
CTCOGTCOH	√			Bound TCOH concentration in blood in free TCOH equivalents (mg/L)
CLivTCOGTCOH	√			Bound TCOH concentration in liver in free TCOH equivalents (mg/L)
AUrnTCOGTCOH	√	√	√	Cumulative amount of total TCOH excreted in urine (mg)
AUrnTCOGTCOH_collect			√	Cumulative amount of total TCOH collected in urine (noncontinuous sampling) (mg)
CDCVGmol			√	DCVG concentration in blood (mmol/L)
CDCVG_ND			√	DCVG nondetects from Lash et al. (1999b)
AUrnNDCVC		√	√	Cumulative amount of NAcDCVC excreted in urine (mg)
AUrnTCTotMole		√		Cumulative amount of TCA+total TCOH excreted in urine (mmol)
TotCTCOH	√	√	√	Total TCOH concentration in blood (mg/L)

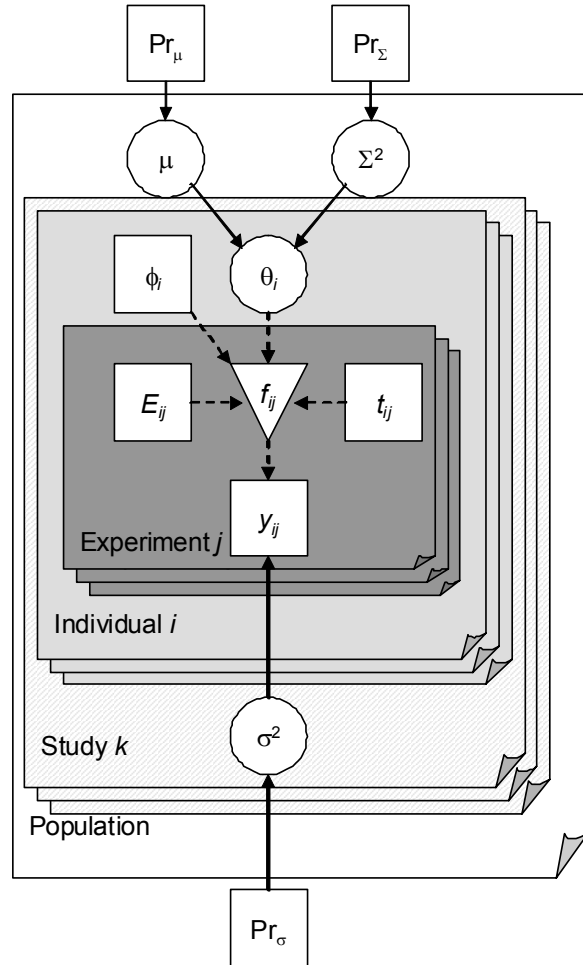
3

*This document is a draft for review purposes only and does not constitute Agency policy.*

1 Rat



Human



2

3

4 **Figure A-6. Updated hierarchical structure for rat and human models.**

5 Symbols have the same meaning as Figure A-1, with modifications for the rat and  
6 human. In particular, in the rat, each “group” consists of animals (usually  
7 comprising multiple dose groups) of the same sex, species, and strain within a  
8 study (possibly reported in more than one publication, but reasonably presumed to  
9 be of animals in the same “lot”). Animals within each group are presumed to be  
10 “identical,” with the same PBPK model parameters, and each such group is  
11 assigned its own set of “residual” error variances  $\sigma^2$ . In humans, each  
12 “individual” is a single person, possibly exposed in multiple experiments, and  
13 each individual is assigned a set of PBPK model parameters drawn from the  
14 population. However, in humans, “residual” error variances are assigned at the  
15 “study” level, rather than the individual or the population level.

1 **A.5. RESULTS OF UPDATED PHYSIOLOGICALLY BASED PHARMACOKINETIC**  
2 **(PBPK) MODEL**

3 The evaluation of the updated PBPK model was discussed in Chapter 3. Detailed results  
4 in the form of tables and figures are provided in this section.

5  
6 **A.5.1. Convergence and Posterior Distributions of Sampled Parameters**

7 For each sampled parameter (population mean and variance and the variance for residual  
8 errors), summary statistics (median, [2.5%, 97.5%] confidence interval) for the posterior  
9 distribution are tabulated in Tables A-9–A-14 below. In addition, the potential scale reduction  
10 factor  $R$ , calculated from comparing four independent chains, is given.

11 In addition, posterior distributions for the group- or individual-specific parameters are  
12 summarized in supplementary figures accessible here:

- 13  
14 • **Mouse:** [Appendix.linked.files\AppA.5.1.Mouse.posterior.by.group.pdf](#)  
15 • **Rat:** [Appendix.linked.files\AppA.5.1.Rat.posterior.by.group.pdf](#)  
16 • **Human:** [Appendix.linked.files\AppA.5.1.Human.posterior.by.group.or.individual.pdf](#)

17  
18 **A.5.2. Comparison of Model Predictions With Data**

19 **A.5.2.1. Mouse Model**

20 **A.5.2.1.1. Group-specific predictions and calibration data.** [See  
21 [Appendix.linked.files\AppA.5.2.1.1.Updated.mouse.group.calib.TCE.DRAFT.pdf.](#)]

22  
23 **A.5.2.1.2. Population-based predictions and calibration data.** [See  
24 [Appendix.linked.files\AppA.5.2.1.2.Updated.mouse.pop.calib.TCE.DRAFT.pdf.](#)]

25  
26 **A.5.2.2. Rat Model**

27 **A.5.2.2.1. Group-specific predictions and calibration data.** [See  
28 [Appendix.linked.files\AppA.5.2.2.1.Updated.rat.group.calib.TCE.DRAFT.pdf.](#)]

29  
30 **A.5.2.2.2. Population-based predictions and calibration data.** [See  
31 [Appendix.linked.files\AppA.5.2.2.2.Updated.rat.pop.calib.TCE.DRAFT.pdf.](#)]

32  
33 **A.5.2.2.3. Population-based predictions and additional evaluation data.** [See  
34 [Appendix.linked.files\AppA.5.2.2.3.Updated.rat.pop.eval.TCE.DRAFT.pdf.](#)]

1  
2  
3

**Table A-9. Posterior distributions for mouse PBPK model population parameters**

Sampled parameter*	Posterior distributions reflecting uncertainty in population distribution			
	Population (geometric) mean		Population (geometric) standard deviation	
	Median (2.5%, 97.5%)	R	Median (2.5%, 97.5%)	R
InQCC	1.237 (0.8972, 1.602)	1	1.402 (1.183, 2.283)	1
InVPRC	0.8076 (0.6434, 1.022)	1	1.224 (1.108, 1.63)	1.001
QFatC	1.034 (0.5235, 1.55)	1	0.436 (0.3057, 0.6935)	1
QGutC	1.183 (1.002, 1.322)	1	0.1548 (0.1101, 0.2421)	1
QLivC	1.035 (0.8002, 1.256)	1	0.1593 (0.1107, 0.2581)	1
QSlwC	0.9828 (0.6043, 1.378)	1	0.275 (0.1915, 0.4425)	1
InDRespC	1.214 (0.7167, 2.149)	1.002	1.215 (1.143, 1.375)	1
QKidC	0.995 (0.5642, 1.425)	1	0.3001 (0.21, 0.48)	1
FracPlasC	0.8707 (0.5979, 1.152)	1.001	0.1903 (0.1327, 0.3039)	1
VFatC	1.329 (0.8537, 1.784)	1.002	0.4123 (0.2928, 0.6414)	1
VGutC	0.9871 (0.817, 1.162)	1	0.1219 (0.085, 0.1965)	1
VLivC	0.8035 (0.5609, 1.093)	1.013	0.2216 (0.1552, 0.3488)	1
VRapC	0.997 (0.8627, 1.131)	1	0.09384 (0.06519, 0.1512)	1
VRespLumC	0.9995 (0.8536, 1.145)	1	0.1027 (0.07172, 0.1639)	1
VRespEffC	1 (0.8537, 1.148)	1.001	0.1032 (0.07176, 0.1652)	1
VKidC	1.001 (0.8676, 1.134)	1	0.09365 (0.06523, 0.1494)	1
VBldC	0.9916 (0.8341, 1.153)	1.001	0.1126 (0.07835, 0.1817)	1
InPBC	0.9259 (0.647, 1.369)	1	1.644 (1.278, 3.682)	1
InPFatC	0.9828 (0.7039, 1.431)	1.001	1.321 (1.16, 2.002)	1.001
InPGutC	0.805 (0.4735, 1.418)	1	1.375 (1.198, 2.062)	1
InPLivC	1.297 (0.7687, 2.039)	1	1.415 (1.21, 2.342)	1
InPRapC	0.9529 (0.5336, 1.721)	1	1.378 (1.203, 2.141)	1
InPRespC	0.9918 (0.5566, 1.773)	1.001	1.378 (1.2, 2.066)	1
InPKidC	1.277 (0.7274, 2.089)	1	1.554 (1.265, 2.872)	1
InPSlwC	0.92 (0.5585, 1.586)	1.001	1.411 (1.209, 2.3)	1.001
InPRBCPlasTCAC	2.495 (1.144, 5.138)	1.001	1.398 (1.178, 2.623)	1.001
InPBodTCAC	0.8816 (0.6219, 1.29)	1.003	1.27 (1.158, 1.609)	1
InPLivTCAC	0.8003 (0.5696, 1.15)	1.003	1.278 (1.157, 1.641)	1.001
InkDissocC	1.214 (0.2527, 4.896)	1.003	2.71 (1.765, 8.973)	1
InBMaxkDC	1.25 (0.6793, 2.162)	1.002	1.474 (1.253, 2.383)	1
InPBodTCOHC	0.8025 (0.5607, 1.174)	1	1.314 (1.17, 1.85)	1.001
InPLivTCOHC	1.526 (0.9099, 2.245)	1	1.399 (1.194, 2.352)	1
InPBodTCOGC	0.4241 (0.1555, 1.053)	1.004	1.398 (1.207, 2.156)	1
InPLivTCOGC	1.013 (0.492, 2.025)	1.002	1.554 (1.279, 2.526)	1
InPeffDCVG	0.9807 (0.008098, 149.6)	1.041	1.406 (1.206, 2.379)	1

*This document is a draft for review purposes only and does not constitute Agency policy.*

**Table A-9. Posterior distributions for mouse PBPK model population parameters (continued)**

Sampled parameter*	Posterior distributions reflecting uncertainty in population distribution			
	Population (geometric) mean		Population (geometric) standard deviation	
	Median (2.5%, 97.5%)	R	Median (2.5%, 97.5%)	R
InkTSD	5.187 (0.3909, 69.34)	1.001	5.858 (2.614, 80)	1
InkAS	1.711 (0.3729, 11.23)	1.001	4.203 (2.379, 18.15)	1
InkTD	0.1002 (0.01304, 0.7688)	1	5.16 (2.478, 60.24)	1
InkAD	0.2665 (0.05143, 1.483)	1.003	4.282 (2.378, 20.21)	1
InkASTCA	3.986 (0.1048, 141.9)	1	5.187 (2.516, 58.72)	1
InkASTCOH	0.7308 (0.006338, 89.75)	1.001	5.047 (2.496, 54.8)	1
InV <sub>MAX</sub> C	0.6693 (0.4093, 1.106)	1.005	1.793 (1.49, 2.675)	1
InK <sub>M</sub> C	0.07148 (0.0323, 0.1882)	1	2.203 (1.535, 4.536)	1.001
InFracOtherC	0.02384 (0.003244, 0.1611)	1.006	1.532 (1.265, 2.971)	1
InFracTCAC	0.4875 (0.2764, 0.8444)	1.002	1.474 (1.258, 2.111)	1
InV <sub>MAX</sub> DCVGC	1.517 (0.02376, 1,421)	1.001	1.53 (1.263, 2.795)	1
InCIDCVGC	0.1794 (0.02333, 79.69)	1.013	1.528 (1.261, 2.922)	1
InV <sub>MAX</sub> KidDCVGC	1.424 (0.04313, 704.9)	1.014	1.533 (1.262, 2.854)	1
InCIKidDCVGC	0.827 (0.04059, 167.2)	1.019	1.527 (1.263, 2.874)	1
InV <sub>MAX</sub> LungLivC	2.903 (0.487, 12.1)	1.001	4.157 (1.778, 29.01)	1.018
InK <sub>M</sub> Clara	0.01123 (0.001983, 0.09537)	1.012	1.629 (1.278, 5.955)	1.003
InFracLungSysC	3.304 (0.2619, 182.1)	1.011	1.543 (1.266, 3.102)	1.001
InV <sub>MAX</sub> TCOHC	1.645 (0.6986, 3.915)	1.005	1.603 (1.28, 2.918)	1
InK <sub>M</sub> TCOH	0.9594 (0.2867, 2.778)	1.007	1.521 (1.264, 2.626)	1
InV <sub>MAX</sub> GlucC	65.59 (27.58, 232.5)	1.018	1.487 (1.254, 2.335)	1
InK <sub>M</sub> Gluc	31.16 (6.122, 137.3)	1.015	1.781 (1.299, 5.667)	1.002
InkMetTCOHC	3.629 (0.7248, 9.535)	1.009	1.527 (1.265, 2.626)	1
InkUrnTCAC	0.1126 (0.04083, 0.2423)	1.012	1.757 (1.318, 3.281)	1.003
InkMetTCAC	0.6175 (0.2702, 1.305)	1.027	1.508 (1.262, 2.352)	1.002
InkBileC	0.9954 (0.316, 3.952)	1.003	1.502 (1.26, 2.453)	1
InkEHRC	0.01553 (0.001001, 0.0432)	1.008	1.534 (1.264, 2.767)	1
InkUrnTCOGC	7.874 (2.408, 50.28)	1	3.156 (1.783, 12.18)	1.001
InFracKidDCVCC	1.931 (0.01084, 113.7)	1.018	1.53 (1.264, 2.77)	1
InkDCVGC	0.2266 (0.001104, 16.46)	1.011	1.525 (1.263, 2.855)	1
InkNATC	0.1175 (0.0008506, 14.34)	1.024	1.528 (1.264, 2.851)	1
InkKidBioactC	0.07506 (0.0009418, 12.35)	1.035	1.527 (1.263, 2.84)	1.001

2  
3  
4  
5  
6  
\*These “sampled parameters” are scaled one or more times (see Table A-4) to obtain a biologically-meaningful parameter, posterior distributions of which are summarized in Tables 3-36 through 3-40). For natural log transformed parameters (name starting with “In”), values are for the population geometric means and standard deviations.

*This document is a draft for review purposes only and does not constitute Agency policy.*

1  
2

**Table A-10. Posterior distributions for mouse residual errors**

Measurement	Residual error geometric standard deviation	
	Median (2.5%, 97.5%)	R
<b>CLnhPPM</b>	1.177 (1.16, 1.198)	1.001
<b>CVen</b>	2.678 (2.354, 3.146)	1.001
<b>CBldMix</b>	1.606 (1.415, 1.96)	1.001
<b>CFat</b>	2.486 (2.08, 3.195)	1
<b>CKid</b>	2.23 (1.908, 2.796)	1
<b>CLiv</b>	1.712 (1.543, 1.993)	1
<b>AExhpost</b>	1.234 (1.159, 1.359)	1
<b>CTCOH</b>	1.543 (1.424, 1.725)	1
<b>CLivTCOH</b>	1.591 (1.454, 1.818)	1
<b>CPlasTCA</b>	1.396 (1.338, 1.467)	1.001
<b>CBldTCA</b>	1.488 (1.423, 1.572)	1.001
<b>CLivTCA</b>	1.337 (1.271, 1.43)	1
<b>AUrnTCA</b>	1.338 (1.259, 1.467)	1
<b>CTCOGTCOH</b>	1.493 (1.38, 1.674)	1.001
<b>CLivTCOGTCOH</b>	1.63 (1.457, 1.924)	1
<b>AUrnTCOGTCOH</b>	1.263 (1.203, 1.355)	1
<b>TotCTCOH</b>	1.846 (1.506, 2.509)	1.002

3  
4

Note: the hierarchical statistical model for residual errors did not separate by group.

1  
2  
3

**Table A-11. Posterior distributions for rat PBPK model population parameters**

Sampled parameter	Posterior distributions reflecting uncertainty in population distribution			
	Population (geometric) mean		Population (geometric) standard deviation	
	Median (2.5%, 97.5%)	R	Median (2.5%, 97.5%)	R
InQCC	1.195 (0.9285, 1.448)	1.034	1.298 (1.123, 2.041)	1.031
InVPRC	0.6304 (0.4788, 0.8607)	1.012	1.446 (1.247, 2.011)	1.005
QFatC	1.167 (0.8321, 1.561)	1	0.4119 (0.2934, 0.6438)	1
QGutC	1.154 (0.988, 1.306)	1	0.1613 (0.1132, 0.2542)	1
QLivC	1.029 (0.8322, 1.223)	1.002	0.1551 (0.1092, 0.2483)	1
QSlwC	0.9086 (0.5738, 1.251)	1.001	0.2817 (0.1968, 0.4493)	1
InDRespC	2.765 (1.391, 5.262)	1.018	1.21 (1.142, 1.358)	1.001
QKidC	1.002 (0.8519, 1.152)	1.001	0.1185 (0.08284, 0.1871)	1
FracPlasC	1.037 (0.8071, 1.259)	1.002	0.1785 (0.1272, 0.2723)	1
VFatC	0.9728 (0.593, 1.378)	1	0.4139 (0.2924, 0.6552)	1.002
VGutC	0.9826 (0.8321, 1.137)	1	0.1187 (0.08296, 0.1873)	1
VLivC	0.9608 (0.7493, 1.19)	1.015	0.1682 (0.1168, 0.2718)	1.001
VRapC	0.9929 (0.8563, 1.133)	1.001	0.1093 (0.07693, 0.175)	1
VRespLumC	1.001 (0.7924, 1.21)	1	0.1636 (0.116, 0.2601)	1
VRespEffC	0.999 (0.7921, 1.208)	1.001	0.1635 (0.1161, 0.2598)	1
VKidC	0.999 (0.8263, 1.169)	1	0.1361 (0.09617, 0.2167)	1
VBldC	1.002 (0.8617, 1.141)	1	0.1096 (0.07755, 0.176)	1
InPBC	0.8551 (0.6854, 1.065)	1.001	1.317 (1.232, 1.462)	1.001
InPFatC	1.17 (0.8705, 1.595)	1.003	1.333 (1.247, 1.481)	1.001
InPGutC	0.8197 (0.5649, 1.227)	1	1.362 (1.198, 1.895)	1
InPLivC	1.046 (0.8886, 1.234)	1.001	1.152 (1.115, 1.214)	1
InPRapC	1.021 (0.6239, 1.675)	1.002	1.373 (1.201, 1.988)	1
InPRespC	0.993 (0.5964, 1.645)	1.001	1.356 (1.197, 1.948)	1
InPKidC	0.9209 (0.6728, 1.281)	1	1.304 (1.201, 1.536)	1
InPSlwC	1.258 (0.9228, 1.711)	1.001	1.364 (1.263, 1.544)	1
InPRBCPlasTCAC	0.9763 (0.6761, 1.353)	1	1.276 (1.159, 1.634)	1
InPBodTCAC	1.136 (0.6737, 1.953)	1.008	1.631 (1.364, 2.351)	1.003
InPLivTCAC	1.283 (0.6425, 2.491)	1.008	1.651 (1.356, 2.658)	1
InkDissocC	1.01 (0.5052, 2.017)	1.002	1.596 (1.315, 2.774)	1
InBMaxkDC	0.9654 (0.5716, 1.733)	1.02	1.412 (1.234, 2.01)	1
InPBodTCOHC	0.9454 (0.4533, 1.884)	1.045	1.734 (1.39, 3.151)	1.002
InPLivTCOHC	0.926 (0.3916, 2.196)	1.013	1.785 (1.382, 4.142)	1.003
InPBodTCOGC	1.968 (0.09185, 14.44)	1.031	1.414 (1.208, 2.571)	1
InPLivTCOGC	7.484 (2.389, 26.92)	1.017	1.41 (1.208, 2.108)	1
InkTSD	3.747 (0.2263, 62.58)	1.01	6.777 (2.844, 87.29)	1

*This document is a draft for review purposes only and does not constitute Agency policy.*



**Table A-11. Posterior distributions for rat PBPK model population parameters (continued)**

Sampled parameter	Posterior distributions reflecting uncertainty in population distribution			
	Population (geometric) mean		Population (geometric) standard deviation	
	Median (2.5%, 97.5%)	<i>R</i>	Median (2.5%, 97.5%)	<i>R</i>
InkAS	2.474 (0.2542, 28.35)	1.004	10.16 (4.085, 143.7)	1
InkAD	0.1731 (0.04001, 0.7841)	1.018	4.069 (2.373, 14.19)	1.009
InkASTCA	1.513 (0.1401, 17.19)	1.002	4.376 (2.43, 22.83)	1
InkASTCOH	0.6896 (0.01534, 25.81)	1.001	4.734 (2.444, 35.2)	1.001
InV <sub>MAX</sub> C	0.8948 (0.6377, 1.293)	1.028	1.646 (1.424, 2.146)	1.021
InK <sub>M</sub> C	0.0239 (0.01602, 0.04993)	1.001	2.402 (1.812, 4.056)	1.001
InFracOtherC	0.344 (0.0206, 1.228)	1.442	3 (1.332, 10.04)	1.353
InFracTCAC	0.2348 (0.122, 0.4616)	1.028	1.517 (1.264, 2.393)	1.001
InV <sub>MAX</sub> DCVGC	7.749 (0.2332, 458.8)	1.088	1.534 (1.262, 2.804)	1.001
InCIDCVGC	0.3556 (0.06631, 2.242)	1.018	1.509 (1.261, 2.553)	1
InV <sub>MAX</sub> KidDCVGC	0.2089 (0.04229, 1.14)	1.011	1.542 (1.263, 2.923)	1.001
InCIKidDCVGC	184 (26.29, 1312)	1.02	1.527 (1.265, 2.873)	1.001
InV <sub>MAX</sub> LungLivC	2.673 (0.4019, 14.16)	1.002	4.833 (1.599, 48.32)	1.002
InK <sub>M</sub> Clara	0.02563 (0.005231, 0.197)	1.01	1.66 (1.279, 18.74)	1.002
InFracLungSysC	2.729 (0.04124, 63.27)	1.027	1.536 (1.267, 2.868)	1.001
InV <sub>MAX</sub> TCOHC	1.832 (0.6673, 6.885)	1.041	1.667 (1.292, 3.148)	1.002
InK <sub>M</sub> TCOH	22.09 (3.075, 131.9)	1.186	1.629 (1.276, 3.773)	1.017
InV <sub>MAX</sub> GlucC	28.72 (10.02, 86.33)	1.225	2.331 (1.364, 5.891)	1.126
InK <sub>M</sub> Gluc	6.579 (1.378, 23.57)	1.119	2.046 (1.309, 10.3)	1.125
InkMetTCOHC	2.354 (0.3445, 15.83)	1.287	1.876 (1.283, 11.82)	1.182
InkUrnTCAC	0.07112 (0.03934, 0.1329)	1.076	1.513 (1.27, 2.327)	1.003
InkMetTCAC	0.3554 (0.1195, 0.8715)	1.036	1.528 (1.263, 2.444)	1.001
InkBileC	8.7 (1.939, 26.71)	1.05	1.65 (1.282, 5.494)	1.017
InkEHRC	1.396 (0.2711, 6.624)	1.091	1.647 (1.277, 5.582)	1.005
InkUrnTCOGC	20.65 (2.437, 138)	1.041	1.595 (1.269, 5.257)	1.026
InkNATC	0.002035 (0.0004799, 0.01019)	1.01	1.523 (1.261, 2.593)	1.001
InkKidBioactC	0.006618 (0.0009409, 0.0367)	1.039	1.52 (1.261, 2.674)	1

*This document is a draft for review purposes only and does not constitute Agency policy.*

**Table A-12. Posterior distributions for rat residual errors**

Measurement	Group	Residual error geometric standard deviation	
		Median (2.5%, 97.5%)	R
CInhPPM	Group 3	1.124 (1.108, 1.147)	1
	Group 16	1.106 (1.105, 1.111)	1
CMixExh	Group 2	1.501 (1.398, 1.65)	1
CArt	Group 2	1.174 (1.142, 1.222)	1
	Group 6	1.523 (1.321, 1.918)	1.002
CVen	Group 4	1.22 (1.111, 1.877)	1
	Group 7	1.668 (1.489, 1.986)	1.001
	Group 8	1.45 (1.234, 2.065)	1.014
	Group 9	1.571 (1.426, 1.811)	1
	Group 10	4.459 (2.754, 6.009)	1
	Group 11	1.587 (1.347, 2.296)	1.002
	Group 16	1.874 (1.466, 2.964)	1.011
	Group 18	1.676 (1.188, 3.486)	1.003
CBldMix	Group 12	1.498 (1.268, 2.189)	1
CFat	Group 9	1.846 (1.635, 2.184)	1
	Group 16	2.658 (1.861, 4.728)	1.001
CGut	Group 9	1.855 (1.622, 2.243)	1
CKid	Group 9	1.469 (1.354, 1.648)	1
CLiv	Group 9	1.783 (1.554, 2.157)	1
	Group 12	1.744 (1.401, 2.892)	1
	Group 16	1.665 (1.376, 2.411)	1.001
CMus	Group 9	1.653 (1.494, 1.919)	1
AExhpost	Group 6	1.142 (1.108, 1.239)	1.003
	Group 10	1.117 (1.106, 1.184)	1.004
	Group 14	1.166 (1.107, 1.475)	1
	Group 15	1.125 (1.106, 1.237)	1
CTCOH	Group 6	1.635 (1.455, 1.983)	1.002
	Group 10	1.259 (1.122, 1.868)	1.009
	Group 11	1.497 (1.299, 1.923)	1.01
	Group 13	1.611 (1.216, 3.556)	1.001
	Group 17	1.45 (1.213, 2.208)	1.004
	Group 18	1.142 (1.107, 1.268)	1
CPlasTCA	Group 4	1.134 (1.106, 1.254)	1
	Group 5	1.141 (1.107, 1.291)	1
	Group 11	1.213 (1.136, 1.381)	1
	Group 19	1.201 (1.145, 1.305)	1

*This document is a draft for review purposes only and does not constitute Agency policy.*

**Table A-12. Posterior distributions for rat residual errors (continued)**

Measurement	Group	Residual error geometric standard deviation	
		Median (2.5%, 97.5%)	R
CBldTCA	Group 4	1.134 (1.106, 1.258)	1
	Group 5	1.14 (1.107, 1.289)	1
	Group 6	1.59 (1.431, 1.878)	1.001
	Group 11	1.429 (1.292, 1.701)	1.001
	Group 17	1.432 (1.282, 1.675)	1.03
	Group 18	1.193 (1.12, 1.358)	1.004
	Group 19	1.214 (1.153, 1.327)	1
CLivTCA	Group 19	1.666 (1.443, 2.104)	1
AUrnTCA	Group 1	1.498 (1.125, 2.18)	1.135
	Group 6	1.95 (1.124, 5.264)	1.003
	Group 8	1.221 (1.146, 1.375)	1.003
	Group 10	1.18 (1.108, 1.444)	1.007
	Group 17	1.753 (1.163, 4.337)	1.001
	Group 19	1.333 (1.201, 1.707)	1
ABileTCOG	Group 6	2.129 (1.128, 5.363)	1.003
CTCOG	Group 17	2.758 (1.664, 5.734)	1.028
AUrnTCOGTCOH	Group 1	1.129 (1.106, 1.232)	1.004
	Group 6	1.483 (1.113, 4.791)	1.002
	Group 8	1.115 (1.106, 1.162)	1
	Group 10	1.145 (1.107, 1.305)	1
	Group 17	2.27 (1.53, 4.956)	1.009
AUrnNDCVC	Group 1	1.168 (1.11, 1.33)	1.002
AUrnTCTotMole	Group 6	1.538 (1.182, 3.868)	1.002
	Group 7	1.117 (1.106, 1.153)	1.001
	Group 14	1.121 (1.106, 1.207)	1
	Group 15	1.162 (1.108, 1.358)	1
TotCTCOH	Group 17	1.488 (1.172, 2.366)	1.015

2  
3  
4  
5  
6  
7  
8  
The nineteen groups are (1) Bernauer et al., 1996; (2) Dallas et al., 1991; (3) Fisher et al., 1989 females; (4) Fisher et al., 1991 females; (5) Fisher et al., 1991 males; (6) Green and Prout, 1985, Prout et al., 1985, male OA rats; (7) Hissink et al., 2002; (8) Kaneko et al., 1994; (9) Keys et al., 2003; (10) Kimmerle and Eben, 1973a; (11) Larson and Bull, 1992a, b; (12) Lee et al., 2000; (13) Merdink et al., 1999; (14) Prout et al., 1985 AP rats; (15) Prout et al., 1985 OM rats; (16) Simmons et al., 2002; (17) Stenner et al., 1997; (18) Templin et al., 1995; (19) Yu et al., 2000.

*This document is a draft for review purposes only and does not constitute Agency policy.*

1  
2  
3

**Table A-13. Posterior distributions for human PBPK model population parameters**

Sampled parameter	Posterior distributions reflecting uncertainty in population distribution			
	Population (geometric) mean		Population (geometric) standard deviation	
	Median (2.5%, 97.5%)	R	Median (2.5%, 97.5%)	R
InQCC	0.837 (0.6761, 1.022)	1.038	1.457 (1.271, 1.996)	1.036
InVPRC	1.519 (1.261, 1.884)	1.007	1.497 (1.317, 1.851)	1.008
QFatC	0.7781 (0.405, 1.143)	1.014	0.6272 (0.4431, 0.9773)	1
QGutC	0.7917 (0.6631, 0.925)	1.017	0.1693 (0.1199, 0.2559)	1.019
QLivC	0.5099 (0.1737, 0.8386)	1.031	0.4167 (0.2943, 0.6324)	1.009
QSlwC	0.7261 (0.4864, 0.9234)	1.011	0.3166 (0.2254, 0.4802)	1.005
InDRespC	0.626 (0.3063, 1.013)	1.197	1.291 (1.158, 2.006)	1.083
QKidC	1.007 (0.9137, 1.103)	1.009	0.1004 (0.07307, 0.1545)	1
FracPlasC	1.001 (0.9544, 1.047)	1.01	0.04275 (0.03155, 0.06305)	1
VFatC	0.788 (0.48, 1.056)	1.005	0.3666 (0.2696, 0.5542)	1
VGutC	1 (0.937, 1.067)	1.007	0.06745 (0.04923, 0.1038)	1
VLivC	1.043 (0.8683, 1.23)	1.047	0.1959 (0.1424, 0.3017)	1.003
VRapC	0.9959 (0.9311, 1.06)	1.006	0.06692 (0.04843, 0.1027)	1
VRespLumC	1.003 (0.8461, 1.164)	1.001	0.1671 (0.1209, 0.255)	1
VRespEffC	1 (0.8383, 1.159)	1.001	0.1672 (0.1215, 0.259)	1
VKidC	0.9965 (0.8551, 1.14)	1.007	0.1425 (0.1037, 0.2183)	1
VBldC	1.013 (0.9177, 1.108)	1.003	0.1005 (0.07265, 0.1564)	1
InPBC	0.9704 (0.8529, 1.101)	1.001	1.216 (1.161, 1.307)	1.002
InPFatC	0.8498 (0.7334, 0.9976)	1.002	1.188 (1.113, 1.366)	1.002
InPGutC	1.095 (0.7377, 1.585)	1.029	1.413 (1.214, 2.05)	1.002
InPLivC	0.9907 (0.6679, 1.441)	1.01	1.338 (1.203, 1.683)	1
InPRapC	0.93 (0.6589, 1.28)	1.003	1.528 (1.248, 2.472)	1.001
InPRespC	1.018 (0.6773, 1.5)	1.015	1.32 (1.192, 1.656)	1
InPKidC	0.9993 (0.8236, 1.219)	1.003	1.155 (1.097, 1.287)	1
InPSlwC	1.157 (0.8468, 1.59)	1.018	1.69 (1.383, 3.157)	1.008
InPRBCPlasTCAC	0.3223 (0.04876, 0.8378)	1.007	5.507 (3.047, 19.88)	1.003
InPBodTCAC	1.194 (0.929, 1.481)	1.043	1.327 (1.185, 1.67)	1.018
InPLivTCAC	1.202 (0.8429, 1.634)	1.046	1.285 (1.162, 1.648)	1.007
InkDissocC	0.9932 (0.9387, 1.053)	1.012	1.043 (1.026, 1.076)	1.003
InBMaxkDC	0.8806 (0.7492, 1.047)	1.038	1.157 (1.085, 1.37)	1.012
InPBodTCOHC	1.703 (1.439, 2.172)	1.019	1.409 (1.267, 1.678)	1.011
InPLivTCOHC	1.069 (0.7643, 1.485)	1.028	1.288 (1.165, 1.629)	1.002
InPBodTCOGC	0.7264 (0.1237, 2.54)	1.003	11.98 (5.037, 185.3)	1.017
InPLivTCOGC	6.671 (1.545, 24.87)	1.225	5.954 (2.653, 23.68)	1.052
InPeffDCVG	0.01007 (0.003264, 0.03264)	1.004	1.385 (1.201, 2.03)	1.001

*This document is a draft for review purposes only and does not constitute Agency policy.*

**Table A-13. Posterior distributions for human PBPK model population parameters (continued)**

Sampled parameter	Posterior distributions reflecting uncertainty in population distribution			
	Population (geometric) mean		Population (geometric) standard deviation	
	Median (2.5%, 97.5%)	R	Median (2.5%, 97.5%)	R
InkASTCA	4.511 (0.04731, 465.7)	1	5.467 (2.523, 71.06)	1
InkASTCOH	8.262 (0.0677, 347.9)	1	5.481 (2.513, 67.86)	1
InV <sub>MAX</sub> C	0.3759 (0.2218, 0.5882)	1.026	2.21 (1.862, 2.848)	1.003
InCIC	12.64 (5.207, 39.96)	1.028	4.325 (2.672, 9.003)	1.016
InFracOtherC	0.1186 (0.02298, 0.2989)	1.061	3.449 (1.392, 9.146)	1.102
InFracTCAC	0.1315 (0.07115, 0.197)	1.026	2.467 (1.916, 3.778)	1.01
InCIDCVGC	2.786 (1.326, 5.769)	1.08	2.789 (1.867, 4.877)	1.02
InK <sub>M</sub> DCVGC	1.213 (0.3908, 4.707)	1.029	4.43 (2.396, 18.56)	1.035
InCIKidDCVGC	0.04538 (0.001311, 0.1945)	1.204	3.338 (1.295, 30.46)	1.095
InK <sub>M</sub> KidDCVGC	0.2802 (0.1096, 1.778)	1.097	1.496 (1.263, 2.317)	1.001
InV <sub>MAX</sub> LungLivC	3.772 (0.8319, 9.157)	1.035	2.228 (1.335, 21.89)	1.014
InK <sub>M</sub> Clara	0.2726 (0.02144, 1.411)	1.041	11.63 (1.877, 682.7)	1.041
InFracLungSysC	24.08 (6.276, 81.14)	1.016	1.496 (1.263, 2.439)	1.001
InCITCOHC	0.1767 (0.1374, 0.2257)	1.011	1.888 (1.624, 2.307)	1.01
InK <sub>M</sub> TCOH	2.221 (1.296, 4.575)	1.02	2.578 (1.782, 4.584)	1.015
InCIGlucC	0.2796 (0.2132, 0.3807)	1.056	1.955 (1.583, 2.418)	1.079
InK <sub>M</sub> Gluc	133.4 (51.56, 277.2)	1.02	1.573 (1.266, 4.968)	1.011
InkMetTCOHC	0.7546 (0.1427, 2.13)	1.007	5.011 (2.668, 15.71)	1.002
InkUrnTCAC	0.04565 (0.0324, 0.06029)	1.005	1.878 (1.589, 2.48)	1.006
InkMetTCAC	0.2812 (0.1293, 0.5359)	1.004	2.529 (1.78, 4.211)	1.002
InkBileC	6.855 (3.016, 20.69)	1.464	1.589 (1.27, 3.358)	1.015
InkEHRC	0.1561 (0.09511, 0.2608)	1.1	1.699 (1.348, 2.498)	1.015
InkUrnTCOGC	15.78 (6.135, 72.5)	1.007	9.351 (4.93, 29.96)	1.003
InkDCVGC	7.123 (5.429, 9.702)	1.026	1.507 (1.311, 1.897)	1.008
InkNATC	0.0003157 (0.0001087, 0.002305)	1.008	1.54 (1.261, 3.306)	1
InkKidBioactC	0.06516 (0.01763, 0.1743)	1.001	1.523 (1.262, 2.987)	1

*This document is a draft for review purposes only and does not constitute Agency policy.*

1  
2

**Table A-14. Posterior distributions for human residual errors**

Measurement	Group	Residual error geometric standard deviation	
		Median (2.5%, 97.5%)	R
RetDose	Group 4	1.131 (1.106, 1.25)	1.001
CAIvPPM	Group 1	1.832 (1.509, 2.376)	1.015
	Group 4	1.515 (1.378, 1.738)	1
	Group 5	1.44 (1.413, 1.471)	1
CVen	Group 1	1.875 (1.683, 2.129)	1.018
	Group 3	1.618 (1.462, 1.862)	1
	Group 4	1.716 (1.513, 2.057)	1.001
	Group 5	2.948 (2.423, 3.8)	1.007
CTCOH	Group 1	1.205 (1.185, 1.227)	1.012
	Group 3	1.213 (1.187, 1.247)	1
	Group 5	2.101 (1.826, 2.571)	1.001
	Group 7	1.144 (1.106, 2.887)	1.123
CPlasTCA	Group 2	1.117 (1.106, 1.17)	1.001
	Group 7	1.168 (1.123, 1.242)	1
CBIdTCA	Group 1	1.138 (1.126, 1.152)	1.003
	Group 2	1.119 (1.106, 1.178)	1
	Group 4	1.488 (1.351, 1.646)	1.018
	Group 5	1.438 (1.367, 1.537)	1.002
zAUrnTCA	Group 1	1.448 (1.414, 1.485)	1.001
	Group 2	1.113 (1.105, 1.149)	1.001
	Group 3	1.242 (1.197, 1.301)	1.001
	Group 4	1.538 (1.441, 1.67)	1
	Group 6	1.158 (1.118, 1.228)	1
	Group 7	1.119 (1.106, 1.181)	1
zAUrnTCA_collect	Group 3	1.999 (1.178, 3.903)	1.003
	Group 5	2.787 (2.134, 4.23)	1.001
AUrnTCOGTCOH	Group 1	1.106 (1.105, 1.112)	1.001
	Group 3	1.11 (1.105, 1.125)	1
	Group 4	1.124 (1.107, 1.151)	1.001
	Group 6	1.117 (1.106, 1.157)	1.001
	Group 7	1.134 (1.106, 1.348)	1.003
AUrnTCOGTCOH_collect	Group 3	1.3 (1.111, 2.333)	1.004
	Group 5	1.626 (1.524, 1.767)	1
CDCVGmol	Group 1	1.53 (1.436, 1.656)	1.009
zAUrnNDCVC	Group 6	1.167 (1.124, 1.244)	1
TotCTCOH	Group 1	1.204 (1.185, 1.226)	1.011
	Group 4	1.247 (1.177, 1.366)	1.009
	Group 5	1.689 (1.552, 1.9)	1.001

3 The seven groups are (1) Fisher et al., 1998; (2) Paycok and Powell, 1945; (3) Kimmerle and Eben, 1973b;  
4 (4) Monster et al., 1976; (5) Chiu et al., 2007; (6) Bernauer et al., 1996; (7) Muller et al., 1974.

*This document is a draft for review purposes only and does not constitute Agency policy.*

1 **A.5.2.3. Human Model**

2 **A.5.2.3.1. Individual-specific predictions and calibration data.** [See  
3 [Appendix.linked.files\AppA.5.2.3.1.Updated.human.indiv.calib.TCE.DRAFT.pdf.](#)]

4  
5 **A.5.2.3.2. Population-based predictions and calibration data.** [See  
6 [Appendix.linked.files\AppA.5.2.3.2.Updated.human.pop.calib.TCE.DRAFT.pdf.](#)]

7  
8 **A.5.2.3.3. Population-based predictions and additional evaluation data.** [See  
9 [Appendix.linked.files\AppA.5.2.3.3.Updated.human.pop.eval.TCE.DRAFT.pdf.](#)]

10  
11 **A.6. EVALUATION OF RECENTLY PUBLISHED TOXICOKINETIC DATA**

12 Several *in vivo* toxicokinetic studies were published or became available during internal  
13 U.S. EPA review and Interagency Consultation, and were not evaluated as part of the originally  
14 planned analyses. Preliminary analyses of these data are summarized here. The general  
15 approach is the same as that used for the evaluation data in the primary analysis—population  
16 predictions from the PBPK model are compared visually with the toxicokinetic data. Figures  
17 with the population-based predictions and these recently published data are in the following  
18 linked files:

- 19  
20 • **Mouse (Kim et al., 2009; Mahle et al., 2001; Green, 2003a, b):**  
21 [Appendix.linked.files\AppA.6.Updated.mouse.pop.eval.TCE.DRAFT.pdf.](#)  
22 • **Rat (Liu et al., 2009; Mahle et al., 2001):**  
23 [Appendix.linked.files\AppA.6.Updated.rat.pop.eval.TCE.DRAFT.pdf.](#)  
24

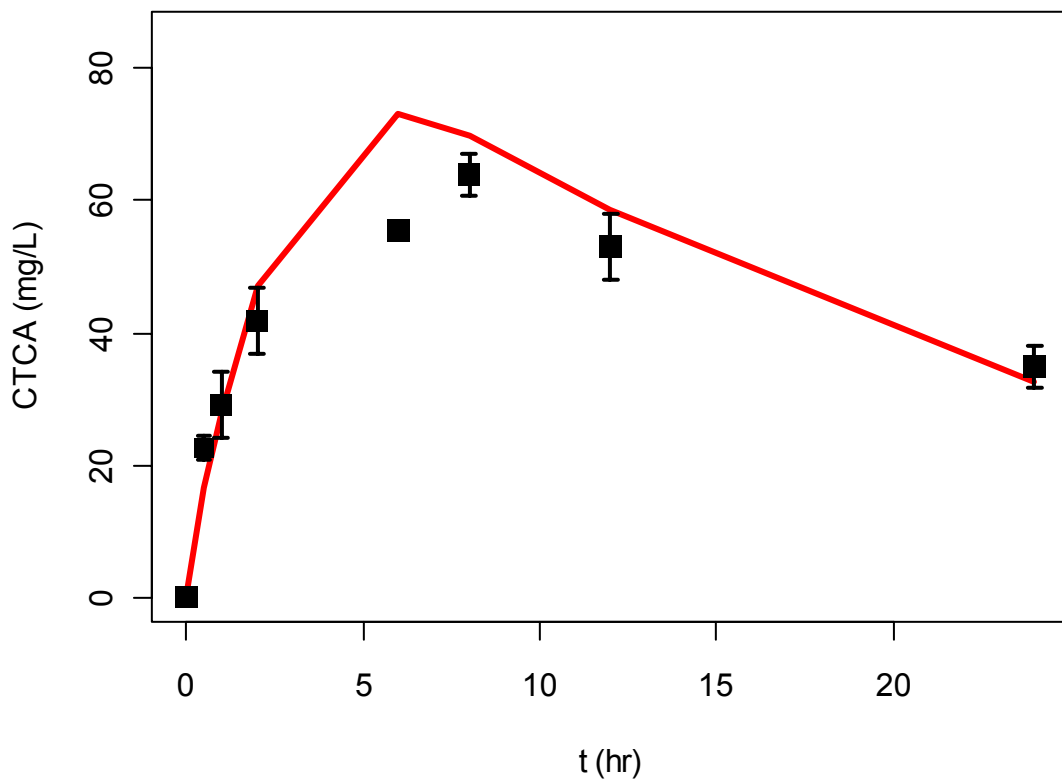
25 **A.6.1. TCE Metabolite Toxicokinetics in Mice: Kim et al. (2009)**

26 Kim et al. (2009) measured TCA, DCA, DCVG, and DCVC in blood of male B6C3F1  
27 mice following a single gavage dose of 2,140 mg/kg. Of these data, only TCA and DCVG blood  
28 concentrations are predicted by the updated PBPK model, so only those data are compared with  
29 PBPK model predictions (prior values for the distribution volume and elimination rate constant  
30 of DCVG were used, as there were no calibration data informing those parameters). These data  
31 were within the inter-quartile region of the PBPK model population predictions.

32 An assessment was made as to whether these data are informative as to the flux of GSH  
33 conjugation in mice. First, the best fitting parameter sample (least squares on TCA and DCVG  
34 in blood, weighted by inverse of the observed variance) from the posterior distribution was  
35 selected out of 50,000 samples generated by Monte Carlo (see Figures A-7 and A-8 for the

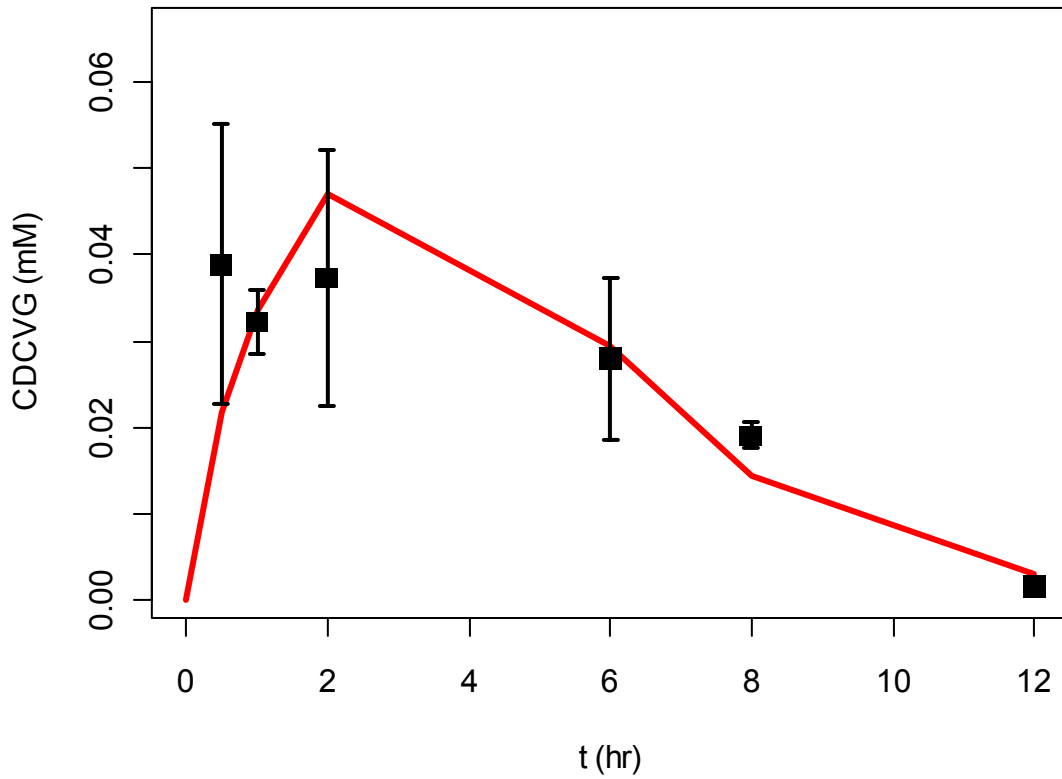
*This document is a draft for review purposes only and does not constitute Agency policy.*

1 comparison with predictions with data). This parameter sample was then used to calculate the  
2 fraction of intake that is predicted by the PBPK model to undergo GSH metabolism for  
3 continuous oral and continuous inhalation exposure, and this point estimate compared to the full  
4 posterior distribution (see Figures A-9 and A-10). The predictions for this “best fitting”  
5 parameter set was similar (within 3-fold) of the median of the full posterior distribution. While a  
6 formal assessment of the impact of these new data (i.e., including its uncertainty and variability)  
7 would require a re-running of the Bayesian analysis, it appears that the median estimates for the  
8 mouse GSH conjugation dose metric used in the dose-response assessment (see Chapter 5) are  
9 reasonably consistent with the Kim et al. (2009) data.

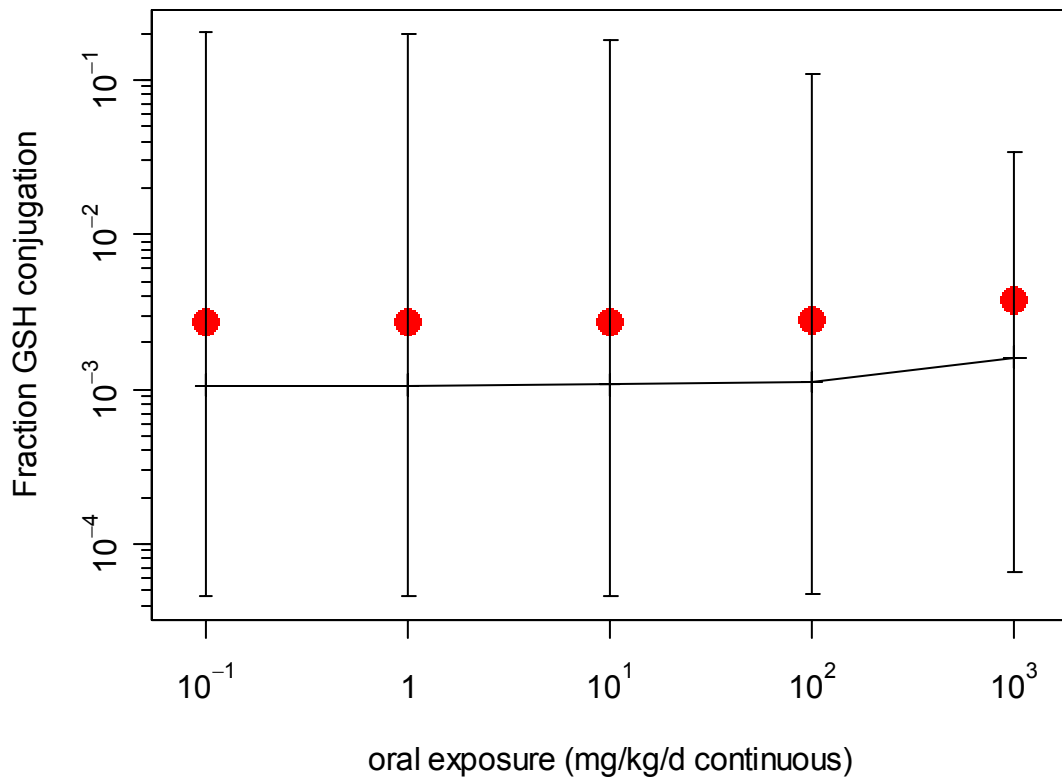


10  
11 **Figure A-7. Comparison of best-fitting (out of 50,000 posterior samples)**  
12 **PBPK model prediction and Kim et al. (2009) TCA blood concentration data**  
13 **for mice gavaged with 2,140 mg/kg TCE. Full population distributions are**  
14 shown in a separate linked file (see text).

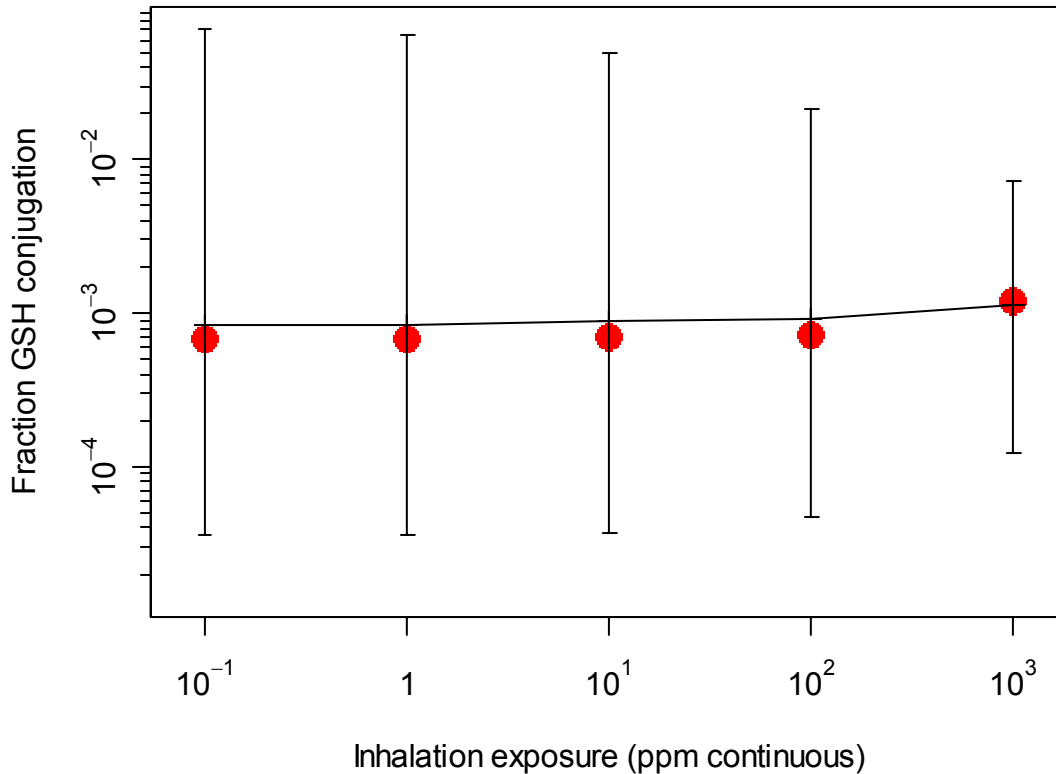




1  
2 **Figure A-8. Comparison of best-fitting (out of 50,000 posterior samples)**  
3 **PBPK model prediction and Kim et al. (2009) DCVG blood concentration**  
4 **data for mice gavaged with 2,140 mg/kg TCE. Full population distributions are**  
5 **shown in a separate linked file (see text).**



1  
2 **Figure A-9. PBPK model predictions for the fraction of intake undergoing**  
3 **GSH conjugation in mice continuously exposed orally to TCE.** Lines and  
4 error bars represent the median and 95<sup>th</sup> percentile confidence interval for the  
5 posterior predictions, respectively (also reported in Section 3.5.7.2.1). Filled  
6 circles represent the predictions from the sample (out of 50,000 total posterior  
7 samples) which provides the best fit to the Kim et al. (2009) TCA and DCVG  
8 blood concentration data for mice gavaged with 2,140 mg/kg TCE.



1  
2 **Figure A-10. PBPK model predictions for the fraction of intake undergoing**  
3 **GSH conjugation in mice continuously exposed via inhalation to TCE.** Lines  
4 and error bars represent the median and 95<sup>th</sup> percentile confidence interval for the  
5 posterior predictions, respectively (also reported in Section 3.5.7.2.1). Filled  
6 circles represent the predictions from the sample (out of 50,000 total posterior  
7 samples) which provides the best fit to the Kim et al. (2009) TCA and DCVG  
8 blood concentration data for mice gavaged with 2,140 mg/kg TCE.  
9

10  
11 An additional note of interest from the Kim et al. (2009) data is the inter-study variability  
12 in TCA kinetics. In particular, the TCA blood concentrations reported by Kim et al. (2009) are  
13 2-fold lower than those reported by Abbas and Fisher (1997) in the same sex and strain of  
14 mouse, with a very similar corn oil gavage dose of 2,000 mg/kg (as compared to 2,140 mg/kg  
15 used in Kim et al., 2009).  
16

17 **A.6.2. TCE Toxicokinetics in Rats: Liu et al. (2009)**

18 Liu et al. (2009) measured TCE in blood of male rats after treatment with TCE by i.v.  
19 injection (0.1, 1.0, or 2.5 mg/kg) or aqueous gavage (0.0001, 0.001, 0.01, 0.1, 1, 2.5, 5, or  
20 10 mg/kg). Almost all of the data from gavage exposures were within the inter-quartile region of

1 the PBPK model population predictions, with all of it within the 95% confidence interval. For  
2 i.v. exposures, the data at 1 and 2.5 mg/kg were well simulated, but the time-course data at  
3 0.1 mg/kg were substantially different in shape from that predicted by the PBPK model, with a  
4 lower initial concentration and longer half-life. The slower elimination rate at 0.1 mg/kg was  
5 noted by the study authors through use of noncompartmental analysis. There is no clear  
6 explanation for this discrepancy, particularly since the gavage data at this and even lower doses  
7 were well predicted by the PBPK model.

### 9 **A.6.3. TCA Toxicokinetics in Mice and Rats: Mahle et al. (2001) and Green (2003a, b)**

10 Three technical reports (Mahle et al., 2001; Green, 2003a, b) described by Sweeney et al.  
11 (2009) contained data on TCA toxicokinetics in mice and rats exposed to TCA in drinking water.  
12 These technical reports were provided to U.S. EPA by the Sweeney et al. (2009) authors.

13 TCA blood and liver concentrations were reported by Mahle et al. (2001) for male  
14 B6C3F1 mice and male Fischer 344 rats exposed to 0.1 g/L to 2 g/L TCA in drinking water for 3  
15 or 14 days (12 to 270 mg/kg/d in mice and 7 to 150 mg/kg/d in rats). For mice, these data were  
16 all within the 95% confidence interval of PBPK model population predictions, with about half of  
17 these data within the interquartile region. For rats, all these data, except those for the 3-day  
18 exposure at 0.1 g/L, were within the 95% confidence interval of the PBPK model predictions. In  
19 addition, the median rat predictions were consistently higher than the data, although this could be  
20 explained by inter-study (strain, lot, etc.) variability.

21 TCA blood concentrations were reported by Green (2003a) for male and female B6C3F1  
22 mice exposed to 0.5 g/L to 2.5 g/L TCA in drinking water for 5 days (130 to 600 mg/kg/d in  
23 males and 160 to 750 mg/kg/d in females). Notably, these animals consumed around twice as  
24 much water per day as compared to the mice reported by Mahle et al. (2001), and therefore  
25 received comparatively higher doses of TCA for the same TCE concentration in drinking water.  
26 In male mice, the data at the lower two doses (130 and 250 mg/kg/d) were within the inter-  
27 quartile region of the PBPK model predictions. The data for male mice at the highest dose  
28 (600 mg/kg/d) were below the inter-quartile region, but within the 95% confidence interval of  
29 the PBPK model predictions. In females, the data at the lower two doses (160 and 360 mg/kg/d)  
30 were mostly below the inter-quartile region, but within the 95% confidence interval of the PBPK  
31 model predictions, while about half the data at the highest dose were just below the 95%  
32 confidence interval.

33 TCA blood, plasma, and liver concentrations were reported by Green (2003b) for male  
34 PPAR $\alpha$ -null mice, male 129/sv mice (the background strain of the PPAR $\alpha$ -null mice), and male  
35 and female B6C3F1 mice, exposed to 1.0 g/L or 2.5 g/L TCA in drinking water for 5 days (male

1 B6C3F1 only) to 14 days.<sup>2</sup> In male PPAR $\alpha$ -null mice, plasma and blood concentrations were  
2 within the inter-quartile region of the PBPK model predictions, while liver concentrations were  
3 below the inter-quartile region but within the 95% confidence interval. In male 129/sv mice, the  
4 plasma concentrations were within the inter-quartile region of the PBPK model predictions,  
5 while blood and liver concentrations were below the inter-quartile region but within the 95%  
6 confidence interval. In male B6C3F1 mice, all data were within the 95% confidence intervals of  
7 the PBPK model predictions, with about half within the inter-quartile region, and the rest above  
8 (plasma concentrations at the lower dose) or below (liver concentrations at all but the lowest  
9 dose at 5 days). In female B6C3F1 mice, plasma concentrations were below the inter-quartile  
10 region but within the 95% confidence region, while liver and blood concentrations were at or  
11 below the lower 95% confidence bound.

12 Overall, the predictions of the TCA submodel of the updated TCE PBPK model appear  
13 consistent with these data on the toxicokinetics of TCA after drinking water exposure in male  
14 rats and male mice. In female mice, the reported concentrations tends to be at the low end of or  
15 lower than those predicted by the PBPK model. Importantly, the data used for calibrating the  
16 mouse PBPK model parameters were predominantly in males, with only Fisher et al. (1991,  
17 1993) reporting TCA plasma levels in female mice after TCE exposure. In addition, median  
18 PBPK model predictions at higher doses (>300 mg/kg/d), even in males, tended to be higher than  
19 the concentrations reported. While TCA kinetics after TCE exposure includes predicted internal  
20 production at these higher levels, previously published data on TCA kinetics alone only included  
21 doses up to 100 mg/kg, and only in males. Therefore, these results suggest that the median  
22 predictions of the TCA sub-model of the updated TCE PBPK model are somewhat less accurate  
23 for female mice and for higher doses of TCA (>300 mg/kg/d) in mice, though the 95%  
24 confidence intervals still cover the majority of the reported data. Finally, the ratio of blood to  
25 liver concentrations of ~1.4 reported in the mouse experiments in Mahle et al. (2001) were  
26 significantly different from the ratios of ~2.3 reported by Green (2003b), a difference for which  
27 there is no clear explanation given the similar experimental designs and common use the  
28 B6C3F1 mouse strain. Because median PBPK model predictions for the blood to liver  
29 concentration ratio for these studies are ~1.3, they are more consistent with the Mahle et al.  
30 (2001) data than with the Green (2003b) data.

31 Sweeney et al. (2009) also suggested that the available data, in conjunction with  
32 deterministic modeling using the TCA portion of the Hack et al. (2006) TCE PBPK model,

---

<sup>2</sup>Sweeney et al. (2009) reported that blood concentrations in Green (2003b) were incorrect due to an arithmetic error  
owing to a change in chemical analytic methodology, and should have been multiplied by 2. This correction was  
included in the present analysis.

*This document is a draft for review purposes only and does not constitute Agency policy.*

1 supported a hypothesis that the bioavailability of TCA in drinking water in mice is substantially  
2 less than 100%. Classically, oral bioavailability is assessed by comparing blood concentration  
3 profiles from oral and i.v. dosing experiments, because blood concentration data from oral  
4 dosing alone cannot distinguish fractional uptake from metabolism. Schultz et al. (1999) made  
5 this comparison in rats at a single dose of 82 mg/kg, and reported an empirical bioavailability of  
6 116%, consistent with complete absorption. *A priori*, there would not seem to be a strong reason  
7 to suspect that oral absorption in mice would be significantly different from that in rats. As  
8 discussed above in the evaluation of Hack et al. (2006) model, available data strongly support  
9 clearance of TCA in addition to urinary excretion, based on the finding of less than 100%  
10 recovery in urine after i.v. dosing. In addition, as the current TCE PBPK model assumes 100%  
11 absorption for orally-administered TCA, and the PBPK model predictions are consistent with  
12 these data, it is likely that the limited bioavailability determined by Sweeney et al. (2009) was  
13 confounded by this additional clearance pathway unaccounted for by Hack et al. (2006).  
14 Therefore, the data are consistent with the combination of 100% absorption for orally-  
15 administered TCA and an additional clearance pathway for TCA other than urinary excretion in  
16 both rats and mice. This hypothesis could be further tested with additional experiments in mice  
17 directly comparing of TCA toxicokinetics (blood or plasma concentrations and urinary  
18 excretion) between i.v. and oral dosing.

19

#### 20 **A.7. UPDATED PHYSIOLOGICALLY BASED PHARMACOKINETIC (PBPK)** 21 **MODEL CODE**

22 The following pages contain the updated PBPK model code for the MCSim software  
23 (version 5.0.0). Additional details on baseline parameter derivations are included as inline  
24 documentation. Example simulation files containing prior distributions and experimental  
25 calibration data are available electronically:

26

- 27 • Mouse: [Appendix.linked.files\TCE.1.2.3.3.Mouse.pop.example.in](#)
- 28 • Rat: [Appendix.linked.files\TCE.1.2.3.3.Rat.pop.example.in](#)
- 29 • Human: [Appendix.linked.files\TCE.1.2.3.3.Human.pop.example.in](#).

30

*This document is a draft for review purposes only and does not constitute Agency policy.*

```

# TCE.risk.1.2.3.3.pop.model -- Updated TCE Risk Assessment Model
#
#### HISTORY OF HACK ET AL. (2006) MODEL
# Model code to correspond to the block diagram version of the model
# Edited by Deborah Keys to incorporate Lapare et al. 1995 data
# Last edited: August 6, 2004
# Translated into MCSim from acslXtreme CSL file by Eric Hack, started 31Aug2004
# Removed nonessential differential equations (i.e., AUCCbld) for MCMC runs.
# Changed QRap and QSlw calculations and added QTot to scale fractional flows
# back to 1 after sampling.
# Finished translating and verifying results on 15Sep2004.
# Changed QSlw calculation and removed QTot 21Sep2004.
# Removed diffusion-limited fat uptake 24Sep2004.
#### HISTORY OF U.S. EPA (2009) MODEL (CHIU ET AL., 2009)
# Extensively revised by U.S. EPA June 2007-June 2008
#   - Fixed hepatic plasma flow for TCA-submodel to include
#     portal vein (i.e., QGutLivPlas -- originally was just
#     QLivPlas, which was only hepatic artery).
#   - Clearer coding and in-line documentation
#   - Single model for 3 species
#   - Revised physiological parameters, with discussion of
#     uncertainty and variability,
#   - In vitro data used for default metabolism parameters,
#     with discussion of uncertainty and variability
#   - added TCE blood compartment
#   - added TCE kidney compartment, with GSH metabolism
#   - added DCVG compartment
#   - added additional outputs available from in vivo data
#   - removed DCA compartment
#   - added IA and PV dosing (for rats)
#   - Version 1.1 -- fixed urinary parameter scaling
#     -- fixed VBod in kUrnTCOG (should be VBodTCOH)
#   - Version 1.1.1 -- changed some truncation limits (in comments only)
#   - Version 1.2 --
#     -- removed TB compartment as currently coded
#     -- added respiratory oxidative metabolism:
#         3 states: AInhResp, AResp, AExhResp
#     -- removed clearance from respiratory metabolism
#   - Version 1.2.1 -- changed oral dosing to be similar to IV
#   - Version 1.2.2 -- fixed default lung metabolism (additional
#     scaling by lung/liver weight ratio)
#   - Version 1.2.3 -- fixed FracKidDCVC scaling
#   - Version 1.2.3.1 -- added output CDCVG_ND (no new dynamics)
#     for non-detects of DCVG in blood
#   - Version 1.2.3.2 -- Exact version of non-detects likelihood
#   - Version 1.2.3.3 -- Error variances changed to "Ve_xxx"
#   NOTE -- lines with comment "(vrisk)" are used only for
#     calculating dose metrics, and are commented out
#     when doing MCMC runs.
#*****
#***           State Variable Specifications           ***
#*****

```

```

States = {
##-- TCE uptake
  AStom,           # Amount of TCE in stomach
  ADuod,          # oral gavage absorption -- mice and rats only
  AExc,           # (vrisk) excreted in feces from gavage (currently 0)
  AO,             # (vrisk) total absorbed
  InhDose,        # Amount inhaled
##-- TCE in the body
  ARap,           # Amount in rapidly perfused tissues
  ASlw,           # Amount in slowly perfused tissues
  AFat,           # Amount in fat
  AGut,           # Amount in gut
  ALiv,           # Amount in liver
  AKid,           # Amount in Kidney -- previously in Rap tissue
  ABld,           # Amount in Blood -- previously in Rap tissue
  AInhResp,       # Amount in respiratory lumen during inhalation
  AResp,          # Amount in respiratory tissue
  AExhResp,       # Amount in respiratory lumen during exhalation
##-- TCA in the body
  AOTCA,          # (vrisk)
  AStomTCA,       # Amount of TCA in stomach
  APlasTCA,       # Amount of TCA in plasma #comment out for
  ABodTCA,        # Amount of TCA in lumped body compartment
  ALivTCA,        # Amount of TCA in liver
##-- TCA metabolized
  AUrnTCA,        # Cumulative Amount of TCA excreted in urine
  AUrnTCA_sat,    # Amount of TCA excreted that during times that had
                  # saturated measurements (for lower bounds)
  AUrnTCA_collect,# Cumulative Amount of TCA excreted in urine during
                  # collection times (for intermittent collection)
##-- TCOH in body
  AOTCOH,         # (vrisk)
  AStomTCOH,      # Amount of TCOH in stomach
  ABodTCOH,       # Amount of TCOH in lumped body compartment
  ALivTCOH,       # Amount of TCOH in liver
##-- TCOG in body
  ABodTCOG,       # Amount of TCOG in lumped body compartment
  ALivTCOG,       # Amount of TCOG in liver
  ABileTCOG,      # Amount of TCOG in bile (incl. gut)
  ARecircTCOG,    # (vrisk)
##-- TCOG excreted
  AUrnTCOG,       # Amount of TCOG excreted in urine
  AUrnTCOG_sat,   # Amount of TCOG excreted that during times that had
                  # saturated measurements (for lower bounds)
  AUrnTCOG_collect,# Cumulative Amount of TCA excreted in urine during
                  # collection times (for intermittent collection)
##-- DCVG in body
  ADCVGIn,        # (vrisk)
  ADCVGMol,       # Amount of DCVG in body in mmoles
  AMetDCVG,       # (vrisk)
##-- DCVC in body
  ADCVCIn,        # (vrisk)
  ADCVC,          # Amount of DCVC in body

```

```

ABioactDCVC,      #(vrisk)
##-- NAcDCVC excreted
AUrnNDCVC,       # Amount of NAcDCVC excreted
##-- Other states for TCE
ACh,             # Amount in closed chamber -- mice and rats only
AExh,            # Amount exhaled
AExhExp, # Amount exhaled during expos [to calc. retention]
##-- Metabolism
AMetLiv1, #(vrisk) Amount metabolized by P450 in liver
AMetLiv2, #(vrisk) Amount metabolized by GSH conjugation in liver
AMetLng,  #(vrisk) Amount metabolized in the lung
AMetKid,  #(vrisk)
AMetTCOHTCA, #(vrisk) Amount of TCOH metabolized to TCA
AMetTCOHGluc, #(vrisk) Amount of TCOH glucuronidated
AMetTCOHOther, #(vrisk)
AMetTCA,  #(vrisk) Amount of TCA metabolized
##-- Other Dose metrics
AUCCBld, #(vrisk)
AUCCLiv, #(vrisk)
AUCCKid, #(vrisk)
AUCCRap, #(vrisk)
AUCCTCOH, #(vrisk)
AUCCBodTCOH, #(vrisk)
AUCTotCTCOH, #(vrisk)
AUCPlasTCAFree, #(vrisk)
AUCPlasTCA, #(vrisk)
AUCLivTCA, #(vrisk)
AUCCDCVG #(vrisk)
};

#####
***      Input Variable Specifications      ***
#####
Inputs = {
##-- TCE dosing
Conc,          # Inhalation exposure conc. (ppm)
IVDose,        # IV dose (mg/kg)
PDose,         # Oral gavage dose (mg/kg)
Drink,        # Drinking water dose (mg/kg/day)
IADose,        # Inter-arterial
PVDose,        # Portal Vein
##-- TCA dosing
IVDoseTCA,    # IV dose (mg/kg) of TCA
PODoseTCA,    # Oral dose (mg/kg) of TCA
##-- TCOH dosing
IVDoseTCOH,   # IV dose (mg/kg) of TCOH
PODoseTCOH,   # Oral dose (mg/kg) of TCOH
##-- Potentially time-varying parameters
QPmeas,       # Measured value of Alveolar ventilation QP
TCAUrnSat,    # Flag for saturated TCA urine
TCOGUrnSat,   # Flag for saturated TCOG urine
UrnMissing    # Flag for missing urine collection times

```

```

};

#####
***      Output Variable Specifications      ***
#####
Outputs = {
#####
*** Outputs for mass balance check
MassBalTCE,
TotDose,
TotTissue,
MassBalTCOH,
TotTCOHIn,
TotTCOHdDose,
TotTissueTCOH,
TotMetabTCOH,
MassBalTCA,
TotTCAIn,
TotTissueTCA,
MassBalTCOG,
TotTCOGIn,
TotTissueTCOG,
MassBalDCVG,
MassBalDCVC,
AUrnNDCVCequiv,

#####
*** Outputs that are potential dose metrics
TotMetab, #(vrisk) Total metabolism
TotMetabBW34, #(vrisk) Total metabolism/BW^3/4
ATotMetLiv, #(vrisk) Total metabolism in liver
AMetLivLiv, #(vrisk) Total oxidation in liver/liver volume
AMetLivOther, #(vrisk) Total "other" oxidation in liver
AMetLivOtherLiv, #(vrisk) Total "other" oxidation in liver/liver vol
AMetLngResp, #(vrisk) oxidation in lung/respiratory tissue volume
AMetGSH, #(vrisk) total GSH conjugation
AMetGSHBW34, #(vrisk) total GSH conjugation/BW^3/4
ABioactDCVCKid, #(vrisk) Amount of DCVC bioactivated/kidney volume

# NEW
TotDoseBW34, #(vrisk) mg intake / BW^3/4
AMetLiv1BW34, #(vrisk) mg hepatic oxidative metabolism / BW^3/4
TotOxMetabBW34, #(vrisk) mg oxidative metabolism / BW^3/4
TotTCAInBW, #(vrisk) TCA production / BW
AMetLngBW34, #(vrisk) oxidation in lung/BW^3/4
ABioactDCVCBW34, #(vrisk) Amount of DCVC bioactivated/BW^3/4
AMetLivOtherBW34, #(vrisk) Total "other" oxidation in liver/BW^3/4

#####
*** Outputs for comparison to in vivo data
# TCE
RetDose, # human - = (InhDose - AExhExp)
CALv, # needed for CALvPPM
CALvPPM, # human
CInhPPM, # mouse, rat

```



```

CInh, # needed for CMixExh
CMixExh, # rat - Mixed exhaled breath (mg/l)
CArt, # rat, human - Arterial blood concentration
CVen, # mouse, rat, human
CBldMix, # rat - Concentration in mixed arterial+venous blood
      # (used for cardiac puncture)
CFat, # mouse, rat - Concentration in fat
CGut, # rat
CRap, # needed for unlumped tissues
CSlw, # needed for unlumped tissues
CHrt, # rat - Concentration in heart tissue [use CRap]
CKid, # mouse, rat - Concentration in kidney
CLiv, # mouse, rat - Concentration in liver
CLung, # mouse, rat - Concentration in lung [use CRap]
CMus, # rat - Concentration in muscle [use CSLw]
CSpl, # rat - Concentration in spleen [use CRap]
CBrn, # rat - Concentration in brain [use CRap]
zAExh, # mouse
zAExhpost, # rat - Amount exhaled post-exposure (mg)

# TCOH
CTCOH, # mouse, rat, human - TCOH concentration in blood
CKidTCOH, # mouse - TCOH concentration in kidney
CLivTCOH, # mouse - TCOH concentration in liver
CLungTCOH, # mouse - TCOH concentration in lung

# TCA
CPlasTCA, # mouse, rat, human - TCA concentration in plasma
CBldTCA, # mouse, rat, human - TCA concentration in blood
CBodTCA, # needed for CKidTCA and CLungTCA
CKidTCA, # mouse - TCA concentration in kidney
CLivTCA, # mouse, rat - TCA concentration in liver
CLungTCA, # mouse - TCA concentration in lung
zAUrnTCA, # mouse, rat, human - Cumulative Urinary TCA
zAUrnTCA_collect, # human - TCA measurements for intermittent collection
zAUrnTCA_sat, # human - Saturated TCA measurements

# TCOG
zABileTCOG, # rat - Amount of TCOG in bile (mg)
CTCOG, # needed for CTCOGTCOH
CTCOGTCOH, # mouse - TCOG concentration in blood (in TCOH-equiv)
CKidTCOGTCOH, # mouse - TCOG concentration in kidney (in TCOH-equiv)
CLivTCOGTCOH, # mouse - TCOG concentration in liver (in TCOH-equiv)
CLungTCOGTCOH, # mouse - TCOG concentration in lung (in TCOH-equiv)
AUrnTCOGTCOH, # mouse, rat, human - Cumulative Urinary TCOG (in TCOH-equiv)
AUrnTCOGTCOH_collect, # human - TCOG (in TCOH-equiv) measurements for
      # intermittent collection
AUrnTCOGTCOH_sat, # human - Saturated TCOG (in TCOH-equiv) measurements

# Other
CDCVGMol, # concentration of DCVG (mmol/l)
CDCVGMol0, # Dummy variable without likelihood (for plotting)#(v1.2.3.1)
CDCVG_ND, # Non-detect of DCVG (<0.05 pmol/ml= 5e-5 mmol/l )#(v1.2.3.1)

```

```

      # Output -ln(likelihood)#(v1.2.3.1)
zAUrnNDCVC, # rat, human - Cumulative urinary NAcDCVC
AUrnTCTotMole, # rat, human - Cumulative urinary TCOH+TCA in mmoles
TotCTCOH, # mouse, human - TCOH+TCOG Concentration (in TCOH-equiv)
TotCTCOHcomp, # ONLY FOR COMPARISON WITH HACK
ATCOG, # ONLY FOR COMPARISON WITH HACK
QPsamp, # human - sampled value of alveolar ventilation rate

```

```
## PARAMETERS #(vrisk)
```

```

QCnow, # (vrisk) #Cardiac output (L/hr)
QP, # (vrisk) #Alveolar ventilation (L/hr)
QFatCtmp, # (vrisk) #Scaled fat blood flow
QGutCtmp, # (vrisk) #Scaled gut blood flow
QLivCtmp, # (vrisk) #Scaled liver blood flow
QSlwCtmp, # (vrisk) #Scaled slowly perfused blood flow
QRapCtmp, # (vrisk) #Scaled rapidly perfused blood flow
QKidCtmp, # (vrisk) #Scaled kidney blood flow
DResp, # (vrisk) #Respiratory lumen:tissue diffusive clearance rate
VFatCtmp, # (vrisk) #Fat fractional compartment volume
VGutCtmp, # (vrisk) #Gut fractional compartment volume
VLivCtmp, # (vrisk) #Liver fractional compartment volume
VRapCtmp, # (vrisk) #Rapidly perfused fractional compartment volume
VRespLumCtmp, # (vrisk) # Fractional volume of respiratory lumen
VRespEffCtmp, # (vrisk) #Effective fractional volume of respiratory tissue
VKidCtmp, # (vrisk) #Kidney fractional compartment volume
VBldCtmp, # (vrisk) #Blood fractional compartment volume
VSlwCtmp, # (vrisk) #Slowly perfused fractional compartment volume
VPlasCtmp, # (vrisk) #Plasma fractional compartment volume
VBodCtmp, # (vrisk) #TCA Body fractional compartment volume [not incl.
blood+liver]
VBodTCOHCtmp, # (vrisk) #TCOH/G Body fractional compartment volume [not incl.
liver]
PB, # (vrisk) #TCE Blood/air partition coefficient
PFat, # (vrisk) #TCE Fat/Blood partition coefficient
PGut, # (vrisk) #TCE Gut/Blood partition coefficient
PLiv, # (vrisk) #TCE Liver/Blood partition coefficient
PRap, # (vrisk) #TCE Rapidly perfused/Blood partition coefficient
PResp, # (vrisk) #TCE Respiratory tissue:air partition coefficient
PKid, # (vrisk) #TCE Kidney/Blood partition coefficient
PSlw, # (vrisk) #TCE Slowly perfused/Blood partition coefficient
TCPlas, # (vrisk) #TCA blood/plasma concentration ratio
PBodTCA, # (vrisk) #Free TCA Body/blood plasma partition coefficient
PLivTCA, # (vrisk) #Free TCA Liver/blood plasma partition coefficient
kDissoc, # (vrisk) #Protein/TCA dissociation constant (umole/L)
BMax, # (vrisk) #Maximum binding concentration (umole/L)
PBodTCOH, # (vrisk) #TCOH body/blood partition coefficient
PLivTCOH, # (vrisk) #TCOH liver/body partition coefficient
PBodTCOG, # (vrisk) #TCOG body/blood partition coefficient
PLivTCOG, # (vrisk) #TCOG liver/body partition coefficient
VDCVG, # (vrisk) #DCVG effective volume of distribution
kAS, # (vrisk) #TCE Stomach absorption coefficient (/hr)
kTSD, # (vrisk) #TCE Stomach-duodenum transfer coefficient (/hr)

```

```

kAD, # (vrisk) #TCE Duodenum absorption coefficient (/hr)
kTD, # (vrisk) #TCE Duodenum-feces transfer coefficient (/hr)
kASTCA, # (vrisk) #TCA Stomach absorption coefficient (/hr)
kASTCOH, # (vrisk) #TCOH Stomach absorption coefficient (/hr)
VMax, # (vrisk) #VMax for hepatic TCE oxidation (mg/hr)
KM, # (vrisk) #KM for hepatic TCE oxidation (mg/L)
FracOther, # (vrisk) #Fraction of hepatic TCE oxidation not to TCA+TCOH
FracTCA, # (vrisk) #Fraction of hepatic TCE oxidation to TCA
VMaxDCVG, # (vrisk) #VMax for hepatic TCE GSH conjugation (mg/hr)
KMDCVG, # (vrisk) #KM for hepatic TCE GSH conjugation (mg/L)
VMaxKidDCVG, # (vrisk) #VMax for renal TCE GSH conjugation (mg/hr)
KMKidDCVG, # (vrisk) #KM for renal TCE GSH conjugation (mg/L)
FracKidDCVC, # (vrisk) #Fraction of renal TCE GSH conj. "directly" to DCVC
# (vrisk) #(i.e., via first pass)
VMaxClara, # (vrisk) #VMax for Tracheo-bronchial TCE oxidation (mg/hr)
KMClara, # (vrisk) #KM for Tracheo-bronchial TCE oxidation (mg/L)
FracLungSys, # (vrisk) #Fraction of respiratory metabolism to systemic circ.
VMaxTCOH, # (vrisk) #VMax for hepatic TCOH->TCA (mg/hr)
KMTCOH, # (vrisk) #KM for hepatic TCOH->TCA (mg/L)
VMaxGluc, # (vrisk) #VMax for hepatic TCOH->TCOG (mg/hr)
KMGluc, # (vrisk) #KM for hepatic TCOH->TCOG (mg/L)
kMetTCOH, # (vrisk) #Rate constant for hepatic TCOH->other (/hr)
kUrnTCA, # (vrisk) #Rate constant for TCA plasma->urine (/hr)
kMetTCA, # (vrisk) #Rate constant for hepatic TCA->other (/hr)
kBile, # (vrisk) #Rate constant for TCOG liver->bile (/hr)
kEHR, # (vrisk) #Lumped rate constant for TCOG bile->TCOH liver (/hr)
kUrnTCOG, # (vrisk) #Rate constant for TCOG->urine (/hr)
kDCVG, # (vrisk) #Rate constant for hepatic DCVG->DCVC (/hr)
kNAT, # (vrisk) #Lumped rate constant for DCVC->Urinary NAcDCVC (/hr)
kKidBioact, # (vrisk) #Rate constant for DCVC bioactivation (/hr)

## Misc
RurnTCA, # (vrisk)
RurnTCOGTCOH, # (vrisk)
RurnNDCVC, # (vrisk)
RAO,
CVenMole,
CPlasTCAMole,
CPlasTCAFreeMole
);

*****
***          Global Constants          ***
*****

# Molecular Weights
MWTCE = 131.39; # TCE
MWDCA = 129.0; # DCA
MWDCVC = 216.1; # DCVC
MWTCA = 163.5; # TCA
MWChlor = 147.5; # Chloral
MWTCOH = 149.5; # TCOH
MWTCOHGluc = 325.53; # TCOH-Gluc

```

```

MWNADCVC = 258.8; # N Acetyl DCVC

# Stoichiometry
StochChlorTCE = MWChlor / MWTCE;
StochTCATCE = MWTCA / MWTCE;
StochTCATCOH = MWTCA / MWTCOH;
StochTCOHTCE = MWTCOH / MWTCE;
StochGlucTCOH = MWTCOHGluc / MWTCOH;
StochTCOHGluc = MWTCOH / MWTCOHGluc;
StochTCEGluc = MWTCE / MWTCOHGluc;
StochDCVCTCE = MWDCVC / MWTCE;
StochN = MWNADCVC / MWDCVC;
StochDCATCE = MWDCA / MWTCE;

*****
***          Global Model Parameters          ***
*****
# These are the actual model parameters used in "dynamics."
# Values that are assigned in the "initialize" section,
# are all set to 1 to avoid confusion.

*****
# Flows
QC = 1; # Cardiac output (L/hr)
QPsamp = 1; # Alveolar ventilation (L/hr)
VFR = 1; # Alveolar ventilation-perfusion ratio
QFatCtmp = 1; # Scaled fat blood flow
QGutCtmp = 1; # Scaled gut blood flow
QLivCtmp = 1; # Scaled liver blood flow
QSlwCtmp = 1; # Scaled slowly perfused blood flow
DResptmp = 1; # Respiratory lumen:tissue diffusive clearance rate (L/hr)
[scaled to QP]
QKidCtmp = 1; # Scaled kidney blood flow
FracPlas = 1; # Fraction of blood that is plasma (1-hematocrit)
*****
# Volumes
VFat = 1; # Fat compartment volume (L)
VGut = 1; # Gut compartment volume (L)
VLiv = 1; # Liver compartment volume (L)
VRap = 1; # Rapidly perfused compartment volume (L)
VRespLum = 1; # Volume of respiratory lumen (L air)
VRespEfftmp = 1; # (vrisk) volume for respiratory tissue (L)
VRespEff = 1; # Effective volume for respiratory tissue (L air) = V(tissue) *
Resp:Air partition coefficient
VKid = 1; # Kidney compartment volume (L)
VBld = 1; # Blood compartment volume (L)
VSlw = 1; # Slowly perfused compartment volume (L)
VPlas = 1; # Plasma compartment volume [fraction of blood] (L)
VBod = 1; # TCA Body compartment volume [not incl. blood+liver] (L)
VBodTCOH = 1; # TCOH/G Body compartment volume [not incl. liver] (L)
*****
# Distribution/partitioning
PB = 1; # TCE Blood/air partition coefficient

```

```

PFat = 1; # TCE Fat/Blood partition coefficient
PGut = 1; # TCE Gut/Blood partition coefficient
PLiv = 1; # TCE Liver/Blood partition coefficient
PRap = 1; # TCE Rapidly perfused/Blood partition coefficient
PResp = 1; # TCE Respiratory tissue:air partition coefficient
PKid = 1; # TCE Kidney/Blood partition coefficient
PSlw = 1; # TCE Slowly perfused/Blood partition coefficient
TCAPlas = 1; # TCA blood/plasma concentration ratio
PBodTCA = 1; # Free TCA Body/blood plasma partition coefficient
PLivTCA = 1; # Free TCA Liver/blood plasma partition coefficient
kDissoc = 1; # Protein/TCA dissociation constant (umole/L)
EMax = 1; # Protein concentration (UNITS?)
PBodTCOH = 1; # TCOH body/blood partition coefficient
PLivTCOH = 1; # TCOH liver/body partition coefficient
PBodTCOG = 1; # TCOG body/blood partition coefficient
PLivTCOG = 1; # TCOG liver/body partition coefficient
VDCVG = 1; # DCVG effective volume of distribution
*****
# Oral absorption
kTSD = 1.4; # TCE Stomach-duodenum transfer coefficient (/hr)
kAS = 1.4; # TCE Stomach absorption coefficient (/hr)
kTD = 0.1; # TCE Duodenum-feces transfer coefficient (/hr)
kAD = 0.75; # TCE Duodenum absorption coefficient (/hr)
kASTCA = 0.75; # TCA Stomach absorption coefficient (/hr)
kASTCOH = 0.75; # TCOH Stomach absorption coefficient (/hr)
*****
# TCE Metabolism
VMax = 1; # VMax for hepatic TCE oxidation (mg/hr)
KM = 1; # KM for hepatic TCE oxidation (mg/L)
FracOther = 1; # Fraction of hepatic TCE oxidation not to TCA+TCOH
FracTCA = 1; # Fraction of hepatic TCE oxidation to TCA
VMaxDCVG = 1; # VMax for hepatic TCE GSH conjugation (mg/hr)
KMDCVG = 1; # KM for hepatic TCE GSH conjugation (mg/L)
VMaxKidDCVG = 1; # VMax for renal TCE GSH conjugation (mg/hr)
KMKidDCVG = 1; # KM for renal TCE GSH conjugation (mg/L)
VMaxClara = 1; # VMax for Tracheo-bronchial TCE oxidation (mg/hr)
KMClara = 1; # KM for Tracheo-bronchial TCE oxidation (mg/L)
# but in units of air concentration
FracLungSys = 1; # Fraction of respiratory oxidative metabolism that
enters systemic circulation

*****
# TCOH metabolism
VMaxTCOH = 1; # VMax for hepatic TCOH->TCA (mg/hr)
KMTCOH = 1; # KM for hepatic TCOH->TCA (mg/L)
VMaxGluc = 1; # VMax for hepatic TCOH->TCOG (mg/hr)
KMGluc = 1; # KM for hepatic TCOH->TCOG (mg/L)
kMetTCOH = 1; # Rate constant for hepatic TCOH->other (/hr)
*****
# TCA metabolism/clearance
kUrnTCA = 1; # Rate constant for TCA plasma->urine (/hr)
kMetTCA = 1; # Rate constant for hepatic TCA->other (/hr)
*****

```

```

# TCOG metabolism/clearance
kBile = 1; # Rate constant for TCOG liver->bile (/hr)
kEHR = 1; # Lumped rate constant for TCOG bile->TCOH liver (/hr)
kUrnTCOG = 1; # Rate constant for TCOG->urine (/hr)
*****
# DCVG metabolism
kDCVG = 1; # Rate constant for hepatic DCVG->DCVC (/hr)
FracKidDCVC = 1; # Fraction of renal TCE GSH conj. "directly" to DCVC
(i.e., via first pass)
*****
# DCVC metabolism/clearance
kNAT = 1; # Lumped rate constant for DCVC->Urinary NAcDCVC (/hr)
kKidBioact = 1; # Rate constant for DCVC bioactivation (/hr)
*****
# Closed chamber and other exposure parameters
Rodents = 1; # Number of rodents in closed chamber data
VCh = 1; # Chamber volume for closed chamber data
kLoss = 1; # Rate constant for closed chamber air loss
CC = 0.0; # Initial chamber concentration (ppm)
TChng = 0.003; # IV infusion duration (hour)
*****
## Flag for species, sex -- these are global parameters
BW = 0.0; # Species-specific defaults during initialization
BW75 = 0.0; # (vrisk) Variable for BW^3/4
Male = 1.0; # 1 = male, 0 = female
Species = 1.0; # 1 = human, 2 = rat, 3 = mouse

*****
### Potentially measured covariates (constants) ###
*****
BWmeas = 0.0; # Body weight
VFatCmeas = 0.0; # Fractional volume fat
PBmeas = 0.0; # Measured blood-air partition coefficient
Hematocritmeas = 0.0; # Measured hematocrit -- used for FracPlas = 1 - Hct
CDCVGmolLD = 5e-5; # Detection limit of CDCVGmol#(v1.2.3.1)

*****
### Global Sampling Parameters ###
*****
# These parameters are potentially sampled/calibrated in the MCMC or MC
# analyses. The default values here are used if no sampled value is given.
# M_ indicates population mean parameters used only in MC sampling
# V_ indicates a population variance parameter used in MC and MCMC sampling

# Flow Rates
lnQCC = 0.0; # Scaled by BW^0.75 and species-specific central estimates
lnVPRC = 0.0; # Scaled to species-specific central estimates

# Fractional Blood Flows to Tissues (fraction of cardiac output)
QFatC = 1.0; # Scaled to species-specific central estimates
QGutC = 1.0; # Scaled to species-specific central estimates
QLivC = 1.0; # Scaled to species-specific central estimates
QSlwC = 1.0; # Scaled to species-specific central estimates

```

```

QKidC      = 1.0;    # Scaled to species-specific central estimates
FracPlasC  = 1.0;    # Scaled to species-specific central estimates
lnDRespC   = 0.0;    # Scaled to alveolar ventilation rate in dynamics

# Fractional Tissue Volumes (fraction of BW)
VFatC      = 1.0;    # Scaled to species-specific central estimates
VGutC      = 1.0;    # Scaled to species-specific central estimates
VLivC      = 1.0;    # Scaled to species-specific central estimates
VRapC      = 1.0;    # Scaled to species-specific central estimates
VRespLumC  = 1.0;    # Scaled to species-specific central estimates
VRespEffC  = 1.0;    # Scaled to species-specific central estimates

VKidC      = 1.0;    # Scaled to species-specific central estimates
VBlcC      = 1.0;    # Scaled to species-specific central estimate

# Partition Coefficients for TCE
lnPBC      = 0.0;    # Scaled to species-specific central estimates
lnPFatC    = 0.0;    # Scaled to species-specific central estimates
lnPGutC    = 0.0;    # Scaled to species-specific central estimates
lnPLivC    = 0.0;    # Scaled to species-specific central estimates
lnPRapC    = 0.0;    # Scaled to species-specific central estimates
lnPRespC   = 0.0;    # Scaled to species-specific central estimates
lnPKidC    = 0.0;    # Scaled to species-specific central estimates
lnPSlwC    = 0.0;    # Scaled to species-specific central estimates

# Partition Coefficients for TCA
lnPRBCPlasTCAC = 0.0; # Scaled to species-specific central estimates
lnPBodTCAC    = 0.0; # Scaled to species-specific central estimates
lnPLivTCAC    = 0.0; # Scaled to species-specific central estimates

# Plasma Binding for TCA
lnkDissocC    = 0.0; # Scaled to species-specific central estimates
lnBMaxkDC     = 0.0; # Scaled to species-specific central estimates

# Partition Coefficients for TCOH and TCOG
lnPBodTCOHC   = 0.0; # Scaled to species-specific central estimates
lnPLivTCOHC   = 0.0; # Scaled to species-specific central estimates
lnPBodTCOGC   = 0.0; # Scaled to species-specific central estimates
lnPLivTCOGC   = 0.0; # Scaled to species-specific central estimates
lnPeffDCVGC   = 0.0; # Scaled to species-specific central estimates

# Oral Absorption rates
lnkTSD        = 0.336;
lnkAS         = 0.336;
lnkTD         = -2.303;
lnkAD         = -0.288;
lnkASTCA      = -0.288;
lnkASTCOH     = -0.288;

# TCE Metabolism
lnVMaxC      = 0.0;    # Scaled by liver weight and species-specific central estimates
lnKMC        = 0.0;    # Scaled to species-specific central estimates
lnClC        = 0.0;    # Scaled to species-specific central estimates

```

```

lnFracOtherC = 0.0;    # Ratio of DCA to non-DCA
lnFracTCAC    = 0.0;    # Ratio of TCA to TCOH
lnVMaxDCVGC  = 0.0;    # Scaled by liver weight and species-specific central
estimates
lnClDCVGC    = 0.0;    # Scaled to species-specific central estimates
lnKMDCVGC    = 0.0;    # Scaled to species-specific central estimates
lnVMaxKidDCVGC = 0.0;    # Scaled by kidney weight and species-specific central
estimates
lnClKidDCVGC = 0.0;    # Scaled to species-specific central estimates
lnKMKidDCVGC = 0.0;    # Scaled to species-specific central estimates
lnVMaxLungLivC = 0.0;    # Ratio of lung Vmax to liver Vmax,
# Scaled to species-specific central estimates
lnKMClara    = 0.0;    # now in units of air concentration

# Clearance in lung
lnFracLungSysC = 0.0;    # ratio of systemic to local clearance of lung
oxidation

# TCOH Metabolism
lnVMaxTCOHC  = 0.0;    # Scaled by BW^0.75
lnClTCOHC    = 0.0;    # Scaled by BW^0.75
lnKMTCOH     = 0.0;    #
lnVMaxGlucC  = 0.0;    # Scaled by BW^0.75
lnClGlucC    = 0.0;    # Scaled by BW^0.75
lnKMGluc     = 0.0;    #
lnkMetTCOHC  = 0.0;    # Scaled by BW^-0.25

# TCA Metabolism/clearance
lnkUrnTCAC   = 0.0;    # Scaled by (plasma volume)^-1 and species-specific
central estimates
lnkMetTCAC   = 0.0;    # Scaled by BW^-0.25

# TCOG excretion and reabsorption
lnkBileC     = 0.0;    # Scaled by BW^-0.25
lnkEHRC      = 0.0;    # Scaled by BW^-0.25
lnkUrnTCOGC  = 0.0;    # Scaled by (blood volume)^-1 and species-specific
central estimates

# DCVG metabolism
lnFracKidDCVCC = 0.0;    # Ratio of "directly" to DCVC to systemic DCVG
lnkDCVGC      = 0.0;    # Scaled by BW^-0.25

# DCVC metabolism
lnkNATC      = 0.0;    # Scaled by BW^-0.25
lnkKidBioactC = 0.0;    # Scaled by BW^-0.25

# Closed chamber parameters
NRodents     = 1;      #
VChC         = 1;      #
lnkLossC     = 0;      #

#*****
# Population means

```

```

#
# These are given truncated normal or uniform distributions, depending on
# what prior information is available. Note that these distributions
# reflect uncertainty in the population mean, not inter-individual
# variability. Normal distributions are truncated at 2, 3, or 4 SD.
# For fractional volumes and flows, 2xSD
# For plasma fraction, 3xSD
# For cardiac output and ventilation-perfusion ratio, 4xSD
# For all others, 3xSD
# For uniform distributions, range of 1e2 to 1e8 fold, centered on
# central estimate.
#
M_lnQCC = 1.0;
M_lnVPRC = 1.0;
M_QFatC = 1.0;
M_QGutC = 1.0;
M_QLivC = 1.0;
M_QSlwC = 1.0;
M_QKidC = 1.0;
M_FracPlasC = 1.0;
M_lnDRespC = 1.0;
M_VFatC = 1.0;
M_VGutC = 1.0;
M_VLivC = 1.0;
M_VRapC = 1.0;
M_VRespLumC = 1.0;
M_VRespEffc = 1.0;
M_VKidC = 1.0;
M_VBldC = 1.0;
M_lnPBC = 1.0;
M_lnPFatC = 1.0;
M_lnPGutC = 1.0;
M_lnPLivC = 1.0;
M_lnPRapC = 1.0;
M_lnPRespC = 1.0;
M_lnPKidC = 1.0;
M_lnPSlwC = 1.0;
M_lnPRBCPlasTCAC = 1.0;
M_lnPBodTCAC = 1.0;
M_lnPLivTCAC = 1.0;
M_lnkDissocC = 1.0;
M_lnBMaxkDC = 1.0;
M_lnPBodTCOHC = 1.0;
M_lnPLivTCOHC = 1.0;
M_lnPBodTCOGC = 1.0;
M_lnPLivTCOGC = 1.0;
M_lnPeffDCVG = 1.0;
M_lnkTSD = 1.0;
M_lnkAS = 1.0;
M_lnkTD = 1.0;
M_lnkAD = 1.0;
M_lnkASTCA = 1.0;
M_lnkASTCOH = 1.0;

```

```

M_lnVMaxC = 1.0;
M_lnKMC = 1.0;
M_lnClC = 1.0;
M_lnFracOtherC = 1.0;
M_lnFracTCAC = 1.0;
M_lnVMaxDCVGC = 1.0;
M_lnClDCVGC = 1.0;
M_lnKMDCVGC = 1.0;
M_lnVMaxKidDCVGC = 1.0;
M_lnClKidDCVGC = 1.0;
M_lnKMKidDCVGC = 1.0;
M_lnVMaxLungLivC = 1.0;
M_lnKMClara = 1.0;
M_lnFracLungSysC = 1.0;
M_lnVMaxTCOHC = 1.0;
M_lnClTCOHC = 1.0;
M_lnkMTCOH = 1.0;
M_lnVMaxGlucC = 1.0;
M_lnClGlucC = 1.0;
M_lnkMGluc = 1.0;
M_lnkMetTCOHC = 1.0;
M_lnkUrnTCAC = 1.0;
M_lnkMetTCAC = 1.0;
M_lnkBileC = 1.0;
M_lnkEHRC = 1.0;
M_lnkUrnTCOGC = 1.0;
M_lnFracKidDCVCC = 1.0;
M_lnkDCVGC = 1.0;
M_lnkNATC = 1.0;
M_lnkKidBioactC = 1.0;

```

```

*****
# Population Variances
#
# These are given InvGamma(alpha,beta) distributions. The parameterization
# for alpha and beta is given by:
# alpha = (n-1)/2
# beta = s^2*(n-1)/2
# where n = number of data points, and s^2 is the sample variance
# Sum(x_i^2)/n - <x>^2.
# Generally, for parameters for which there is no direct data, assume a
# value of n = 5 (alpha = 2). For a sample variance s^2, this gives
# an expected value for the standard deviation <sigma> = 0.9*s,
# a median [2.5%,97.5%] of 1.1*s [0.6*s,2.9*s].
#
V_lnQCC = 1.0;
V_lnVPRC = 1.0;
V_QFatC = 1.0;
V_QGutC = 1.0;
V_QLivC = 1.0;
V_QSlwC = 1.0;
V_QKidC = 1.0;

```

```

V_FracPlasC      = 1.0;
V_lnDRespC      = 1.0;
V_VFatC         = 1.0;
V_VGutC         = 1.0;
V_VLivC         = 1.0;
V_VRapC         = 1.0;
V_VRespLumC     = 1.0;
V_VRespEffC     = 1.0;
V_VKidC         = 1.0;
V_VBldC         = 1.0;
V_lnPBC         = 1.0;
V_lnPFatC       = 1.0;
V_lnPGutC       = 1.0;
V_lnPLivC       = 1.0;
V_lnPRapC       = 1.0;
V_lnPRespC      = 1.0;
V_lnPKidC       = 1.0;
V_lnPSlwC       = 1.0;
V_lnPRBCPlasTCAC = 1.0;
V_lnPBodTCAC    = 1.0;
V_lnPLivTCAC    = 1.0;
V_lnkDissocC    = 1.0;
V_lnBMaxkDC     = 1.0;
V_lnPBodTCOHC   = 1.0;
V_lnPLivTCOHC   = 1.0;
V_lnPBodTCOGC   = 1.0;
V_lnPLivTCOGC   = 1.0;
V_lnPeffDCVG    = 1.0;
V_lnkTSD        = 1.0;
V_lnkAS         = 1.0;
V_lnkTD         = 1.0;
V_lnkAD         = 1.0;
V_lnkASTCA      = 1.0;
V_lnkASTCOH     = 1.0;
V_lnVMaxC       = 1.0;
V_lnkMC         = 1.0;
V_lnClC         = 1.0;
V_lnFracOtherC  = 1.0;
V_lnFracTCAC    = 1.0;
V_lnVMaxDCVGC   = 1.0;
V_lnClDCVGC     = 1.0;
V_lnkMDCVGC     = 1.0;
V_lnVMaxKidDCVGC = 1.0;
V_lnClKidDCVGC  = 1.0;
V_lnkMKKidDCVGC = 1.0;
V_lnVMaxLungLivC = 1.0;
V_lnkMClara     = 1.0;
V_lnFracLungSysC = 1.0;
V_lnVMaxTCOHC   = 1.0;
V_lnClTCOHC     = 1.0;
V_lnkMTCOH      = 1.0;
V_lnVMaxGlucC   = 1.0;
V_lnClGlucC     = 1.0;

```

```

V_lnkMGluc      = 1.0;
V_lnkMetTCOHC   = 1.0;
V_lnkUrnTCAC    = 1.0;
V_lnkMetTCAC    = 1.0;
V_lnkBileC      = 1.0;
V_lnkEHRC       = 1.0;
V_lnkUrnTCOGC   = 1.0;
V_lnFracKidDCVCC = 1.0;
V_lnkDCVGC      = 1.0;
V_lnkNATC       = 1.0;
V_lnkKidBioactC = 1.0;

```

```

#*****
# Measurement error variances for output

```

```

Ve_RetDose      = 1;
Ve_CALv         = 1;
Ve_CALvPPM      = 1;
Ve_CInhPPM      = 1;
Ve_CInh         = 1;
Ve_CMixExh      = 1;
Ve_CArt         = 1;
Ve_CVen         = 1;
Ve_CBldMix      = 1;

```

```

Ve_CFat         = 1;
Ve_CGut         = 1;
Ve_CRap         = 1;
Ve_CSlw         = 1;
Ve_CHrt         = 1;
Ve_CKid         = 1;
Ve_CLiv         = 1;
Ve_CLung        = 1;
Ve_CMus         = 1;
Ve_CSpl         = 1;
Ve_CBrn         = 1;
Ve_zAExh        = 1;
Ve_zAExhpost    = 1;

```

```

Ve_CTOH         = 1;
Ve_CKidTCOH     = 1;
Ve_CLivTCOH     = 1;
Ve_CLungTCOH    = 1;

```

```

Ve_CPlasTCA     = 1;
Ve_CBldTCA      = 1;
Ve_CBodTCA      = 1;
Ve_CKidTCA      = 1;
Ve_CLivTCA      = 1;
Ve_CLungTCA     = 1;
Ve_zAUrnTCA     = 1;

```

```

Ve_zAUrnTCA_collect = 1;
Ve_zAUrnTCA_sat = 1;

Ve_zABileTCOG = 1;
Ve_CTCOG = 1;
Ve_CTCOGTCOH = 1;
Ve_CKidTCOGTCOH = 1;
Ve_CLivTCOGTCOH = 1;
Ve_CLungTCOGTCOH = 1;
Ve_AUrnTCOGTCOH = 1;
Ve_AUrnTCOGTCOH_collect = 1;

Ve_AUrnTCOGTCOH_sat = 1;

Ve_CDCVGmol = 1;
Ve_zAUrnNDCVC = 1;
Ve_AUrnTCTotMole = 1;
Ve_TotCTCOH = 1;
Ve_QPsamp = 1;

*****
*** Defaults for input parameters ***
*****
##-- TCE dosing
Conc = 0.0; # Inhalation exposure conc. (ppm)
IVDose = 0.0; # IV dose (mg/kg)
PDose = 0.0; # Oral gavage dose (mg/kg)
Drink = 0.0; # Drinking water dose (mg/kg/day)
IADose = 0.0; # Intraarterial dose (mg/kg)
PVDose = 0.0; # Portal vein dose (mg/kg)

##-- TCA dosing
IVDoseTCA = 0.0;# IV dose (mg/kg) of TCA
PODoseTCA = 0.0;# Oral dose (mg/kg) of TCA

##-- TCOH dosing
IVDoseTCOH = 0.0;# IV dose (mg/kg) of TCOH
PODoseTCOH = 0.0;# Oral dose (mg/kg) of TCOH

##-- Potentially time-varying parameters
QPmeas = 0.0; # Measured value of Alveolar ventilation QP
TCAUrnSat = 0.0;# Flag for saturated TCA urine
TCOGUrnSat = 0.0;# Flag for saturated TCOG urine
UrnMissing = 0.0;# Flag for missing urine collection times

Initialize {

*****
*** Parameter Initialization and Scaling ***
*****
# Model Parameters (used in dynamics):
# QC Cardiac output (L/hr)
# VPR Ventilation-perfusion ratio
# QPsamp Alveolar ventilation (L/hr)

```

```

# QFatCtmp Scaled fat blood flow
# QGutCtmp Scaled gut blood flow
# QLivCtmp Scaled liver blood flow
# QSlwCtmp Scaled slowly perfused blood flow
# DRespTmp Respiratory lumen:tissue diffusive clearance rate
# QKidCtmp Scaled kidney blood flow
# FracPlas Fraction of blood that is plasma (1-hematocrit)
# VFat Fat compartment volume (L)
# VGut Gut compartment volume (L)
# VLiv Liver compartment volume (L)
# VRap Rapidly perfused compartment volume (L)
# VRespLum Volume of respiratory lumen (L air)
# VRespEff Effective volume of respiratory tissue (L air)
# VKid Kidney compartment volume (L)
# VBld Blood compartment volume (L)
# VSlw Slowly perfused compartment volume (L)
# VPlas Plasma compartment volume [fraction of blood] (L)
# VBod TCA Body compartment volume [not incl. blood+liver]
(L)
# VBodTCOH TCOH/G Body compartment volume [not incl. liver] (L)
# PB TCE Blood/air partition coefficient
# PFat TCE Fat/Blood partition coefficient
# PGut TCE Gut/Blood partition coefficient
# PLiv TCE Liver/Blood partition coefficient
# PRap TCE Rapidly perfused/Blood partition coefficient
# PResp TCE Respiratory tissue:air partition coefficient
# PKid TCE Kidney/Blood partition coefficient
# PSlw TCE Slowly perfused/Blood partition coefficient
# TCAPlas TCA blood/plasma concentration ratio
# PBodTCA Free TCA Body/blood plasma partition coefficient
# PLivTCA Free TCA Liver/blood plasma partition coefficient
# kDissoc Protein/TCA dissociation constant (umole/L)
# BMax Maximum binding concentration (umole/L)
# PBodTCOH TCOH body/blood partition coefficient
# PLivTCOH TCOH liver/body partition coefficient
# PBodTCOG TCOG body/blood partition coefficient
# PLivTCOG TCOG liver/body partition coefficient
# kAS TCE Stomach absorption coefficient (/hr)
# kTSD TCE Stomach-duodenum transfer coefficient (/hr)
# kAD TCE Duodenum absorption coefficient (/hr)
# kTD TCE Duodenum-feces transfer coefficient (/hr)
# kASTCA TCA Stomach absorption coefficient (/hr)
# kASTCOH TCOH Stomach absorption coefficient (/hr)
# VMax VMax for hepatic TCE oxidation (mg/hr)
# KM KM for hepatic TCE oxidation (mg/L)
# FracOther Fraction of hepatic TCE oxidation not to TCA+TCOH
# FracTCA Fraction of hepatic TCE oxidation to TCA
# VMaxDCVG VMax for hepatic TCE GSH conjugation (mg/hr)
# KMDCVG KM for hepatic TCE GSH conjugation (mg/L)
# VMaxKidDCVG VMax for renal TCE GSH conjugation (mg/hr)
# KMKidDCVG KM for renal TCE GSH conjugation (mg/L)
# VMaxClara VMax for Tracheo-bronchial TCE oxidation (mg/hr)
# KMClara KM for Tracheo-bronchial TCE oxidation (mg/L)

```

10/20/09

*This document is a draft for review purposes only and does not constitute Agency policy*

A-91

DRAFT: DO NOT CITE OR QUOTE

```
#      FracLungSys      Fraction of respiratory metabolism to systemic circ.      #      lnPLivTCAC
#      VMaxTCOH      VMax for hepatic TCOH->TCA (mg/hr)      #      lnkDissocC
#      KMTCOH      KM for hepatic TCOH->TCA (mg/L)      #      lnBMaxkDC
#      VMaxGluc      VMax for hepatic TCOH->TCOG (mg/hr)      #      lnPBodTCOHC
#      KMGluc      KM for hepatic TCOH->TCOG (mg/L)      #      lnPLivTCOHC
#      kMetTCOH      Rate constant for hepatic TCOH->other (/hr)      #      lnPBodTCOGC
#      kUrnTCA      Rate constant for TCA plasma->urine (/hr)      #      lnPLivTCOGC
#      kMetTCA      Rate constant for hepatic TCA->other (/hr)      #      lnPeffDCVG
#      kBile      Rate constant for TCOG liver->bile (/hr)      #      lnkTSD
#      kEHR      Lumped rate constant for TCOG bile->TCOH liver (/hr)      #      lnkAS
#      kUrnTCOG      Rate constant for TCOG->urine (/hr)      #      lnkTD
#      kDCVG      Rate constant for hepatic DCVG->DCVC (/hr)      #      lnkAD
#      FracKidDCVC      Fraction of renal TCE GSH conj. "directly" to DCVC      #      lnkASTCA
#      (i.e., via first pass)      #      lnkASTCOH
#      VDCVG      DCVG effective volume of distribution      #      lnVMaxC
#      kNAT      Lumped rate constant for DCVC->Urinary NAcDCVC (/hr)      #      lnkMC
#      kKidBioact      Rate constant for DCVC bioactivation (/hr)      #      lnClC
#      Rodents      Number of rodents in closed chamber data      #      lnFracOtherC
#      VCh      Chamber volume for closed chamber data      #      lnFracTCAC
#      kLoss      Rate constant for closed chamber air loss      #      lnVMaxDCVGC
# Parameters used (not assigned here)      #      lnClDCVGC
#      BW      Body weight in kg      #      lnKMDCVGC
#      Species      1 = human (default), 2 = rat, 3 = mouse      #      lnVMaxKidDCVGC
#      Male      0 = female, 1 (default) = male      #      lnClKidDCVGC
#      CC      Closed chamber initial concentration      #      lnKMKidDCVGC
# Sampling/scaling parameters (assigned or sampled)      #      lnVMaxLungLivC
#      lnQCC      #      lnKMClara
#      lnVPRC      #      lnFracLungSysC
#      lnDRespC      #      lnVMaxTCOHC
#      QFatC      #      lnClTCOHC
#      QGutC      #      lnKMTCOH
#      QLivC      #      lnVMaxGlucC
#      QSlwC      #      lnClGlucC
#      QKidC      #      lnKMGluc
#      FracPlasC      #      lnkMetTCOHC
#      VFatC      #      lnkUrnTCAC
#      VGutC      #      lnkMetTCAC
#      VLivC      #      lnkBileC
#      VRapC      #      lnkEHRC
#      VRespLumC      #      lnkUrnTCOGC
#      VRespEffC      #      lnFracKidDCVCC
#      VKidC      #      lnkDCVGC
#      VBldC      #      lnkNATC
#      lnPBC      #      lnkKidBioactC
#      lnPFatC      #      NRodents
#      lnPGutC      #      VChC
#      lnPLivC      #      lnkLossC
#      lnPRapC      # Input parameters
#      lnPSlwC      #      none
#      lnPRespC      # Notes:
#      lnPKidC      #*****
#      lnPRBCPlasTCAC      # use measured value of > 0, otherwise use 0.03 for mouse,
#      lnPBodTCAC      #      0.3 for rat, 60 for female human, 70 for male human
```



```

    BW = (BWmeas > 0.0 ? BWmeas : (Species == 3 ? 0.03 : (Species == 2 ? 0.3 :
(Male == 0 ? 60.0 : 70.0) )));

```

```

    BW75 = pow(BW, 0.75);
    BW25 = pow(BW, 0.25);

```

```

# Cardiac Output and alveolar ventilation (L/hr)

```

```

    QC = exp(lnQCC) * BW75 *      # Mouse, Rat, Human (default)
      (Species == 3 ? 11.6 : (Species == 2 ? 13.3 : 16.0) );
    # Mouse: CO=13.98 +/- 2.85 ml/min, BW=30 g (Brown et al. 1997, Tab. 22)
    #   Uncertainty CV is 0.20
    # Rat: CO=110.4 ml/min +/- 15.6, BW=396 g (Brown et al. 1997, Tab. 22,
    #   p 441). Uncertainty CV is 0.14.
    # Human: Average of Male CO=6.5 l/min, BW=73 kg
    #   and female CO= 5.9 l/min, BW=60 kg (ICRP #89, sitting at rest)
    #   From Price et al. 2003, estimates of human perfusion rate were
    #   4.7~6.5 for females and 5.5~7.1 l/min for males (note
    #   portal blood was double-counted, and subtracted off here)
    #   Thus for uncertainty use CV of 0.2, truncated at 4xCV
    #   Variability from Price et al. (2003) had CV of 0.14~0.20,
    #   so use 0.2 as central estimate

```

```

    VPR = exp(lnVPRC) *
      (Species == 3 ? 2.5 : (Species == 2 ? 1.9 : 0.96) );
    # Mouse: QP/BW=116.5 ml/min/100 g (Brown et al. 1997, Tab. 31), VPR=2.5
    #   Assume uncertainty CV of 0.2 similar to QC, truncated at 4xCV
    #   Consistent with range of QP in Tab. 31
    # Rat: QP/BW=52.9 ml/min/100 g (Brown et al. 1997, Tab. 31), VPR=1.9
    #   Assume uncertainty CV of 0.3 similar to QC, truncated at 4xCV
    #   Used larger CV because Tab. 31 shows a very large range of QP
    # Human: Average of Male VE=9 l/min, resp. rate=12 /min,
    #   dead space=0.15 l (QP=7.2 l/min), and Female
    #   VE=6.5 l/min, resp. rate=14 /min, dead space=0.12 l
    #   (QP=4.8 l/min), VPR = 0.96
    #   Assume uncertainty CV of 0.2 similar to QC, truncated at 4xCV
    #   Consistent with range of QP in Tab. 31

```

```

    QPsamp = QC*VPR;

```

```

#   Respiratory diffusion flow rate
#   Will be scaled by QP in dynamics
#   Use log-uniform distribution from 1e-5 to 10
    DResptmp = exp(lnDRespC);

```

```

# Fractional Flows scaled to the appropriate species

```

```

# Fat = Adipose only
# Gut = GI tract + pancreas + spleen (all drain to portal vein)
# Liv = Liver, hepatic artery
# Slw = Muscle + Skin
# Kid = Kidney
# Rap = Rapidly perfused (rest of organs, plus bone marrow, lymph, etc.),
#   derived by difference in dynamics
#
# Mouse and rat data from Brown et al. (1997). Human data from
#   ICRP-89 (2002), and is sex-specific.

```

```

    QFatCtmp = QFatC *
      (Species == 3 ? 0.07 : (Species == 2 ? 0.07 : (Male == 0 ? 0.085 : 0.05)
));

```

```

));

```

```

    QGutCtmp = QGutC *
      (Species == 3 ? 0.141 : (Species == 2 ? 0.153 : (Male == 0 ? 0.21 : 0.19)
));

```

```

));

```

```

    QLivCtmp = QLivC *
      (Species == 3 ? 0.02 : (Species == 2 ? 0.021 : 0.065) );
    QSlwCtmp = QSlwC *
      (Species == 3 ? 0.217 : (Species == 2 ? 0.336 : (Male == 0 ? 0.17 : 0.22)
));

```

```

));

```

```

    QKidCtmp = QKidC *
      (Species == 3 ? 0.091 : (Species == 2 ? 0.141 : (Male == 0 ?
0.17 : 0.19) ));

```

```

# Plasma Flows to Tissues (L/hr)

```

```

## Mice and rats from Hejtmancik et al. 2002,
##   control F344 rats and B6C3F1 mice at 19 weeks of age
## However, there appear to be significant strain differences in rodents, so
##   assume uncertainty CV=0.2 and variability CV=0.2.
## Human central estimate from ICRP. Well measured in humans, from Price et al.,
##   human SD in hematocrit was 0.029 in females, 0.027 in males,
##   corresponding to FracPlas CV of 0.047 in females and
##   0.048 in males. Use rounded CV = 0.05 for both uncertainty and
variability
## Use measured 1-hematocrit if available
## Truncate distributions at 3xCV to encompass clinical "normal range"
    FracPlas = (Hematocritmeas > 0.0 ? (1-Hematocritmeas) : (FracPlasC *
      (Species == 3 ? 0.52 : (Species == 2 ? 0.53 : (Male == 0 ? 0.615 :
0.567)))));

```

```

# Tissue Volumes (L)

```

```

# Fat = Adipose only
# Gut = GI tract (not contents) + pancreas + spleen (all drain to portal vein)
# Liv = Liver
# Rap = Brain + Heart + (Lungs-TB) + Bone marrow + "Rest of the body"
# VResp = Tracheobronchial region (trachea+bronchial basal+
#   bronchial secretory+bronchiolar)
# Kid = Kidney
# Bld = Blood
# Slw = Muscle + Skin, derived by difference
# residual (assumed unperfused) = (Bone-Marrow)+GI contents+other
#
# Mouse and rat data from Brown et al. (1997). Human data from
#   ICRP-89 (2002), and is sex-specific.

```

```

    VFat = BW * (VFatCmeas > 0.0 ? VFatCmeas : (VFatC * (Species == 3 ? 0.07 :
      (Species == 2 ? 0.07 : (Male == 0 ? 0.317 : 0.199) ))));

```

```

    VGut = VGutC * BW *
      (Species == 3 ? 0.049 : (Species == 2 ? 0.032 : (Male == 0 ? 0.022 :
0.020) ));

```

```

    VLiv = VLivC * BW *

```

```

(Species == 3 ? 0.055 : (Species == 2 ? 0.034 : (Male == 0 ? 0.023 :
0.025) ));
VRap = VRapC * BW *
(Species == 3 ? 0.100 : (Species == 2 ? 0.088 : (Male == 0 ? 0.093 :
0.088) ));
VRespLum = VRespLumC * BW *
(Species == 3 ? (0.00014/0.03) : (Species == 2 ? (0.0014/0.3) : (0.167/70)
)); # Lumenal volumes from Styrene model (Sarangapani et al. 2002)
VRespEfftmp = VRespEffC * BW *
(Species == 3 ? 0.0007 : (Species == 2 ? 0.0005 : 0.00018 ));
# Respiratory tract volume is TB region
# will be multiplied by partition coef. below
VKid = VKidC * BW *
(Species == 3 ? 0.017 : (Species == 2 ? 0.007 : (Male == 0 ? 0.0046 :
0.0043) ));
VBld = VBldC * BW *
(Species == 3 ? 0.049 : (Species == 2 ? 0.074 : (Male == 0 ? 0.068 :
0.077) ));
VSlw = (Species == 3 ? 0.8897 : (Species == 2 ? 0.8995 : (Male == 0 ?
0.85778 : 0.856))) * BW
- VFat - VGut - VLiv - VRap - VRespEfftmp - VKid - VBld;
# Slowly perfused:
# Baseline mouse: 0.8897-0.049-0.017-0.0007-0.1-0.055-0.049-0.07= 0.549
# Baseline rat: 0.8995 -0.074-0.007-0.0005-0.088-0.034-0.032-0.07= 0.594
# Baseline human F: 0.85778-0.068-0.0046-0.00018-0.093-0.023-0.022-0.317= 0.33
# Baseline human M: 0.856-0.077-0.0043-0.00018-0.088-0.025-0.02-0.199= 0.4425

VPlas = FracPlas * VBld;
VBod = VFat + VGut + VRap + VRespEfftmp + VKid + VSlw; # For TCA
VBodTCOH = VBod + VBld; # for TCOH and TCOG -- body without liver

# Partition coefficients
PB = (PBmeas > 0.0 ? PBmeas : (exp(lnPBC) * (Species == 3 ? 15. : (Species ==
2 ? 22. : 9.5 )))); # Blood-air
# Mice: pooling Abbas and Fisher 1997, Fisher et al. 1991
# each a single measurement, with overall CV = 0.07.
# Given small number of measurements, and variability
# in rat, use CV of 0.25 for uncertainty and variability.
# Rats: pooling Sato et al. 1977, Gargas et al. 1989,
# Barton et al. 1995, Simmons et al. 2002, Koizumi 1989,
# Fisher et al. 1989. Fisher et al. measurement substantially
# smaller than others (15 vs. 21~26). Recent article
# by Rodriguez et al. 2007 shows significant change with
# age (13.1 at PND10, 17.5 at adult, 21.8 at aged), also seems
# to favor lower values than previously reported. Therefore
# use CV = 0.25 for uncertainty and variability.
# Humans: pooling Sato and Nakajima 1979, Sato et al. 1977,
# Gargas et al. 1989, Fiserova-Bergerova et al. 1984,
# Fisher et al. 1998, Koizumi 1989
# Overall variability CV = 0.185. Consistent with
# within study inter-individual variability CV = 0.07~0.22.
# Study-to-study, sex-specific means range 8.1~11, so
# uncertainty CV = 0.2.

```

```

PFat = exp(lnPFatC) * # Fat/blood
(Species == 3 ? 36. : (Species == 2 ? 27. : 67. ));
# Mice: Abbas and Fisher 1997. Single measurement. Use
# rat uncertainty of CV = 0.3.
# Rats: Pooling Barton et al. 1995, Sato et al. 1977,
# Fisher et al. 1989. Recent article by Rodriguez et al.
# (2007) shows higher value of 36., so assume uncertainty
# CV of 0.3.
# Humans: Pooling Fiserova-Bergerova et al. 1984, Fisher et al. 1998,
# Sato et al. 1977. Variability in Fat:Air has CV = 0.07.
# For uncertainty, dominated by PB uncertainty CV = 0.2
# For variability, add CVs in quadrature for
# sqrt(0.07^2+0.185^2)=0.20
PGut = exp(lnPGutC) * # Gut/blood
(Species == 3 ? 1.9 : (Species == 2 ? 1.4 : 2.6 ));
# Mice: Geometric mean of liver, kidney
# Rats: Geometric mean of liver, kidney
# Humans: Geometric mean of liver, kidney
# Uncertainty of CV = 0.4 due to tissue extrapolation
PLiv = exp(lnPLivC) * # Liver/blood
(Species == 3 ? 1.7 : (Species == 2 ? 1.5 : 4.1 ));
# Mice: Fisher et al. 1991, single datum, so assumed uncert CV = 0.4
# Rats: Pooling Barton et al. 1995, Sato et al. 1977,
# Fisher et al. 1989, with little variation (range 1.3~1.7).
# Recent article by Rodriguez et al. reports 1.34. Use
# uncertainty CV = 0.15.
# Humans: Pooling Fiserova-Bergerova et al. 1984, Fisher et al. 1998
# almost 2-fold difference in Liver:Air values, so uncertainty
# CV = 0.4
PRap = exp(lnPRapC) * # Rapidly perfused/blood
(Species == 3 ? 1.9 : (Species == 2 ? 1.3 : 2.6 ));
# Mice: Similar to liver, kidney. Uncertainty CV = 0.4 due to
# tissue extrapolation
# Rats: Use brain values Sato et al. 1977. Recent article by
# Rodriguez et al. (2007) reports 0.99 for brain. Uncertainty
# CV of 0.4 due to tissue extrapolation.
# Humans: Use brain from Fiserova-Bergerova et al. 1984
# Uncertainty of CV = 0.4 due to tissue extrapolation
PResp = exp(lnPRespC) * # Resp/blood =
(Species == 3 ? 2.6 : (Species == 2 ? 1.0 : 1.3 ));
# Mice: Abbas and Fisher 1997, single datum, so assumed uncert CV = 0.4
# Rats: Sato et al. 1977, single datum, so assumed uncert CV = 0.4
# Humans: Pooling Fiserova-Bergerova et al. 1984, Fisher et al. 1998
# > 2-fold difference in lung:air values, so uncertainty
# CV = 0.4
VRespEff = VRespEfftmp * PResp * PB; # Effective air volume
PKid = exp(lnPKidC) * # Slowly perfused/blood
(Species == 3 ? 2.1 : (Species == 2 ? 1.3 : 1.6 ));
# Mice: Abbas and Fisher 1997, single datum, so assumed uncert CV = 0.4
# Rats: Pooling Barton et al. 1995, Sato et al. 1977. Recent article
# by Rodriguez et al. (2007) reports 1.01, so use uncertainty
# CV of 0.3. Pooled variability CV = 0.39.
# Humans: Pooling Fiserova-Bergerova et al. 1984, Fisher et al. 1998

```

```

# For uncertainty, dominated by PB uncertainty CV = 0.2
# Variability in kidney:air CV = 0.23, so add to PB variability
# in quadrature sqrt(0.23^2+0.185^2)=0.30
Pslw = exp(lnPslwC) * # Slowly perfused/blood
      (Species == 3 ? 2.4 : (Species == 2 ? 0.58 : 2.1 ));
# Mice: Muscle - Abbas and Fisher 1997, single datum, so assumed
# uncert CV = 0.4
# Rats: Pooling Barton et al. 1995, Sato et al. 1977,
# Fisher et al. 1989. Recent article by Rodriguez et al. (2007)
# reported 0.72, so use uncertainty CV of 0.25. Variability
# in Muscle:air and muscle:blood ~ CV = 0.3
# Humans: Pooling Fiserova-Bergerova et al. 1984, Fisher et al. 1998
# Range of values 1.4~2.4, so uncertainty CV = 0.3
# Variability in muscle:air CV = 0.3, so add to PB variability
# in quadrature sqrt(0.3^2+0.185^2)=0.35

# TCA partitioning
TCAPlas = FracPlas + (1 - FracPlas) * 0.5 * exp(lnPRBCPlasTCAC);
# Blood/Plasma concentration ratio. Note dependence
# on fraction of blood that is plasma. Here
# exp(lnPRBCPlasTCA) = partition coefficient
# C(blood minus plasma)/C(plasma)
# Default of 0.5, corresponding to Blood/Plasma
# concentration ratio of 0.76 in
# rats (Schultz et al 1999)
# For rats, Normal uncertainty with GSD = 1.4
# For mice and humans, diffuse prior uncertainty of
# 100-fold up/down
PBodTCA = TCAPlas * exp(lnPBodTCAC) *
      (Species == 3 ? 0.88 : (Species == 2 ? 0.88 : 0.52 ));
# Note -- these were done at 10-20 microg/ml (Abbas and Fisher 1997),
# which is 1.635-3.27 mmol/ml (1.635-3.27 x 10^6 microM).
# At this high concentration, plasma binding should be
# saturated -- e.g., plasma albumin concentration was
# measured to be P=190-239 microM in mouse, rat, and human
# plasma by Lumpkin et al. 2003, or > 6800 molecules of
# TCA per molecule of albumin. So the measured partition
# coefficients should reflect free blood-tissue partitioning.
# Used muscle values, multiplied by blood:plasma ratio to get
# Body:Plasma partition coefficient
# Rats = mice from Abbas and Fisher 1997
# Humans from Fisher et al. 1998
# Uncertainty in mice, humans GSD = 1.4
# For rats, GSD = 2.0, based on difference between mice
# and humans.
PLivTCA = TCAPlas * exp(lnPLivTCAC) *
      (Species == 3 ? 1.18 : (Species == 2 ? 1.18 : 0.66 ));
# Multiplied by blood:plasma ratio to get Liver:Plasma
# Rats = mice from Abbas and Fisher 1997
# Humans from Fisher et al. 1998
# Uncertainty in mice, humans GSD = 1.4
# For rats, GSD = 2.0, based on difference between mice
# and humans.

# Binding Parameters for TCA
# GM of Lumpkin et al. 2003; Schultz et al. 1999;
# Templin et al. 1993, 1995; Yu et al. 2000
# Protein/TCA dissociation constant (umole/L)
# note - GSD = 3.29, 1.84, and 1.062 for mouse, rat, human
kDissoc = exp(lnkDissocC) *
      (Species == 3 ? 107. : (Species == 2 ? 275. : 182. ));
# BMax = NSites * Protein concentration. Sampled parameter is
# BMax/kD (determines binding at low concentrations)
# note - GSD = 1.64, 1.60, 1.20 for mouse, rat, human
BMax = kDissoc * exp(lnBMaxkDC) *
      (Species == 3 ? 0.88 : (Species == 2 ? 1.22 : 4.62 ));

# TCOH partitioning
# Data from Abbas and Fisher 1997 (mouse) and Fisher et al.
# 1998 (human). For rat, used mouse values.
# Uncertainty in mice, humans GSD = 1.4
# For rats, GSD = 2.0, based on difference between mice
# and humans.
PBodTCOH = exp(lnPBodTCOHC) *
      (Species == 3 ? 1.11 : (Species == 2 ? 1.11 : 0.91 ));
PLivTCOH = exp(lnPLivTCOHC) *
      (Species == 3 ? 1.3 : (Species == 2 ? 1.3 : 0.59 ));

# TCOG partitioning
# Use TCOH as a proxy, but uncertainty much greater
# (e.g., use uniform prior, 100-fold up/down)
PBodTCOG = exp(lnPBodTCOGC) *
      (Species == 3 ? 1.11 : (Species == 2 ? 1.11 : 0.91 ));
PLivTCOG = exp(lnPLivTCOGC) *
      (Species == 3 ? 1.3 : (Species == 2 ? 1.3 : 0.59 ));

# DCVG distribution volume
# exp(lnPeffDCVG) is the effective partition coefficient for
# the "body" (non-blood) compartment
# Diffuse prior distribution: loguniform 1e-3 to 1e3
VDCVG = VBld + # blood plus body (with "effective" PC)
      exp(lnPeffDCVG) * (VBod + VLiv);

# Absorption Rate Constants (/hr)
# All priors are diffuse (log)uniform distributions
# transfer from stomach centered on 1.4/hr, range up or down 100-fold,
# based on human stomach half-time of 0.5 hr.
kTSD = exp(lnkTSD);
# stomach absorption centered on 1.4/hr, range up or down 1000-fold
kAS = exp(lnkAS);
# assume no fecal excretion -- 100% absorption
kTD = 0.0 * exp(lnkTD);
# intestinal absorption centered on 0.75/hr, range up or down
# 1000-fold, based on human transit time of small intestine
# of 4 hr (95% throughput in 4 hr)

```

This document is a draft for review purposes only and does not constitute Agency policy

```

kAD = exp(lnkAD);
kASTCA = exp(lnkASTCA);
kASTCOH = exp(lnkASTCOH);

# TCE Oxidative Metabolism Constants
# For rodents, in vitro microsomal data define priors (pooled).
# For human, combined in vitro microsomoal+hepatocellular individual data
#   define priors.
# All data from Elfarra et al. 1998; Lipscomb et al. 1997, 1998a,b
# For VMax, scaling from in vitro data were (Barter et al. 2007):
#   32 mg microsomal protein/g liver
#   99 x 1e6 hepatocytes/g liver
#   Here, human data assumed representative of mouse and rats.
# For KM, two different scaling methods were used for microsomes:
#   Assume microsomal concentration = liver concentration, and
#   use central estimate of liver:blood PC (see above)
#   Use measured microsomo:air partition coefficient (1.78) and
#   central estimate of blood:air PC (see above)
# For human KM from hepatocytes, used measured human hepatocyte:air
#   partition coefficient (21.62, Lipscomb et al. 1998), and
#   central estimate of blood:air PC.
# Note that to that the hepatocyte:air PC is similar to that
#   found in liver homogenates (human: 29.4+/-5.1 from Fiserova-
#   Bergerova et al. 1984, and 54 for Fisher et al. 1998; rat:
#   27.2+/-3.4 from Gargas et al. 1989, 62.7 from Koisumi 1989,
#   43.6 from Sato et al. 1977; mouse: 23.2 from Fisher et al. 1991).
# For humans, sampled parameters are VMax and ClC (VMax/KM), due to
#   improved convergence. VMax is kept as a parameter because it
#   appears less uncertain (i.e., more consistent across microsomal
#   and hepatocyte data).

# Central estimate of VMax is 342, 76.2, and 32.3 (micromol/min/
#   kg liver) for mouse, rat, human. Converting to /hr by
#   * (60 min/hr * 0.1314 mg/micromol) gives
#   2700, 600, and 255 mg/hr/kg liver
# Observed variability of about 2-fold GSD. Assume 2-fold GSD for
#   both uncertainty and variability
VMax = Vliv*exp(lnVMaxC)*
  (Species == 3 ? 2700. : (Species == 2 ? 600. : 255.));

# For mouse and rat central estimates for KM are 0.068~1.088 and
#   0.039~0.679 mmol/l in blood, depending on the scaling
#   method used. Taking the geometric mean, and converting
#   to mg/l by 131.4 mg/mmol gives 36. and 21. mg/l in blood.
# For human, central estimate
#   for Cl are 0.306~3.95 l/min/kg liver. Taking the geometric
#   mean and converting to /hr gives a central estimate of
#   66. l/hr/kg.
#   KM is then derived from KM = VMax/(Cl*Vliv) (central estimate
#   of
# Note uncertainty due to scaling is about 4-fold.
#   Variability is about 3-fold in mice, 1.3-fold in rats, and
#   2- to 4- fold in humans (depending on scaling).

KM = (Species == 3 ? 36.*exp(lnKMC) : (Species == 2 ? 21.*exp(lnKMC) :
VMax/(Vliv*66.*exp(lnClC))));

# Oxidative metabolism splits
#   Fractional split of TCE to DCA
#   exp(lnFracOtherC) = ratio of DCA to non-DCA
#   Diffuse prior distribution: loguniform 1e-4 to 1e2
FracOther = exp(lnFracOtherC)/(1+exp(lnFracOtherC));
# Fractional split of TCE to TCA
#   exp(lnFracTCAC) = ratio of TCA to TCOH
#   TCA/TCOH = 0.1 from Lipscomb et al. 1998 using fresh hepatocytes,
#   but TCA/TCOH ~ 1 from Bronley-DeLancey et al 2006
#   GM = 0.32, GSD = 3.2
FracTCA = 0.32*exp(lnFracTCAC)*(1-FracOther)/(1+0.32*exp(lnFracTCAC));

# TCE GSH Metabolism Constants
# Human in vitro data from Lash et al. 1999, define human priors.
#
#           VMax (nmol/min/      KM (mM)           CLeff (ml/min/
#           g tissue)                g tissue)
# -----
#           [high affinity pathway only] [total]
# Human liver cytosol:    ~423           0.0055-0.023       21.2~87.0
# Human liver cytosol+   ~211           --                --
#   microsomes
#
#           [total]           [total]           [total]
# Human hepatocytes*     12~30**        0.012-0.039***     0.2~0.5****
# Human kidney cytosol:   81            0.0164-0.0263      3.08-4.93
#
# * estimated visually from Fig 1, Lash et al. 1999
# ** Fig 1A, data from 50~500 ppm headspace at 60 min
#   and Fig 1B, data at 100~5000 ppm in headspace for 120 min
# *** Fig 1B, 30~100 ppm headspace, converted to blood concentration
#   using blood:air PC of 9.5
# **** Fig 1A, data at 50 ppm headspace at 120 min and Fig 1B, data at
#   25 and 50 ppm headspace at 120 min.
# Overall, human liver hepatocytes are probably most like the
#   intact liver (e.g., accounting for the competition between
#   GSH conjugation and oxidation). So central estimates based
#   on those: CLeff ~ 0.32 ml/min/g tissue, KM ~ 0.022 mM in blood.
#   CLeff converted to 19 l/hr/kg; KM converted to 2.9 mg/l in blood
#   However, uncertainty in CLeff is large (values in cytosol
#   ~100-fold larger). Moreover, Green et al. 1997 reported
#   DCVG formation in cytosol that was ~30,000-fold smaller
#   than Lash et al. (1998) in cytosol, which would be a VMax
#   ~300-fold smaller than Lash et al. (1998) in hepatocytes.
#   Uncertainty in KM appears smaller (~4-fold)
#   CLC: GM = 19., GSD = 100; KM: GM = 2.9., GSD = 4.
#   In addition, at a single concentration, the variability
#   in human liver cytosol samples had a GSD=1.3.
# For the human kidney, the kidney cytosol values are used, with the same
#   uncertainty as for the liver. Note that the DCVG formation rates
#   in rat kidney cortical cells and rat cytosol are quite similar
#   (see below).
#   CLC: GM = 230., GSD = 100; KM: GM = 2.7., GSD = 4.

```

```

# Rat and mouse in vitro data from Lash et al. 1995,1998 define rat and mouse
# priors. However, rats and mice are only assayed at 1 and 2 mM
# providing only a bound on VMax and very little data on KM.
#           Rate at 2 mM      Equivalent      CLeff
#           (nmol/min/      blood conc.      at 2 mM
#           g tissue)        (mM)            (ml/min/
#                               g tissue)
# -----
# Rat   hepatocytes:  4.4~16      2.0            0.0022~0.0079
#       liver cytosol: 8.0~12      1.7~2.0        0.0040~0.0072
#       kidney cells: 0.79~1.1  2.2            0.00036~0.00049
#       kidney cytosol: 0.53~0.75  1.1~2.0        0.00027~0.00068
# Mouse liver cytosol: 36~40      1.1~2.0        0.018~0.036
#       kidney cytosol: 6.2~9.3      0.91~2.0      0.0031~0.0102
#
# In most cases, rates were increased over the same sex/species at 1 mM,
# indicating VMax has not yet been reached. The values between cells
# and cytosol are more much consistent that in the human data.
# These data therefore put a lower bound on VMax and a lower bound
# on CLC. To account for in vitro-in vivo uncertainty, the lower
# bound of the prior distribution is set 100-fold below the central
# estimate of the measurements here. In addition, Green et al.
# (1997) found values 100-fold smaller than Lash et al. 1995, 1998.
# Therefore diffuse prior distributions set to 1e-2~1e4.
# Rat liver: Bound on VMax of 4.4~16, with GM of 8.4. Converting to
# mg/hr/kg tissue (* 131.4 ng/nmol * 60 min/hr * 1e3 g/kg / 1e6 mg/ng)
# gives a central estimate of 66. mg/hr/kg tissue. Bound on CL of
# 0.0022~0.0079, with GM of 0.0042. Converting to l/hr/kg tissue
# (* 60 min/hr) gives 0.25 l/hr/kg tissue.
# Rat kidney: Bound on VMax of 0.53~1.1, with GM of 0.76. Converting
# to mg/hr/kg tissue gives a central estimate of 6.0 mg/hr/kg.
# Bound on CL of 0.00027~0.00068, with GM of 0.00043. Converting
# to l/hr/kg tissue gives 0.026 l/hr/kg tissue.
# Mouse liver: Bound on VMax of 36~40, with GM of 38. Converting
# to mg/hr/kg tissue gives a central estimate of 300. mg/hr/kg.
# Bound on CL of 0.018~0.036, with GM of 0.025. Converting
# to l/hr/kg tissue gives 1.53 l/hr/kg tissue.
# Mouse kidney: Bound on VMax of 6.2~9.3, with GM of 7.6. Converting
# to mg/hr/kg tissue gives a central estimate of 60. mg/hr/kg.
# Bound on CL of 0.0031~0.0102, with GM of 0.0056. Converting
# to l/hr/kg tissue gives 0.34 l/hr/kg tissue.

VMaxDCVG = VLiv*(Species == 3 ? (300.*exp(lnVMaxDCVGC)) : (Species == 2 ?
(66.*exp(lnVMaxDCVGC)) : (2.9*19.*exp(lnClDCVGC+lnKMDCVGC)))));
KMDCVG = (Species == 3 ? (VMaxDCVG/(VLiv*1.53*exp(lnClDCVGC))) : (Species ==
2 ? (VMaxDCVG/(VLiv*0.25*exp(lnClDCVGC))) : 2.9*exp(lnKMDCVGC)));
VMaxKidDCVG = VKid*(Species == 3 ? (60.*exp(lnVMaxKidDCVGC)) : (Species ==
2 ? (6.0*exp(lnVMaxKidDCVGC)) : (2.7*230.*exp(lnClKidDCVGC+lnKMKidDCVGC)))));
KMKidDCVG = (Species == 3 ? (VMaxKidDCVG/(VKid*0.34*exp(lnClKidDCVGC))) :
(Species == 2 ? (VMaxKidDCVG/(VKid*0.026*exp(lnClKidDCVGC)))) :
2.7*exp(lnKMKidDCVGC)));

# TCE Metabolism Constants for Chloral Kinetics in Lung (mg/hr)

```

```

# Scaled to liver VMax using data from Green et al. (1997)
# in microsomal preparations (nmol/min/mg protein) at ~1 mM.
# For humans, used detection limit of 0.03
# Additional scaling by lung/liver weight ratio
# from Brown et al. Table 21 (mouse and rat) or
# ICRP Pub 89 Table 2.8 (Human female and male)
# Uncertainty ~ 3-fold truncated at 3 GSD
VMaxClara = exp(lnVMaxLungLivC) * VMax *
(Species == 3 ? (1.03/1.87*0.7/5.5):(Species == 2 ?
(0.08/0.82*0.5/3.4):(0.03/0.33*(Male == 0 ? (0.42/1.4) : (0.5/1.8)))));
KMClara = exp(lnKMClara);
# Fraction of Respiratory Metabolism that goes to system circulation
# (translocated to the liver)
FracLungSys = exp(lnFracLungSysC)/(1 + exp(lnFracLungSysC));

# TCOH Metabolism Constants (mg/hr)
# No in vitro data. So use diffuse priors of
# 1e-4 to 1e4 mg/hr/kg^0.75 for VMax
# (4e-5 to 4000 mg/hr for rat),
# 1e-4 to 1e4 mg/l for KM,
# and 1e-5 to 1e3 l/hr/kg^0.75 for CL
# (2e-4 to 2.4e4 l/hr for human)
VMaxTCOH = BW75*
(Species == 3 ? (exp(lnVMaxTCOHC)) : (Species == 2 ?
(exp(lnVMaxTCOHC)) : (exp(lnClTCOHC+lnKMTCOH))));
KMTCOH = exp(lnKMTCOH);
VMaxGluc = BW75*
(Species == 3 ? (exp(lnVMaxGlucC)) : (Species == 2 ?
(exp(lnVMaxGlucC)) : (exp(lnClGlucC+lnKMGluc))));
KMGluc = exp(lnKMGluc);
# No in vitro data. So use diffuse priors of
# 1e-5 to 1e3 kg^0.25/hr (3.5e-6/hr to 3.5e2/hr for human)
kMetTCOH = exp(lnkMetTCOHC) / BW25;

# TCA kinetic parameters
# Central estimate based on GFR clearance per unit body weight
# 10.0, 8.7, 1.8 ml/min/kg for mouse, rat, human
# (= 0.6, 0.522, 0.108 l/hr/kg) from Lin 1995.
# = CL_GFR / BW (BW=0.02 for mouse, 0.265 for rat, 70 for human)
# kUrn = CL_GFR / VPlas
# Diffuse prior with uncertainty of up,down 100-fold
kUrnTCA = exp(lnkUrnTCAC) * BW / VPlas *
(Species == 3 ? 0.6 : (Species == 2 ? 0.522 : 0.108));
# No in vitro data. So use diffuse priors of
# 1e-4 to 1e2 /hr/kg^0.25 (0.3/hr to 35/hr for human)
kMetTCA = exp(lnkMetTCAC) / BW25;

# TCOG kinetic parameters
# No in vitro data. So use diffuse priors of
# 1e-4 to 1e2 /hr/kg^0.25 (0.3/hr to 35/hr for human)
kBile = exp(lnkBileC) / BW25;
kEHR = exp(lnkEHRC) / BW25;
# Central estimate based on GFR clearance per unit body weight

```

```

#           10.0, 8.7, 1.8 ml/min/kg for mouse, rat, human
#           (= 0.6, 0.522, 0.108 l/hr/kg) from Lin 1995.
#           = CL_GFR / BW (BW=0.02 for mouse, 0.265 for rat, 70 for human)
#           kUrn = CL_GFR / VBld
#           Diffuse prior with Uncertainty of up,down 1000-fold
kUrnTCOG = exp(lnkUrnTCOGC) * BW / (VBodTCOH * PBodTCOG) *
          (Species == 3 ? 0.6 : (Species == 2 ? 0.522 : 0.108));

# DCVG Kinetics (/hr)
# Fraction of renal TCE GSH conj. "directly" to DCVC via "first pass"
# exp(lnFracOtherCC) = ratio of direct/non-direct
# Diffuse prior distribution: loguniform 1e-3 to 1e3
# FIXED in v1.2.3
# In ".in" files, set to 1, so that all kidney GSH conjugation
# is assumed to directly produce DCVC (model lacks identifiability
# otherwise).
FracKidDCVC = exp(lnFracKidDCVCC) / (1 + exp(lnFracKidDCVCC));
# No in vitro data. So use diffuse priors of
#           1e-4 to 1e2 /hr/kg^0.25 (0.3/hr to 35/hr for human)
kDCVG = exp(lnkDCVGC) / BW25;

# DCVC Kinetics in Kidney (/hr)
# No in vitro data. So use diffuse priors of
#           1e-4 to 1e2 /hr/kg^0.25 (0.3/hr to 35/hr for human)
kNAT = exp(lnkNATC) / BW25;
kKidBioact = exp(lnkKidBioactC) / BW25;

# CC data initialization
Rodents = (CC > 0 ? NRodents : 0.0); # Closed chamber simulation
VCh = (CC > 0 ? VChC - (Rodents * BW) : 1.0);
# Calculate net chamber volume
kLoss = (CC > 0 ? exp(lnkLossC) : 0.0);

*****
***           State Variable Initialization and Scaling           ***
*****
# NOTE: All State Variables are automatically set to 0 initially,
# unless re-initialized here

          Ach = (CC * VCh * MWTCE) / 24450.0; # Initial amount in chamber
);
##### End of Initialization #####

Dynamics{
*****
***           Dynamic physiological parameter scaling           ***
*****
# State Variables with dynamics:
#           none
# Input Variables:
#           QPmeas

# Other State Variables and Global Parameters:
#           QC
#           VPR
#           DResptmp
#           QPsamp
#           QFatCtmp
#           QGutCtmp
#           QLivCtmp
#           QSlwCtmp
#           QKidCtmp
#           FracPlas
# Temporary variables used:
#           none
# Temporary variables assigned:
#           QP
#           DResp
#           QCnow
#           QFat
#           QGut
#           QLiv
#           QSlw
#           QKid
#           QGutLiv
#           QRap
#           QCPlas
#           QBodPlas
#           QGutLivPlas
# Notes:
*****
# QP uses QPmeas if value is > 0, otherwise uses sampled value
          QP = (QPmeas > 0 ? QPmeas : QPsamp);
          DResp = DResptmp * QP;

# QCnow uses QPmeas/VPR if QPmeas > 0, otherwise uses sampled value
          QCnow = (QPmeas > 0 ? QPmeas/VPR : QC);

# These done here in dynamics in case QCnow changes
# Blood Flows to Tissues (L/hr)
          QFat = (QFatCtmp) * QCnow; #
          QGut = (QGutCtmp) * QCnow; #
          QLiv = (QLivCtmp) * QCnow; #
          QSlw = (QSlwCtmp) * QCnow; #

          QKid = (QKidCtmp) * QCnow; #
          QGutLiv = QGut + QLiv; #
          QRap = QCnow - QFat - QGut - QLiv - QSlw - QKid;
          QRapCtmp = QRap/QCnow; #(vrisk)
          QBod = QCnow - QGutLiv;

# Plasma Flows to Tissues (L/hr)
          QCPlas = FracPlas * QCnow; #
          QBodPlas = FracPlas * QBod; #

```

10/20/09

A-98

DRAFT: DO NOT CITE OR QUOTE

This document is a draft for review purposes only and does not constitute Agency policy

```

QGutLivPlas = FracPlas * QGutLiv; #

#####
***          Exposure and Absorption calculations          ***
#####
# State Variables with dynamics:
#   AStom
#   ADuod
#   AStomTCA
#   AStomTCOH
# Input Variables:
#   IVDose
#   PDose
#   Drink
#   Conc
#   IVDoseTCA
#   PODoseTCA
#   IVDoseTCOH
#   PODoseTCOH
# Other State Variables and Global Parameters:
#   ACh
#   CC
#   VCh
#   MWTCE
#   BW
#   TChng
#   kAS
#   kTSD
#   kAD
#   kTD
#   kASTCA
#   kASTCOH
# Temporary variables used:
#   none
# Temporary variables assigned:
#   kIV - rate into CVen
#   kIA - rate into CArt
#   kPV - rate into portal vein
#   kStom - rate into stomach
#   kDrink - incorporated into RAO
#   RAO - rate into gut (oral absorption - both gavage and drinking water)
#   CIinh - inhalation exposure concentration
#   kIVTCA - rate into blood
#   kStomTCA - rate into stomach
#   kPOTCA - rate into liver (oral absorption)
#   kIVTCOH - rate into blood
#   kStomTCOH - rate into stomach
#   kPOTCOH - rate into liver (oral absorption)
# Notes:
# For oral dosing, using "Spikes" for instantaneous inputs
# Inhalation Concentration (mg/L)
#   CIinh uses Conc when open chamber (CC=0) and
#   ACh/VCh when closed chamber CC>0.

```

```

#####
#### TCE DOSING
## IV route
    kIV = (IVDose * BW) / TChng; # IV infusion rate (mg/hr)
                                     # (IVDose constant for duration TChng)
    kIA = (IADose * BW) / TChng;      # IA infusion rate (mg/hr)
    kPV = (PVDose * BW) / TChng;      # PV infusion rate (mg/hr)
    kStom = (PDose * BW) / TChng; # PO dose rate (into stomach) (mg/hr)

## Oral route
# Amount of TCE in stomach -- for oral dosing only (mg)
    dt(AStom) = kStom - AStom * (kAS + kTSD);

# Amount of TCE in duodenum -- for oral dosing only (mg)
    dt(ADuod) = (kTSD * AStom) - (kAD + kTD) * ADuod;
# Rate of absorption from drinking water
    kDrink = (Drink * BW) / 24.0; # Ingestion rate via drinking water (mg/hr)
# Total rate of absorption including gavage and drinking water
    RAO = kDrink + (kAS * AStom) + (kAD * ADuod);
## Inhalation route
    CIinh = (CC > 0 ? ACh/VCh : Conc*MWTCE/24450.0); # in mg/l

#### TCA Dosing
    kIVTCA = (IVDoseTCA * BW) / TChng; # TCA IV infusion rate (mg/hr)
    kStomTCA = (PODoseTCA * BW) / TChng; # TCA PO dose rate into stomach
    dt(AStomTCA) = kStomTCA - AStomTCA * kASTCA;
    kPOTCA = AStomTCA * kASTCA; # TCA oral absorption rate (mg/hr)

#### TCOH Dosing
    kIVTCOH = (IVDoseTCOH * BW) / TChng; # TCOH IV infusion rate (mg/hr)
    kStomTCOH = (PODoseTCOH * BW) / TChng; # TCOH PO dose rate into stomach
    dt(AStomTCOH) = kStomTCOH - AStomTCOH * kASTCOH;
    kPOTCOH = AStomTCOH * kASTCOH; # TCOH oral absorption rate (mg/hr)

#####
***          TCE Model          ***
#####
# State Variables with dynamics:
#   ARap,          # Amount in rapidly perfused tissues
#   ASlw,          # Amount in slowly perfused tissues
#   AFat,          # Amount in fat
#   AGut,          # Amount in gut
#   ALiv,          # Amount in liver
#   AIinhResp,
#   AResp,
#   AExhResp,
#   AKid,          # Amount in Kidney -- currently in Rap tissue
#   ABld,          # Amount in Blood -- currently in Rap tissue
#   ACh,          # Amount of TCE in closed chamber
# Input Variables:
#   none
# Other State Variables and Global Parameters:

```

10/20/09

This document is a draft for review purposes only and does not constitute Agency policy

A-99

DRAFT: DO NOT CITE OR QUOTE

```

# VRap
# PRap
# VSlw
# PSlw
# VFat
# PFat
# VGut
# PGut
# VLiv
# PLiv
# VRespLum
# VRespEff
# FracLungSys
# VKid
# PKid
# VBld
# VMaxClara
# KMClara
# PB
# Rodents
# VCh
# kLoss
# VMax
# KM
# VMaxDCVG
# KMDCVG
# VMaxKidDCVG
# KMKidDCVG
# Temporary variables used:
# QM
# QFat
# QGutLiv
# QSlw
# QRap
# QKid
# kIV
# QCnow
# CInh
# QP
# RAO
# Temporary variables assigned:
# QM
# CRap
# CSlw
# CFat
# CGut
# CLiv
# CInhResp
# CResp
# CExhResp
# ExhFactor
# CMixExh
# CKid

```

```

# CVRap
# CVSlw
# CVFat
# CVGut
# CVLiv
# CVTB
# CVKid
# CVen
# RAMetLng
# CArt_tmp
# CArt
# CALv
# RAMetLiv1
# RAMetLiv2
# RAMetKid
# Notes:
#*****
#
#****Blood (venous)*****
# Tissue Concentrations (mg/L)
# CRap = ARap/VRap;
# CSlw = ASlw/VSlw;
# CFat = AFat/VFat;
# CGut = AGut/VGut;
# CLiv = ALiv/VLiv;
# CKid = AKid/VKid;
# Venous Concentrations (mg/L)
# CVRap = CRap / PRap;
# CVSlw = CSlw / PSlw;
# CVFat = CFat / PFat;
# CVGut = CGut / PGut;
# CVLiv = CLiv / PLiv;
# CVKid = CKid / PKid;
# Concentration of TCE in mixed venous blood (mg/L)
# CVen = ABld/VBld;
# Dynamics for blood
# dt(ABld) = (QFat*CVFat + QGutLiv*CVLiv + QSlw*CVSlw +
# QRap*CVRap + QKid*CVKid + kIV) - CVen * QCnow;
#****Gas exchange and Respiratory Metabolism*****
#
# QM = QP/0.7; # Minute-volume
# CInhResp = AInhResp/VRespLum;
# CResp = AResp/VRespEff;
# CExhResp = AExhResp/VRespLum;
# dt(AInhResp) = (QM*CInh + DResp*(CResp-CInhResp) - QM*CInhResp);
# RAMetLng = VMaxClara * CResp / (KMClara + CResp);
# dt(AResp) = (DResp*(CInhResp + CExhResp - 2*CResp) - RAMetLng);
# CArt_tmp = (QCnow*CVen + QP*CInhResp) / (QCnow + (QP/PB));
# dt(AExhResp) = (QM*(CInhResp-CExhResp) + QP*(CArt_tmp/PB-CInhResp) +
# DResp*(CResp-CExhResp));
# CMixExh = (CExhResp > 0 ? CExhResp : 1e-15); # mixed exhaled breath

```



```

# Concentration in alveolar air (mg/L)
# Correction factor for exhaled air to account for
# absorption/desorption/metabolism in respiratory tissue
# = 1 if DResp = 0
ExhFactor_den = (QP * CART_tmp / PB + (QM-QP)*CInhResp);
ExhFactor = (ExhFactor_den > 0) ? (
    QM * CMixExh / ExhFactor_den) : 1;
# End-exhaled breath (corrected for absorption/
# desorption/metabolism in respiratory tissue)
CALV = CART_tmp / PB * ExhFactor;
# Concentration in arterial blood entering circulation (mg/L)
CART = CART_tmp + kIA/QCnow; # add inter-arterial dose

#****Other dynamics for inhalation/exhalation ****
# Dynamics for amount of TCE in closed chamber
dt(ACh) = (Rodents * (QM * CMixExh - QM * ACh/VCh)) - (kLoss * ACh);

#**** Non-metabolizing tissues ****
# Amount of TCE in rapidly perfused tissues (mg)
dt(ARap) = QRap * (CART - CVRap);
# Amount of TCE in slowly perfused tissues
dt(ASlw) = QSlw * (CART - CVSlw);
# Amount of TCE in fat tissue (mg)
dt(AFat) = QFat*(CART - CVFat);
# Amount of TCE in gut compartment (mg)
dt(AGut) = (QGut * (CART - CVGut)) + RAO;

#**** Liver ****
# Rate of TCE oxidation by P450 to TCA, TCOH, and other (DCA) in liver (mg/hr)
RAMetLiv1 = (VMax * CVLiv) / (KM + CVLiv);
# Rate of TCE metabolized to DCVG in liver (mg)
RAMetLiv2 = (VMaxDCVG * CVLiv) / (KMDCVG + CVLiv);
# Dynamics for amount of TCE in liver (mg)
dt(ALiv) = (QLiv * (CART - CVLiv)) + (QGut * (CVGut - CVLiv))
    - RAMetLiv1 - RAMetLiv2 + kPV; # added PV dose

#**** Kidney ****
# Rate of TCE metabolized to DCVG in kidney (mg) #
RAMetKid = (VMaxKidDCVG * CVKid) / (KMKidDCVG + CVKid);
# Amount of TCE in kidney compartment (mg)
dt(AKid) = (QKid * (CART - CVKid)) - RAMetKid;

#**** TCOH Sub-model ****
# State Variables with dynamics:
# ABodTCOH
# ALivTCOH
# Input Variables:
# none
# Other State Variables and Global Parameters:
# ABileTCOG

```

```

# kEHR
# VBodTCOH
# PBodTCOH
# VLiv
# PLivTCOH
# VMaxTCOH
# KMTCOH
# VMaxGluc
# KMGluc
# kMetTCOH - hepatic metabolism of TCOH (e.g., to DCA)
# FracOther
# FracTCA
# StochTCOHTCE
# StochTCOHGluc
# FracLungSys
# Temporary variables used:
# QBod
# QGutLiv
# QCnow
# kPOTCOH
# RAMetLiv1
# RAMetLng
# Temporary variables assigned:
# CVBodTCOH
# CVLivTCOH
# CTCOH
# RAMetTCOHTCA
# RAMetTCOHGluc
# RAMetTCOH
# RAREcircTCOG
# Notes:
#**** Blood (venous=arterial) ****
# Venous Concentrations (mg/L)
CVBodTCOH = ABodTCOH / VBodTCOH / PBodTCOH;
CVLivTCOH = ALivTCOH / VLiv / PLivTCOH;
CTCOH = (QBod * CVBodTCOH + QGutLiv * CVLivTCOH + kIVTCOH)/QCnow;

#**** Body ****
# Amount of TCOH in body
dt(ABodTCOH) = QBod * (CTCOH - CVBodTCOH);

#**** Liver ****
# Rate of oxidation of TCOH to TCA (mg/hr)
RAMetTCOHTCA = (VMaxTCOH * CVLivTCOH) / (KMTCOH + CVLivTCOH);
# Amount of glucuronidation to TCOG (mg/hr)
RAMetTCOHGluc = (VMaxGluc * CVLivTCOH) / (KMGluc + CVLivTCOH);
# Amount of TCOH metabolized to other (e.g., DCA)
RAMetTCOH = kMetTCOH * ALivTCOH;
# Amount of TCOH-Gluc recirculated (mg)
RAREcircTCOG = kEHR * ABileTCOG;
# Amount of TCOH in liver (mg)

```

```

dt(ALivTCOH) = kPOTCOH + QGutLiv * (CTCOH - CVLivTCOH)
              - RAMetTCOH - RAMetTCOHTCA - RAMetTCOHGluc
              + ((1.0 - FracOther - FracTCA) * StochTCOHTCE *
                 (RAMetLivl + FracLungSys*RAMetLng))
              + (StochTCOHGluc * RARecircTCOG);

#####
***                               TCA Sub-model                               ***
#####
# State Variables with dynamics:
#   APlasTCA
#   ABodTCA
#   ALivTCA
#   AUrnTCA
#   AUrnTCA_sat
#   AUrnTCA_collect
# Input Variables:
#   TCAUrnSat
#   UrnMissing
# Other State Variables and Global Parameters:
#   VPlas
#   MWTCA
#   kDissoc
#   BMax
#   kMetTCA -- hepatic metabolism of TCA (e.g., to DCA)
#   VBod
#   PBodTCA
#   PLivTCA
#   kUrnTCA
#   FracTCA
#   StochTCATCE
#   StochTCATCOH
#   FracLungSys
# Temporary variables used:
#   kIVTCA
#   kPOTCA
#   QBodPlas
#   QGutLivPlas
#   QCPlas
#   RAMetLivl
#   RAMetTCOHTCA
#   RAMetLng
# Temporary variables assigned:
#   CPlasTCA
#   CPlasTCAMole
#   a, b, c
#   CPlasTCAFreeMole
#   CPlasTCAFree
#   APlasTCAFree
#   CPlasTCABnd
#   CBodTCAFree
#   CLivTCAFree
#   CBodTCA

#   CLivTCA
#   CVBodTCA
#   CVLivTCA
#   RUrnTCA
#   RAMetTCA
# Notes:
#####
**** Plasma #####
# Concentration of TCA in plasma (umoles/L)
  CPlasTCA = (APlasTCA<1.0e-15 ? 1.0e-15 : APlasTCA/VPlas);
# Concentration of free TCA in plasma in (umoles/L)
  CPlasTCAMole = (CPlasTCA / MWTCA) * 1000.0;
  a = kDissoc+BMax-CPlasTCAMole;
  b = 4.0*kDissoc*CPlasTCAMole;
  c = (b < 0.01*a*a ? b/2.0/a : sqrt(a*a+b)-a);
  CPlasTCAFreeMole = 0.5*c;
# Concentration of free TCA in plasma (mg/L)
  CPlasTCAFree = (CPlasTCAFreeMole * MWTCA) / 1000.0;
  APlasTCAFree = CPlasTCAFree * VPlas;
# Concentration of bound TCA in plasma (mg/L)
  CPlasTCABnd = (CPlasTCA<CPlasTCAFree ? 0 : CPlasTCA-CPlasTCAFree);
# Concentration in body and liver
  CBodTCA = (ABodTCA<0 ? 0 : ABodTCA/VBod);
  CLivTCA = (ALivTCA<1.0e-15 ? 1.0e-15 : ALivTCA/VLiv);
# Total concentration in venous plasma (free+bound)
  CVBodTCAFree = (CBodTCA / PBodTCA); # free in equilibrium
  CVBodTCA = CPlasTCABnd + CVBodTCAFree;
  CVLivTCAFree = (CLivTCA / PLivTCA);
  CVLivTCA = CPlasTCABnd + CVLivTCAFree; # free in equilibrium
# Rate of urinary excretion of TCA
  RUrnTCA = kUrnTCA * APlasTCAFree;
# Dynamics for amount of total (free+bound) TCA in plasma (mg)
  dt(APlasTCA) = kIVTCA + (QBodPlas*CVBodTCA) + (QGutLivPlas*CVLivTCA)
                - (QCPlas * CPlasTCA) - RUrnTCA;

**** Body #####
# Dynamics for amount of TCA in the body (mg)
  dt(ABodTCA) = QBodPlas * (CPlasTCAFree - CVBodTCAFree);

**** Liver #####
# Rate of metabolism of TCA
  RAMetTCA = kMetTCA * ALivTCA;
# Dynamics for amount of TCA in the liver (mg)
  dt(ALivTCA) = kPOTCA + QGutLivPlas*(CPlasTCAFree - CVLivTCAFree)
                - RAMetTCA + (FracTCA * StochTCATCE *
                               (RAMetLivl + FracLungSys*RAMetLng))
                + (StochTCATCOH * RAMetTCOHTCA);

**** Urine #####
# Dynamics for amount of TCA in urine (mg)
  dt(AUrnTCA) = RUrnTCA;
  dt(AUrnTCA_sat) = TCAUrnSat*(1-UrnMissing)* RUrnTCA;
# Saturated, but not missing collection times

```

```

dt(AUrnTCA_collect) = (1-TCAUrnSat)*(1-UrnMissing)*RUrnTCA;
# Not saturated and not missing collection times

#*****
#***                               TCOG Sub-model                               ***
#*****
# State Variables with dynamics:
#   ABodTCOG
#   ALivTCOG
#   ABileTCOG
#   AUrnTCOG
#   AUrnTCOG_sat
#   AUrnTCOG_collect
# Input Variables:
#   TCOGUrnSat
#   UrnMissing
# Other State Variables and Global Parameters:
#   VBodTCOH
#   VLiv
#   PBodTCOG
#   PLivTCOG
#   kUrnTCOG
#   kBile
#   StochGlucTCOH
# Temporary variables used:
#   QBod
#   QGutLiv
#   QCnow
#   RAMetTCOHGluc
#   RAREcircTCOG
# Temporary variables assigned:
#   CVBodTCOG
#   CVLivTCOG
#   CTCOG
#   RUrnTCOG
#   RBileTCOG
# Notes:
#*****
#*** Blood (venous=arterial) *****
# Venous Concentrations (mg/L)
  CVBodTCOG = ABodTCOG / VBodTCOH / PBodTCOG;
  CVLivTCOG = ALivTCOG / VLiv / PLivTCOG;
  CTCOG = (QBod * CVBodTCOG + QGutLiv * CVLivTCOG)/QCnow;
#*** Body *****
# Amount of TCOG in body
  RUrnTCOG = kUrnTCOG * ABodTCOG;
  dt(ABodTCOG) = QBod * (CTCOG - CVBodTCOG) - RUrnTCOG;
  RUrnTCOGTCOH = RUrnTCOG*StochTCOHGluc; #(vrisk)
#*** Liver *****
# Amount of TCOG in liver (mg)
  RBileTCOG = kBile * ALivTCOG;
  dt(ALivTCOG) = QGutLiv * (CTCOG - CVLivTCOG)
    + (StochGlucTCOH * RAMetTCOHGluc) - RBileTCOG;

```

```

#*** Bile *****
# Amount of TCOH-Gluc excreted into bile (mg)
  dt(ABileTCOG) = RBileTCOG - RAREcircTCOG;

#*** Urine *****
# Amount of TCOH-Gluc excreted in urine (mg)
  dt(AUrnTCOG) = RUrnTCOG;
  dt(AUrnTCOG_sat) = TCOGUrnSat*(1-UrnMissing)*RUrnTCOG;
# Saturated, but not missing collection times
  dt(AUrnTCOG_collect) = (1-TCOGUrnSat)*(1-UrnMissing)*RUrnTCOG;
# Not saturated and not missing collection times

#*****
#***                               DCVG Sub-model                               ***
#*****
# State Variables with dynamics:
#   ADCVGmol
# Input Variables:
#   none
# Other State Variables and Global Parameters:
#   kDCVG
#   FracKidDCVC # Fraction of kidney DCVG going to DCVC in first pass
#   VDCVG
# Temporary variables used:
#   RAMetLiv2
#   RAMetKid
# Temporary variables assigned:
#   RAMetDCVGmol
#   CDCVGmol
# Notes:
#   Assume negligible GGT activity in liver as compared to kidney,
#   supported by in vitro data on GGT (even accounting for 5x
#   greater liver mass relative to kidney mass), as well as lack
#   of DCVC detected in blood.
#   "FracKidDCVC" Needed to account for "first pass" in
#   kidney (TCE->DCVG->DCVC without systemic circulation of DCVG).
#*****
# Rate of metabolism of DCVG to DCVC
  RAMetDCVGmol = kDCVG * ADCVGmol;
# Dynamics for DCVG in blood
  dt(ADCVGmol) = (RAMetLiv2 + RAMetKid*(1-FracKidDCVC)) / MWTCE
    - RAMetDCVGmol;
# Concentration of DCVG in blood (in mmoles/l)
  CDCVGmol = ADCVGmol / VDCVG;

#*****
#***                               DCVC Sub-model                               ***
#*****
# State Variables with dynamics:
#   ADCVC
#   AUrnNDCVC
# Input Variables:

```

```

# none
# Other State Variables and Global Parameters:
# MWDCVC
# FracKidDCVC
# StochDCVCTCE
# kNAT
# kKidBioact
# StochN
# Temporary variables used:
# RAMetDCVGmol
# RAMetKid
# Temporary variables assigned:
# RAUrndCVC
# Notes:
# Cannot detect DCVC in blood, so assume all is locally generated
# and excreted or bioactivated in kidney.
#*****
# Amount of DCVC in kidney (mg)
  dt(ADCVC) = RAMetDCVGmol * MWDCVC
              + RAMetKid * FracKidDCVC * StochDCVCTCE
              - ((kNAT + kKidBioact) * ADCVC);
# Rate of NAcDCVC excretion into urine (mg)
  RAUrndCVC = kNAT * ADCVC;
# Dynamics for amount of N Acetyl DCVC excreted (mg)
  dt(AUrndCVC) = StochN * RAUrndCVC;
  RUrndCVC = StochN * RAUrndCVC; # (vrisk)
#*****
#*** Total Mass Balance ***
#*****
#**** Mass Balance for TCE *****
# Total intake from inhalation (mg)
  Rinhdose = QM * CInh;
  dt(Inhdose) = Rinhdose;
# Amount of TCE absorbed by non-inhalation routes (mg)
  dt(AO) = RAO + kIV + kIA + kPV; # (vrisk)
# Total dose
  TotDose = InhDose + AO; # (vrisk)
# Total in tissues
  TotTissue = # (vrisk)
              ARap + ASlw + AFat + AGut + ALiv + AKid + ABld + # (vrisk)
              AInhResp + AResp + AExhResp; # (vrisk)
# Total metabolized
  dt(AMetLng) = RAMetLng; # (vrisk)
  dt(AMetLiv1) = RAMetLiv1; # (vrisk)
  dt(AMetLiv2) = RAMetLiv2; # (vrisk)
  dt(AMetKid) = RAMetKid; # (vrisk)
  ATotMetLiv = AMetLiv1 + AMetLiv2; # (vrisk)
  TotMetab = AMetLng + ATotMetLiv + AMetKid; # (vrisk)
  AMetLivOther = AMetLiv1 * FracOther; # (vrisk)
  AMetGSH = AMetLiv2 + AMetKid; # (vrisk)
# Amount of TCE excreted in feces (mg)
  RAExc = kTD * ADuod; # (vrisk)
  dt(AExc) = RAExc; # (vrisk)

```

```

# Amount exhaled (mg)
  RAExh = QM * CMixExh;
  dt(AExh) = RAExh;
# Mass balance
  TCEDiff = TotDose - TotTissue - TotMetab; # (vrisk)
  MassBaltCE = TCEDiff - AExc - AExh; # (vrisk)

#**** Mass Balance for TCOH *****
# Total production/intake of TCOH
  dt(ARecircTCOG) = RARecircTCOG; # (vrisk)
  dt(AOTCOH) = kPOTCOH + kIVTCOH; # (vrisk)
  TotTCOHIn = AOTCOH + ((1.0 - FracOther - FracTCA) * # (vrisk)
                StochTCOHTCE * (AMetLiv1 + FracLungSys*AMetLng)) + # (vrisk)
                (StochTCOHGluc * ARecircTCOG); # (vrisk)
  TotTCOHDose = AOTCOH + ((1.0 - FracOther - FracTCA) * # (vrisk)
                    StochTCOHTCE * (AMetLiv1 + FracLungSys*AMetLng)); # (vrisk)
# Total in tissues
  TotTissueTCOH = ABodTCOH + ALivTCOH; # (vrisk)
# Total metabolism of TCOH
  dt(AMetTCOHTCA) = RAMetTCOHTCA; # (vrisk)
  dt(AMetTCOHGluc) = RAMetTCOHGluc; # (vrisk)
  dt(AMetTCOHOther) = RAMetTCOH; # (vrisk)
  TotMetabTCOH = AMetTCOHTCA + AMetTCOHGluc + AMetTCOHOther; # (vrisk)
# Mass balance
  MassBaltTCOH = TotTCOHIn - TotTissueTCOH - TotMetabTCOH; # (vrisk)

#**** Mass Balance for TCA *****
# Total production/intake of TCA
  dt(AOTCA) = kPOTCA + kIVTCA; # (vrisk)
  TotTCAln = AOTCA + (FracTCA*StochTCATCE*(AMetLiv1 + # (vrisk)
                    FracLungSys*AMetLng)) + (StochTCATCOH*AMetTCOHTCA); # (vrisk)
# Total in tissues
  TotTissueTCA = APlasTCA + ABodTCA + ALivTCA; # (vrisk)
# Total metabolism of TCA
  dt(AMetTCA) = RAMetTCA; # (vrisk)
# Mass balance
  TCADiff = TotTCAln - TotTissueTCA - AMetTCA; # (vrisk)
  MassBaltTCA = TCADiff - AUrnTCA; # (vrisk)

#**** Mass Balance for TCOG *****
# Total production of TCOG
  TotTCOGIn = StochGlucTCOH * AMetTCOHGluc; # (vrisk)
# Total in tissues
  TotTissueTCOG = ABodTCOG + ALivTCOG + ABileTCOG; # (vrisk)
# Mass balance
  MassBaltTCOG = TotTCOGIn - TotTissueTCOG - # (vrisk)
                ARecircTCOG - AUrnTCOG; # (vrisk)

#**** Mass Balance for DCVG *****
# Total production of DCVG
  dt(ADCVGIn) = (RAMetLiv2 + RAMetKid*(1-FracKidDCVC)) / MWTCCE; # (vrisk)
# Metabolism of DCVG
  dt(AMetDCVG) = RAMetDCVGmol; # (vrisk)

```

```

# Mass balance
  MassBalDCVG = ADCVGIN - ADCVGMol - AMetDCVG; #(vrisk)

##### Mass Balance for DCVC #####
# Total production of DCVC
  dt(ADCVCIn) = RAMetDCVGMol * MWDCVC #(vrisk)
    + RAMetKid * FracKidDCVC * StochDCVCTCE;#(vrisk)
# Bioactivation of DCVC
  dt(ABioactDCVC) = (kKidBioact * ADCVC);#(vrisk)
# Mass balance
  AUrnNDCVCequiv = AUrnNDCVC/StochN;
  MassBalDCVC = ADCVCIn - ADCVC - ABioactDCVC - AUrnNDCVCequiv;#(vrisk)

#####
***          Dynamic Outputs          ***
#####
# Amount exhaled during exposure (mg)
  dt(AExhExp) = (CInh > 0 ? RAExh : 0);

#####
***          Dose Metrics          ***
#####
##### AUCs in mg-hr/L unless otherwise noted #####
#AUC of TCE in arterial blood
  dt(AUCCBld) = CArt; #(vrisk)
#AUC of TCE in liver
  dt(AUCCLiv) = CLiv; #(vrisk)
#AUC of TCE in kidney
  dt(AUCCKid) = CKid; #(vrisk)
#AUC of TCE in rapidly perfused
  dt(AUCCRap) = CRap; #(vrisk)
#AUC of TCOH in blood
  dt(AUCCTCOH) = CTCOH; #(vrisk)
#AUC of TCOH in body
  dt(AUCCBodTCOH) = ABodTCOH / VBodTCOH; #(vrisk)
#AUC of free TCA in the plasma (mg/L * hr)
  dt(AUCPlasTCAFree) = CPlasTCAFree; #(vrisk)
#AUC of total TCA in plasma (mg/L * hr)
  dt(AUCPlasTCA) = CPlasTCA; #(vrisk)
#AUC of TCA in liver (mg/L * hr)
  dt(AUCLivTCA) = CLivTCA; #(vrisk)
#AUC of total TCOH (free+gluc) in TCOH-equiv in blood (mg/L * hr)
  dt(AUCTotTCOH) = CTCOH + CTCOGTCOH; #(vrisk)
#AUC of DCVG in blood (mmol/L * hr) -- NOTE moles, not mg
  dt(AUCCDCVG) = CDCVGMol; #(vrisk)
);
##### End of Dynamics #####

CalcOutputs(

##### Static outputs for comparison to data #####
# TCE

```

```

RetDose = ((InhDose-AExhExp) > 0 ? (InhDose - AExhExp) : 1e-15);
CALVPPM = (CALV < 1.0e-15 ? 1.0e-15 : CALV * (24450.0 / MWTCE));
CInhPPM = (ACh < 1.0e-15 ? 1.0e-15 : ACh/VCh*24450.0/MWTCE);
  # CInhPPM Only used for CC inhalation
CArt = (CArt < 1.0e-15 ? 1.0e-15 : CArt);
CVen = (CVen < 1.0e-15 ? 1.0e-15 : CVen);
CBldMix = (CArt+CVen)/2;
CFat = (CFat < 1.0e-15 ? 1.0e-15 : CFat);
CGut = (CGut < 1.0e-15 ? 1.0e-15 : CGut);
CRap = (CRap < 1.0e-15 ? 1.0e-15 : CRap);
CSlw = (CSlw < 1.0e-15 ? 1.0e-15 : CSlw);
CHrt = CRap;
CKid = (CKid < 1.0e-15 ? 1.0e-15 : CKid);
CLiv = (CLiv < 1.0e-15 ? 1.0e-15 : CLiv);
CLung = CRap;
CMus = (CSlw < 1.0e-15 ? 1.0e-15 : CSlw);
CSpl = CRap;
CBrn = CRap;
zAExh = (AExh < 1.0e-15 ? 1.0e-15 : AExh);
zAExhpost = ((AExh - AExhExp) < 1.0e-15 ? 1.0e-15 : AExh - AExhExp);

# TCOH
CTCOH = (CTCOH < 1.0e-15 ? 1.0e-15 : CTCOH);
CBodTCOH = (ABodTCOH < 1.0e-15 ? 1.0e-15 : ABodTCOH/VBodTCOH);
CKidTCOH = CBodTCOH;
CLivTCOH = (ALivTCOH < 1.0e-15 ? 1.0e-15 : ALivTCOH/VLiv);
CLungTCOH = CBodTCOH;

# TCA
CPlasTCA = (CPlasTCA < 1.0e-15 ? 1.0e-15 : CPlasTCA);
CBldTCA = CPlasTCA*TCAPlas;
CBodTCA = (CBodTCA < 1.0e-15 ? 1.0e-15 : CBodTCA);
CLivTCA = (CLivTCA < 1.0e-15 ? 1.0e-15 : CLivTCA);
CKidTCA = CBodTCA;
CLungTCA = CBodTCA;
zAUrnTCA = (AUrnTCA < 1.0e-15 ? 1.0e-15 : AUrnTCA);
zAUrnTCA_sat = (AUrnTCA_sat < 1.0e-15 ? 1.0e-15 : AUrnTCA_sat);
zAUrnTCA_collect = (AUrnTCA_collect < 1.0e-15 ? 1.0e-15 :
AUrnTCA_collect);
# TCOG
zABileTCOG = (ABileTCOG < 1.0e-15 ? 1.0e-15 : ABileTCOG);
# Concentrations are in TCOH-equivalents
CTCOG = (CTCOG < 1.0e-15 ? 1.0e-15 : CTCOG);
CTCOGTCOH = (CTCOG < 1.0e-15 ? 1.0e-15 : StochTCOHGluc*CTCOG);
CBodTCOGTCOH = (ABodTCOG < 1.0e-15 ? 1.0e-15 :
StochTCOHGluc*ABodTCOG/VBodTCOH);
CKidTCOGTCOH = CBodTCOGTCOH;
CLivTCOGTCOH = (ALivTCOG < 1.0e-15 ? 1.0e-15 :
StochTCOHGluc*ALivTCOG/VLiv);
CLungTCOGTCOH = CBodTCOGTCOH;
AUrnTCOGTCOH = (AUrnTCOG < 1.0e-15 ? 1.0e-15 : StochTCOHGluc*AUrnTCOG);
AUrnTCOGTCOH_sat = (AUrnTCOG_sat < 1.0e-15 ? 1.0e-15 :
StochTCOHGluc*AUrnTCOG_sat);
AUrnTCOGTCOH_collect = (AUrnTCOG_collect < 1.0e-15 ? 1.0e-15 :
StochTCOHGluc*AUrnTCOG_collect);

```

```

# Other
CDCVGmol = (CDCVGmol < 1.0e-15 ? 1.0e-15 : CDCVGmol);
CDCVGmol0 = CDCVGmol; #(v1.2.3.2)
CDCVG_NDtmp = CDFNormal(3*(1-CDCVGmol/CDCVGmolLD));
      # Assuming LD = 3*sigma_blank, Normally distributed
CDCVG_ND = ( CDCVG_NDtmp < 1.0 ? ( CDCVG_NDtmp >= 1e-100 ? -
log(CDCVG_NDtmp) : -log(1e-100)) : 1e-100 );
      #(v1.2.3.2)
zAUrnNDCVC = (AUrnNDCVC < 1.0e-15 ? 1.0e-15 : AUrnNDCVC);
AUrnTCTotMole = zAUrnTCA / MWTCA + AUrnTCOGTCOH / MWTCOH;
TotCTCOH = CTCOH + CTCOGTCOH;
TotCTCOHcomp = CTCOH + CTCOG; # ONLY FOR COMPARISON WITH HACK
ATCOG = ABodTCOG + ALivTCOG; # ONLY FOR COMPARISON WITH HACK

# Misc
CVenMole = CVen / MWTCE;
CPlasTCAMole = (CPlasTCAMole < 1.0e-15 ? 1.0e-15 : CPlasTCAMole);
CPlasTCAFreeMole = (CPlasTCAFreeMole < 1.0e-15 ? 1.0e-15 :
CPlasTCAFreeMole);

#**** Additional Dose Metrics ****
#
      TotTCAInBW = TotTCAIn/BW;#(vrisk)

# Scaled by BW^3/4
TotMetabBW34 = TotMetab/BW75;#(vrisk)
AMetGSHBW34 = AMetGSH/BW75;#(vrisk)
TotDoseBW34 = TotDose/BW75;#(vrisk)
AMetLivlBW34 = AMetLivl/BW75;#(vrisk)
TotOxMetabBW34 = (AMetLng+AMetLivl)/BW75;#(vrisk)

AMetLngBW34 = AMetLng/BW75; #(vrisk)
ABioactDCVCBW34 = ABioactDCVC/BW75;#(vrisk)
AMetLivOtherBW34 = AMetLivOther/BW75; #(vrisk)

# Scaled by tissue volume
AMetLivlLiv = AMetLivl/VLiv; #(vrisk)
AMetLivOtherLiv = AMetLivOther/VLiv; #(vrisk)
AMetLngResp = AMetLng/VRespEfftmp; #(vrisk)
ABioactDCVKid = ABioactDCVC/VKid;#(vrisk)

#**** Fractional Volumes

VFatCtmp = VFat/BW; #(vrisk)
VGutCtmp = VGut/BW; #(vrisk)
VLivCtmp = VLiv/BW; #(vrisk)
VRapCtmp = VRap/BW; #(vrisk)
VRespLumCtmp = VRespLum/BW; #(vrisk)
VRespEffCtmp = VRespEfftmp/BW; #(vrisk)
VKidCtmp = VKid/BW; #(vrisk)
VBldCtmp = VBld/BW; #(vrisk)
VSlwCtmp = VSlw/BW; #(vrisk)
VPlasCtmp = VPlas/BW; #(vrisk)
VBodCtmp = VBod/BW; #(vrisk)
VBodTCOHCtmp = VBodTCOH/BW; #(vrisk)

```

## 1 A.8. REFERENCES

- 2 Abbas R, Seckel CS, MacMahon KL, Fisher JW. (1997). Determination of kinetic rate constants for chloral hydrate,  
3 trichloroethanol, trichloroacetic acid, and dichloroacetic acid—a physiologically based modeling approach.  
4 *Toxicologist* **36**:32-33.
- 5 Abbas R, Fisher JW. (1997). physiologically based pharmacokinetic model for trichloroethylene and its metabolites,  
6 chloral hydrate, trichloroacetate, dichloroacetate, trichloroethanol, and trichloroethanol glucuronide in B6C3F1  
7 mice. *Toxicol Appl Pharmacol.* **147**:15–30.
- 8 Andersen, M. E., Gargas, M. L., Clewell, H. J., 3rd, and Severyn, K. M. (1987). Quantitative evaluation of the  
9 metabolic interactions between trichloroethylene and 1,1-dichloroethylene *in vivo* using gas uptake methods. *Toxicol*  
10 *Appl Pharmacol* **89**, 149–157.
- 11 Araki, S. (1978). The effects of water restriction and water loading on urinary excretion of lead, delta-  
12 aminolevulinic acid and coproporphyrin. *Br J Ind Med.* **35**(4):312–7.
- 13 Barter, Z. E., Bayliss, M. K., Beaune, P. H., Boobis, A. R., Carlile, D. J., Edwards, R. J., Houston, J. B., Lake, B. G.,  
14 Lipscomb, J. C., Pelkonen, O. R., Tucker, G. T., and Rostami-Hodjegan, A. (2007). Scaling factors for the  
15 extrapolation of *in vivo* metabolic drug clearance from *in vitro* data: reaching a consensus on values of human  
16 microsomal protein and hepatocellularity per gram of liver. *Curr Drug Metab* **8**, 33–45.
- 17 Barton, H. A., Creech, J. R., Godin, C. S., Randall, G. M., and Seckel, C. S. (1995). Chloroethylene mixtures:  
18 pharmacokinetic modeling and *in vitro* metabolism of vinyl chloride, trichloroethylene, and trans-1,2-  
19 dichloroethylene in rat. *Toxicol Appl Pharmacol* **130**, 237–247.
- 20 Bartonicek, V. (1962). Metabolism and excretion of trichloroethylene after inhalation by human subjects. *Br J*  
21 *Indust Med.* **19**:134–141.
- 22 Bernauer, U., Birner, G., Dekant, W., and Henschler, D. (1996). Biotransformation of trichloroethene: dose-  
23 dependent excretion of 2,2,2-trichloro-metabolites and mercapturic acids in rats and humans after inhalation. *Arch*  
24 *Toxicol* **70**, 338–346.
- 25 Birner G, Vamvakas S, Dekant W, Henschler D. (1993). Nephrotoxic and genotoxic N-acetyl-S-dichlorovinyl-L-  
26 cysteine is a urinary metabolite after occupational 1,1,2-trichloroethene exposure in humans: implications for the  
27 risk of trichloroethene exposure. *Environ Health Perspect.* **99**:281–4.
- 28 Bloemen, L. J., Monster, A. C., Kezic, S., Commandeur, J. N., Veulemans, H., Vermeulen, N. P., and Wilmer, J. W.  
29 (2001). Study on the cytochrome P-450- and glutathione-dependent biotransformation of trichloroethylene in  
30 humans. *Int Arch Occup Environ Health* **74**, 102–108.
- 31 Bois FY. (2000a). Statistical analysis of Fisher et al. PBPK model of trichloroethylene kinetics. *Environ Health*  
32 *Perspect.* **108 Suppl 2**:275–82.
- 33 Bois FY. (2000b). Statistical analysis of Clewell et al. PBPK model of trichloroethylene kinetics. *Environ Health*  
34 *Perspect.* **108 Suppl 2**:307–16.
- 35 Bronley-DeLancey, A., McMillan, D. C., McMillan, J. M., Jollow, D. J., Mohr, L. C., and Hoel, D. G. (2006).  
36 Application of cryopreserved human hepatocytes in trichloroethylene risk assessment: relative disposition of chloral  
37 hydrate to trichloroacetate and trichloroethanol. *Environ Health Perspect* **114**, 1237–1242.
- 38 Brown RP, Delp MD, Lindstedt SL, Rhomberg LR, Beliles RP. (1997). Physiological parameter values for  
39 physiologically based pharmacokinetic models. *Toxicol Ind Health.* **13**:407–84.

*This document is a draft for review purposes only and does not constitute Agency policy.*

- 1 Chiu, WA; Bois, RY. (2006) Revisiting the population toxicokinetics of tetrachloroethylene. *Arch Toxicol*  
2 80(6):382–385.
- 3 Chiu, W. A., Micallef, S., Monster, A. C., and Bois, F. Y. (2007). Toxicokinetics of inhaled trichloroethylene and  
4 tetrachloroethylene in humans at 1 ppm: empirical results and comparisons with previous studies. *Toxicol Sci* **95**,  
5 23–36.
- 6 Clewell HJ 3rd, Gentry PR, Covington TR, Gearhart JM. (2000). Development of a physiologically based  
7 pharmacokinetic model of trichloroethylene and its metabolites for use in risk assessment. *Environ Health Perspect.*  
8 **108 Suppl 2**:283–305.
- 9 Dallas, C. E., Gallo, J. M., Ramanathan, R., Muralidhara, S., and Bruckner, J. V. (1991). Physiological  
10 pharmacokinetic modeling of inhaled trichloroethylene in rats. *Toxicol Appl Pharmacol* **110**, 303–314.
- 11 Elfarra, A. A., Krause, R. J., Last, A. R., Lash, L. H., and Parker, J. C. (1998). Species- and sex-related differences  
12 in metabolism of trichloroethylene to yield chloral and trichloroethanol in mouse, rat, and human liver microsomes.  
13 *Drug Metab Dispos* **26**, 779–785.
- 14 Ertle T, Henschler D, Müller G, Spassowski M. (1972). Metabolism of trichloroethylene in man. I. The significance  
15 of trichloroethanol in long-term exposure conditions. *Arch Toxikol.* **29**:171–88.
- 16 Fernandez, J. G., Droz, P. O., Humbert, B. E., and Caperos, J. R. (1977). Trichloroethylene exposure. Simulation of  
17 uptake, excretion, and metabolism using a mathematical model. *Br J Ind Med* **34**, 43–55.
- 18 Fiserova-Bergerova, V., Tichy, M., and Di Carlo, F. J. (1984). Effects of biosolubility on pulmonary uptake and  
19 disposition of gases and vapors of lipophilic chemicals. *Drug Metab Rev* **15**, 1033–1070.
- 20 Fisher JW. (2000). Physiologically based pharmacokinetic models for trichloroethylene and its oxidative  
21 metabolites. *Environ Health Perspect.* **108 Suppl 2**:265–73.
- 22 Fisher JW, Allen BC. (1993). Evaluating the risk of liver cancer in humans exposed to trichloroethylene using  
23 physiological models. *Risk Anal.* **13**(1):87–95.
- 24 Fisher, J. W., Whittaker, T. A., Taylor, D. H., Clewell, H. J., 3rd, and Andersen, M. E. (1989). Physiologically based  
25 pharmacokinetic modeling of the pregnant rat: a multiroute exposure model for trichloroethylene and its metabolite,  
26 trichloroacetic acid. *Toxicol Appl Pharmacol* **99**, 395–414.
- 27 Fisher JW, Gargas ML, Allen BC, Andersen ME. (1991). Physiologically based pharmacokinetic modeling with  
28 trichloroethylene and its metabolite, trichloroacetic acid, in the rat and mouse. *Toxicol Appl Pharmacol.*  
29 **109**:183–95.
- 30 Fisher, J. W., Mahle, D., and Abbas, R. (1998). A human physiologically based pharmacokinetic model for  
31 trichloroethylene and its metabolites, trichloroacetic acid and free trichloroethanol. *Toxicol Appl Pharmacol* **152**,  
32 339–359.
- 33 Gargas, M. L., Burgess, R. J., Voisard, D. E., Cason, G. H., and Andersen, M. E. (1989). Partition coefficients of  
34 low-molecular-weight volatile chemicals in various liquids and tissues. *Toxicol Appl Pharmacol* **98**, 87–99.
- 35 Gelfand, A.E., Smith, A.F.M. (1990). Sampling-based approaches to calculating marginal densities. *J Am Stat*  
36 *Assoc.* **85**:398–409.
- 37 Gelman A, Bois F, Jiang J. (1996). Physiological pharmacokinetic analysis using population modeling and  
38 informative prior distributions. *J Am Stat Assoc.* **91**:1400–1412.

*This document is a draft for review purposes only and does not constitute Agency policy.*



- 1 Gelman A, Carlin JB, Stern HS, Rubin DB. (2004). Bayesian Data Analysis. New York: Chapman & Hall/CRC.
- 2 Gilks, W.R., Richardson, S., Spiegelhalter, D.J., eds. (1996) Markov Chain Monte Carlo in Practice. New York:  
3 Chapman & Hall/CRC Press.
- 4 Green, T. (2003a) The concentrations of trichloroacetic acid in blood following administration of trichloroacetic  
5 acid in drinking water. Central Toxicology Laboratory, Alderley Park Macclesfield, Cheshire, UK.
- 6 Green, T. (2003b) The concentrations of trichloroacetic acid in blood following administration of trichloroacetic  
7 acid in drinking water. Central Toxicology Laboratory, Alderley Park Macclesfield, Cheshire, UK.
- 8 Green, T., and Prout, M. S. (1985). Species differences in response to trichloroethylene. II. Biotransformation in rats  
9 and mice. *Toxicol Appl Pharmacol* 79, 401–411.
- 10 Green, T., Mainwaring, G. W., and Foster, J. R. (1997). Trichloroethylene-induced mouse lung tumors: studies of  
11 the mode of action and comparisons between species. *Fundam Appl Toxicol* 37, 125–130.
- 12 Greenberg, M. S., Burton, G. A., and Fisher, J. W. (1999). Physiologically based pharmacokinetic modeling of  
13 inhaled trichloroethylene and its oxidative metabolites in B6C3F1 mice. *Toxicol Appl Pharmacol* 154, 264–278.
- 14 Hack CE, Chiu WA, Jay Zhao Q, Clewell HJ.(2006). Bayesian population analysis of a harmonized physiologically  
15 based pharmacokinetic model of trichloroethylene and its metabolites. *Regul Toxicol Pharmacol*. 46:63–83.
- 16 Hejtmančik MR, Trela BA, Kurtz PJ, Persing RL, Ryan MJ, Yarrington JT, Chhabra RS. (2002). Comparative  
17 gavage subchronic toxicity studies of o-chloroaniline and m-chloroaniline in F344 rats and B6C3F1 mice. *Toxicol*  
18 *Sci*. 69:234–43.
- 19 Hissink, E. M., Bogaards, J. J. P., Freidg, A. P., Commandeur, J. N. M., Vermeulen, N. P. E., and van Bladeren, P. J.  
20 (2002). The use of *in vitro* metabolic parameters and physiologically based pharmacokinetic (PBPK) modeling to  
21 explore the risk assessment of trichloroethylene. *Environmental Toxicology and Pharmacology* 11, 259–271.
- 22 ICRP (International Commission on Radiological Protection). (2003) Basic anatomical and physiological data for  
23 use in radiological protection: Reference values, 89. Oxford; New York: Pergamon Press.
- 24 Jakobson, I., Holmberg, B., and Ekner, A. (1986). Venous blood levels of inhaled trichloroethylene in female rats  
25 and changes induced by interacting agents. *Acta Pharmacol Toxicol (Copenh)* 59, 135–143.
- 26 Kaneko, T., Wang, P. Y., and Sato, A. (1994). Enzymes induced by ethanol differently affect the pharmacokinetics  
27 of trichloroethylene and 1,1,1-trichloroethane. *Occup Environ Med* 51, 113–119.
- 28 Keys, D. A., Bruckner, J. V., Muralidhara, S., and Fisher, J. W. (2003). Tissue dosimetry expansion and cross-  
29 validation of rat and mouse physiologically based pharmacokinetic models for trichloroethylene. *Toxicol Sci* 76,  
30 35–50.
- 31 Kim, S; Kim, D; Pollack, GM; et al. (2009) Pharmacokinetic analysis of trichloroethylene metabolism in male  
32 B6C3F1 mice: Formation and disposition of trichloroacetic acid, dichloroacetic acid,  
33 S-(1,2-dichlorovinyl)glutathione and S-(1,2-dichlorovinyl)-L-cysteine. *Toxicol Appl Pharmacol* 238(1):90-99.  
34 Epub 2009 May 3.
- 35 Kimmerle, G., Eben, A. (1973a). Metabolism, excretion and toxicology of trichloroethylene after inhalation. I.  
36 Experimental exposure on rats. *Arch Toxicol* 30:115–126.
- 37 Kimmerle, G., Eben, A. (1973b). Metabolism, excretion and toxicology of trichloroethylene after inhalation. II.  
38 Experimental human exposure. *Arch Toxicol* 30:127–138.

*This document is a draft for review purposes only and does not constitute Agency policy.*

- 1 Koizumi, A. (1989). Potential of physiologically based pharmacokinetics to amalgamate kinetic data of  
2 trichloroethylene and tetrachloroethylene obtained in rats and man. *Br J Ind Med* **46**, 239–249.
- 3 Laparé S, Tardif R, Brodeur J.(1995). Effect of various exposure scenarios on the biological monitoring of  
4 organicsolvents in alveolar air. II. 1,1,1-Trichloroethane and trichloroethylene. *Int Arch Occup Environ Health*.  
5 **67**:375–94.
- 6 Larson, J. L., and Bull, R. J. (1992a). Metabolism and lipoperoxidative activity of trichloroacetate and  
7 dichloroacetate in rats and mice. *Toxicol Appl Pharmacol* **115**, 268–277.
- 8 Larson, J. L., and Bull, R. J. (1992b). Species differences in the metabolism of trichloroethylene to the carcinogenic  
9 metabolites trichloroacetate and dichloroacetate. *Toxicol Appl Pharmacol* **115**, 278–285.
- 10 Lash, L. H., Tokarz, J. J., and Pegouske, D. M. (1995). Susceptibility of primary cultures of proximal tubular and  
11 distal tubular cells from rat kidney to chemically induced toxicity. *Toxicology* **103**, 85–103.
- 12 Lash, L. H., Visarius, T. M., Sall, J. M., Qian, W., and Tokarz, J. J. (1998). Cellular and subcellular heterogeneity of  
13 glutathione metabolism and transport in rat kidney cells. *Toxicology* **130**, 1–15.
- 14 Lash LH, Lipscomb JC, Putt DC, Parker JC. (1999a). Glutathione conjugation of trichloroethylene in human liver  
15 and kidney: kinetics and individual variation. *Drug Metab Dispos*. **27**:351–359.
- 16 Lash LH, Putt DA, Brashear WT, Abbas R, Parker JC, Fisher JW. (1999b). Identification of S-(1,2-  
17 dichlorovinyl)glutathione in the blood of human volunteers exposed to trichloroethylene. *J Toxicol Environ Health*  
18 *A*. **56**:1–21.
- 19 Lash LH, Putt DA, Parker JC. (2006). Metabolism and tissue distribution of orally administered trichloroethylene in  
20 male and female rats: identification of glutathione- and cytochrome P-450-derived metabolites in liver, kidney,  
21 blood, and urine. *J Toxicol Environ Health A*. **69**:1285–309.
- 22 Lee, K. M., Bruckner, J. V., Muralidhara, S., and Gallo, J. M. (1996). Characterization of presystemic elimination of  
23 trichloroethylene and its nonlinear kinetics in rats. *Toxicol Appl Pharmacol* **139**, 262–271.
- 24 Lee, K. M., Muralidhara, S., Schnellmann, R. G., and Bruckner, J. V. (2000). Contribution of direct solvent injury to  
25 the dose-dependent kinetics of trichloroethylene: portal vein administration to rats. *Toxicol Appl Pharmacol* **164**,  
26 46–54.
- 27 Lin JH. (1995). Species similarities and differences in pharmacokinetics. *Drug Metab Dispos*. **23**:1008–21.
- 28 Lipscomb, J. C., Garrett, C. M., and Snawder, J. E. (1997). Cytochrome P450-dependent metabolism of  
29 trichloroethylene: interindividual differences in humans. *Toxicol Appl Pharmacol* **142**, 311–318.
- 30 Lipscomb, J. C., Garrett, C. M., and Snawder, J. E. (1998a). Use of Kinetic and Mechanistic Data in Species  
31 Extrapolation of Bioactivation: Cytochrome-P450 Dependent Trichloroethylene Metabolism at Occupationally  
32 Relevant Concentrations. *J Occup Health* **40**, 110–117.
- 33 Lipscomb, J. C., Fisher, J. W., Confer, P. D., and Byczkowski, J. Z. (1998b). *In vitro to in vivo* extrapolation for  
34 trichloroethylene metabolism in humans. *Toxicol Appl Pharmacol* **152**, 376–387.
- 35 Liu, Y; Bartlett, MG; White, CA; et al. (2009) Presystemic elimination of trichloroethylene in rats following  
36 environmentally relevant oral exposures. *Drug Metab Dispos* (10):1994-1998. Epub 2009 Jul 6.

*This document is a draft for review purposes only and does not constitute Agency policy.*

- 1 Lumpkin, M. H., Bruckner, J. V., Campbell, J. L., Dallas, C. E., White, C. A., and Fisher, J. W. (2003). Plasma  
2 binding of trichloroacetic acid in mice, rats, and humans under cancer bioassay and environmental exposure  
3 conditions. *Drug Metab Dispos* **31**, 1203–1207.
- 4 Mahle, DA; Godfrey, RJ; Buttler, GW; et al. (2001) Pharmacokinetics and metabolism of dichloroacetic acid and  
5 trichloroacetic acid administered in drinking water in rats and mice. United States Air Force Research Laboratory,  
6 Wright Patterson Air Force Base, OH. AFRL-HE-WP-TR-2001-0059.
- 7 Merdink, J. L., Gonzalez-Leon, A., Bull, R. J., and Schultz, I. R. (1998). The extent of dichloroacetate formation  
8 from trichloroethylene, chloral hydrate, trichloroacetate, and trichloroethanol in B6C3F1 mice. *Toxicol Sci* **45**,  
9 33–41.
- 10 Merdink, J. L., Stenner, R. D., Stevens, D. K., Parker, J. C., and Bull, R. J. (1999). Effect of enterohepatic  
11 circulation on the pharmacokinetics of chloral hydrate and its metabolites in F344 rats. *J Toxicol Environ Health A*  
12 **57**, 357–368.
- 13 Monster, A. C., Boersma, G., and Duba, W. C. (1976). Pharmacokinetics of trichloroethylene in volunteers,  
14 influence of workload and exposure concentration. *Int Arch Occup Environ Health* **38**, 87–102.
- 15 Monster, A. C., Boersma, G., and Duba, W. C. (1979). Kinetics of trichloroethylene in repeated exposure of  
16 volunteers. *Int Arch Occup Environ Health* **42**, 283–292.
- 17 Müller G, Spassowski M, Henschler D. (1972). Trichloroethylene exposure and trichloroethylene metabolites in  
18 urine and blood. *Arch. Toxicol.* **29**:335–340.
- 19 Muller, G., Spassovski, M., and Henschler, D. (1974). Metabolism of trichloroethylene in man. II. Pharmacokinetics  
20 of metabolites. *Arch Toxicol* **32**, 283–295.
- 21 Muller, G., Spassowski, M., and Henschler, D. (1975). Metabolism of trichloroethylene in man. III. Interaction of  
22 trichloroethylene and ethanol. *Arch Toxicol* **33**, 173–189.
- 23 Okino MS, Chiu WA, Evans MV, Power FW, Lipscomb JC, Tornero-Velez R, Dary CC, Blancato JN, Chen C .  
24 2005. Suitability of Using *In Vitro* and Computationally Estimated Parameters in Simplified Pharmacokinetic  
25 Models. *Drug Metab Rev* 2005; 37(suppl. 2):162.
- 26 Paycok, Z.V., Powell, J.F. (1945). The excretion of sodium trichloroacetate. *J Pharmacol Exper Therapeut.* **85**:  
27 289–293.
- 28 Plummer M, Best N, Cowles K, Vines K. (2008). *coda: Output analysis and diagnostics for MCMC*. R package  
29 version 0.13-3.
- 30 Price PS, Conolly RB, Chaisson CF, Gross EA, Young JS, Mathis ET, Tedder DR. (2003). Modeling interindividual  
31 variation in physiological factors used in PBPK models of humans. *Crit Rev Toxicol.* **33**:469–503.
- 32 Prout, M. S., Provan, W. M., and Green, T. (1985). Species differences in response to trichloroethylene. I.  
33 Pharmacokinetics in rats and mice. *Toxicol Appl Pharmacol* **79**, 389–400.
- 34 Rodriguez, CE; Mahle, DA; Gearhart, JM; et al. (2007) Predicting age-appropriate pharmacokinetics of six volatile  
35 organic compounds in the rat utilizing physiologically based pharmacokinetic modeling. *Toxicol Sci* 98(1) :43-56.
- 36 Sarangapani R, Gentry PR, Covington TR, Teeguarden JG, Clewell HJ 3rd. (2003). Evaluation of the potential  
37 impact of age- and gender-specific lung morphology and ventilation rate on the dosimetry of vapors. *Inhal Toxicol.*  
38 **15**:987–1016.

*This document is a draft for review purposes only and does not constitute Agency policy.*

- 1 Sato, A., Nakajima, T., Fujiwara, Y., and Murayama, N. (1977). A pharmacokinetic model to study the excretion of  
2 trichloroethylene and its metabolites after an inhalation exposure. *Br J Ind Med* **34**, 56–63.
- 3 Sato, A., and Nakajima, T. (1979). Partition coefficients of some aromatic hydrocarbons and ketones in water, blood  
4 and oil. *Br J Ind Med* **36**, 231–234.
- 5 Schultz, I. R., Merdink, J. L., Gonzalez-Leon, A., and Bull, R. J. (1999). Comparative toxicokinetics of chlorinated  
6 and brominated haloacetates in F344 rats. *Toxicol Appl Pharmacol* **158**, 103–114.
- 7 Simmons, J. E., Boyes, W. K., Bushnell, P. J., Raymer, J. H., Limsakun, T., McDonald, A., Sey, Y. M., and Evans,  
8 M. V. (2002). A physiologically based pharmacokinetic model for trichloroethylene in the male long-Evans rat.  
9 *Toxicol Sci* **69**, 3–15.
- 10 Stenner, R. D., Merdink, J. L., Stevens, D. K., Springer, D. L., and Bull, R. J. (1997). Enterohepatic recirculation of  
11 trichloroethanol glucuronide as a significant source of trichloroacetic acid. Metabolites of trichloroethylene. *Drug*  
12 *Metab Dispos* **25**, 529–535.
- 13 Stewart, R. D., Dodd, H. C., Gay, H. H., and Erley, D. S. (1970). Experimental human exposure to trichloroethylene.  
14 *Arch Environ Health* **20**, 64–71.
- 15 Sweeney, LM; Kirman, CR; Gargas, ML; et al. (2009) Contribution of trichloroacetic acid to liver tumors observed  
16 in perchloroethylene (perc)-exposed mice. *Toxicology* 260(1-3):77-83. Epub 2009 Mar 24.
- 17 Templin, M. V., Parker, J. C., and Bull, R. J. (1993). Relative formation of dichloroacetate and trichloroacetate from  
18 trichloroethylene in male B6C3F1 mice. *Toxicol Appl Pharmacol* **123**, 1–8.
- 19 Templin, M. V., Stevens, D. K., Stenner, R. D., Bonate, P. L., Tuman, D., and Bull, R. J. (1995). Factors affecting  
20 species differences in the kinetics of metabolites of trichloroethylene. *J Toxicol Environ Health* **44**, 435–447.
- 21 Trevisan A, Giraldo M, Borella M, Maso S. (2001). Historical control data on urinary and renal tissue biomarkers in  
22 naive male Wistar rats. *J Appl Toxicol*. 21(5):409-13.
- 23 Triebig, G., Essing, H.-G., Schaller, K.-H., Valentin, H. (1976). Biochemical and psychological examinations of test  
24 subjects exposed to trichloroethylene. *Zbl. Bakt. Hyg., I. Abt. Orig. B* **163**: 383–416.
- 25 Yu, K. O., Barton, H. A., Mahle, D. A., and Frazier, J. M. (2000). *In vivo* kinetics of trichloroacetate in male Fischer  
26 344 rats. *Toxicol Sci* **54**, 302–311.

*This document is a draft for review purposes only and does not constitute Agency policy.*